TECHNISCHE UNIVERSITÄT
CAROLO-WILHELMINA
ZU BRAUNSCHWEIG

High-throughput metabolome analysis of transposon mutants of *Corynebacterium glutamicum* and quenching of microbial metabolism

Von der Fakultät für Lebenswissenschaften
der Technischen Universität Carolo-Wilhelmina
zu Braunschweig

zur Erlangung des Grades einer
Doktorin der Naturwissenschaften
(Dr. rer. nat.)

genehmigte
D i s s e r t a t i o n

von Jana Spura
aus Torgau

1. Referentin oder Referent:	Professor Dr. Dietmar Schomburg
2. Referentin oder Referent:	Professor Dr. Dieter Jahn
eingereicht am:	15.12.2008
mündliche Prüfung (Disputation) am:	24.02.2009

Druckjahr 2009

Vorveröffentlichungen der Dissertation

Teilergebnisse aus dieser Arbeit wurden mit Genehmigung der Fakultät für Lebenswissenschaften, vertreten durch den Mentor der Arbeit, in folgenden Beiträgen vorab veröffentlicht:

Publikationen

Börner, J., Buchinger, S. & Schomburg, D. A high-throughput method for microbial metabolome analysis using gas chromatography/mass spectrometry. Analytical Biochemistry 367: 143-151 (2007)

Spura, J. & Schomburg D. Hochdurchsatzmetabolomanalyse von Mikro-organismen. Laborwelt 6: 21-24 (2008)

Tagungsbeiträge

Börner, J., Buchinger, S. & Schomburg, D. High-throughput method for microbial metabolome analysis. (Poster) European BioPerspectives, Köln (2007).

Börner, J., Buchinger, S. & Schomburg, D. High-throughput method for microbial metabolome analysis. (Poster) ProkaGENOMICS, Göttingen (2007).

Spura, J., Reimer, L., Lühr, T. & Schomburg, D. Screening of transposon mutants of *Corynebacterium glutamicum* using a high-throughput method for microbial metabolome analysis. (Vortrag) European BioPerspectives, Hannover (2008).

Reimer, L., Spura, J., Wieloch, P., Schreiber, K. & Schomburg, D Quenching of different microorganisms for metabolome analysis using an ethanol/sodium chloride-quenchingsolution (Poster) European BioPerspectives, Hannover (2008).

Table of contents

Abstract

A suitable method is the prerequisite for comprehensive screening performances. Therefore, an analytical method for high-throughput metabolome analysis on basis of our well established standard method was developed. Fast metabolome analysis was done using gas chromatography/mass spectrometry. Two major advantages were parallelization of operations and partial automation. In short this means a clear reduction of time needed for the pre-analytical steps. The standard error between independent samples of the model organism *Corynebacterium glutamicum* raised on the same plate was decreased to 13%. Additionally, the runtime of a single measurement was decreased, allowing an increased number of measurements per day. The adaptation of our internal standard library achieved 650 quantifiable peaks per single GC/MS run.

With this method around 320 transposon mutants of *Corynebacterium glutamicum* were investigated, and suitable screening criteria were developed to identify mutants with significant changes of their phenotype. First indicators regarding this research came from a comparison of mutant and wild type raised on the same plate. But for a clear differentiation of changes caused by gene deletion and those resulting from biological and environmental variations, a wild type reference list was created. A threshold for each metabolite was calculated revealing significant differences.

The last part of this thesis deals with the development of a quenching method applicable for different microorganisms. An ethanol quenching procedure, established earlier in our group, was optimized, and evaluated against results coming from published quenching tests for three different organisms: *Corynebacterium glutamicum, Escherichia coli* and *Saccharomyces cerevisiae*. The ethanol quenching method in most cases produced the highest number of detected metabolites, and had a low standard error. Also, this samples showed the highest range of relative concentrations of identified metabolites.

Kurzzusammenfassung

Ein umfassendes und erfolgreiches *Screening* ist nur mit einer geeigneten Methode möglich. Deshalb wurde im Rahmen dieser Arbeit eine Hochdurchsatzmethode zur Metabolomanalyse entwickelt. Grundlage war die Standardmethode unserer Arbeitsgruppe. Die Metabolomanalyse wurde unter Verwendung der Gaschromatographie/Massenspektrometrie durchgeführt. Hauptvorteile waren Parallelisierung und Teilautomatisierung, die zu einer Verringerung der benötigten Zeit für die Probenvorbereitung führten. Der Standardfehler unabhängiger Proben des Modellorganismus *Corynebacterium glutamicum* wurde auf 13% reduziert. Außerdem wurde die Laufzeit einer Messung verkürzt und so die Anzahl pro Tag erhöht. Die Anpassung unserer internen Standardbibliothek führte zu 650 quantifizierbaren Peaks je GC/MS-Lauf.

Diese Methode wurde verwendet, um zirka 320 Transposonmutanten von *Corynebacterium glutamicum* zu untersuchen und geeignete Kriterien für das *Screening* nach Mutanten mit signifikanten Veränderungen des Phänotyps zu entwickeln. Zuerst erfolgte der direkte Vergleich gemeinsam kultivierter Mutanten- und Wildtypproben. Allerdings konnte nicht zwischen Veränderungen durch Gendeletion und biologischen und umweltbedingten Schwankungen unterschieden werden. Deshalb wurde eine Referenzliste erstellt. Die Ermittlung eines für jeden Metaboliten spezifischen Schwellenwerts ließ signifikante Veränderungen erkennen.

Im letzten Teil der Arbeit wurde eine Quenchingmethode für unterschiedliche Mikroorganismen untersucht. Dafür wurde eine bereits vorhandene Ethanolquenchmethode unserer Arbeitsgruppe optimiert und an verschiedenen Organismen - *Corynebacterium glutamicum, Escherichia coli* und *Saccharomyces cerevisiae* - sowie im direkten Vergleich zu publizierten Methoden evaluiert. Das Quenchen mit Ethanol lieferte in den meisten Fällen die höchste Anzahl sowie die höchsten relativen Konzentrationen identifizierter Metabolite verbunden mit geringen Standardfehlern.

Abbreviations & Formula

2D-PAGE	two-dimensional polyacrylamid gel electrophoresis
A	diffusion influenced by packing of the column
Abs.	absolute
ADC	analog to digital conversion
AMDIS	Automated Mass Spectral Deconvolution and Identification System
AMP	Adenosine-5'-monophosphate
APCI	atmospheric pressure chemical ionization
B	longitudinal diffusion
B2P6	bank 2 plate 6
BHI	brain heart infusion medium (complex medium)
BLAST	Basic Local Alignment Search Tool
bp	base pair(s)
BRENDA	*Braunschweiger Enzymdatenbank (Braunschweig enzyme database)*
BSA	N,O-bis(trimethylsilyl)acetamid
BSTFA	N,O-bis(trimethylsilyl)trifuoracetamid
$b_{0.5}$	width in half height of the peak
C	term for reaching the equilibrium
CDW	cell dry weight
CE	capillary electrophoresis
C. glutamicum	*Corynebacterium glutamicum*
CI	chemical ionization
Δ	delta, difference
DB-5MS	chromatographic column, fused silica
DNA	deoxyribonucleic acid
e	unit charge
eV	electron voltage
E. coli	*Escherichia coli*
EDTA	Ethylenediaminetetraacetic acid
EI	electron ionization, electron impact ionization
E_{kin}	kinetic energy

$Error_{Ref}$	standard error of a metabolite from the wild type reference list
ESI	electrospray ionization
ESOMs	emergent self organizing maps
EQ	ethanol quenching
g	acceleration of gravity
GC	gas chromatography, gas chromatograph
GC-GC	tandem gas chromatography
GSQ	cold glycerin saline quenching
h	hour
H_{eff}	height of effective theoretical plates
i	control variable
IS*6100*	insertion sequence 6100
K_D	distribution coefficient
Kan^R	kanamycin resistance marker
KEGG	Kyoto Encyclopedia of Genes and Genomes
L	length of GC column in mm
l	length of the flight tube
LB	Luria-Bertani medium
LC	liquid chromatography
m	ion mass
Mb	mega bases
ml, l	milliliter, liter
mm	millimeter
MM1	minimal medium
MALDI	matrix assisted laser desorption ionization
MCP	micro channel plate
mM	milli-molar
mRNA	messenger ribonucleic acid
MS	mass spectrometry, mass spectrometer
MS/MS	tandem mass spectrometry
MSTFA	N-methyl-N-trimethylsilyltrifluoroacetamid
MT	relative concentration of metabolite in mutant sample

MudPIT	multidimensional protein identification technology
MQ	methanol quenching
n	series of measurements
NCBI	National Center for Biotechnology Information
N_{eff}	number of effective theoretical plates
NIST	National Institute of Standards and Technology
NMR	nuclear magnetic resonance spectroscopy
OD	optical density
ori	origin of replication
pAT6100	plasmid 6100
PP	polypropylene
PS	polystyrene
PTV	programmed temperature vaporizer
r	Pearson correlation coefficient
Ref	relative concentration of the metabolite from the wild type reference list
RI	retention index, Kovàts' index
RNA	ribonucleic acid
RP4*mob*	mobilizable part of the cloning vector pK18*mob2*
pK18*mob2*	vector
pM	pico-molar
s	standard deviation
s_{rel}	relative error
s_f	Gauss error after
$s_{\bar{x}}$	standard error
T	temperature
TAE	Tris-Acetate-EDTA
TE	Tris-EDTA
T_{Met}	metabolite threshold
t	flight time of an ion
t_i	retention time of the unknown substance i
t_S	net retention time

t_R	gross retention time
t_T	dead time
t_x	retention time of alkane eluting before elution of unknown substance
t_y	retention time of alkane eluting after elution of unknown substance
TIC	total ion current
TMS	trimethylsilyl
TOF	time of flight mass spectrometer
u	carrier velocity
U	acceleration velocity
UQ	unquenched, standard method
U/ml	units per milliliter
v/v	volume per volume
w/v	weight per volume
x	number of carbon atoms contained in alkane eluting before elution of unknown substance
x_i	single measurement
$\overline{x}$	mean value
y	number of carbon atoms contained in alkane eluting after elution of unknown substance
z	ion charge
µm	micrometer

1 Introduction

In the continually growing field of systems biology knowledge about all gene functions present within an organism is an important task. This is necessary for the construction of complete regulatory networks and e.g. predictions by computer models. But information available so far from genome data and annotation are incomplete. Further information is necessary to close existing gaps in networks. Hence, analyzing the changes in the metabolome of mutants will contribute to enhanced knowledge. The metabolome is farther way from gene expression and thus more closely reflects cell activity on a functional level, comprising the potential to map the function of unknown genes and to characterize the phenotype (Garcia et al., 2008, Plassmeier et al., 2007).
Below a short introduction into the "omics"-technologies is presented, with a special focus on metabolomics and its potential in functional genomics. The organisms on which the research is based are introduced afterwards.

1.1 Systems biology

Only a few years ago each cellular and biochemical component (genes, proteins or metabolites) was studied as a single subject (De Keersmaecker et al., 2006). Now in the field of systems biology the so called "omics"-technologies (genomics, transcriptomics, proteomics and metabolomics) have been combined, with the intention to provide explanations of biologic phenomena by using information from all components (e.g. DNA, RNA, proteins, metabolites) within a cell or an organism (Liu, 2005). Main objectives are the understanding of the structure and the dynamic of the system (Kitano, 2002).

1.1.1 Genomics

The genome is the entirety of all genes present in an organism. In the field of genomics intensive research is going on to identify the whole DNA sequence of a microorganism. Bioinformatics tools are used for the prediction of genes and operons. Databases are

searched to identify homologous proteins and functions for the predicted genes. Whole genome sequences are completed by annotation (Wendisch et al., 2006). In contrast to all other “omics”-technologies, genomics is the one dealing with the stable genome, defining the phenotype of an organism.

1.1.2 Transcriptomics

The messenger RNAs represent the transcriptome of a microorganism which is studied in transcriptomics. All mRNAs as well as their relative abundance inside a cell at a given time and under a defined set of conditions are investigated in the transcriptomics approach. The high-throughput technology of microarrays is mostly used for investigation, where the expression of the genes is monitored (Schena et al., 1995). Analyses are made with gene chips. Models of transcriptional regulatory and metabolic networks are generated to predict the results of phenotyping and gene expression experiments. Furthermore, these models are used to identify gaps and unknown components as well as interactions in such networks (Covert et al., 2004).

1.1.3 Proteomics

The proteome of a cell or organism comprises all existing proteins at a specific time as well as under defined conditions - and it is the subject of investigation in proteomics. In contrast to the genome, which is static, the proteome is highly dynamic what means it responds on environmental changes or exposure of agents and its composition underlies permanent adaptation in a qualitative and quantitative manner; new proteins become synthesized and others degraded.

Proteomics can lead to information about biological mechanisms much faster than the single-protein approach (Abbott, 1999).

Proteins are composed of 20 different amino acids, leading to highly diverse physicochemical properties. Furthermore, they fulfill different and very important functions: proteins are, for example, catalysts of metabolism and regulators of processes

(Wendisch et al, 2006).

Today, the protein composition of a cell is normally analyzed with one of the two following techniques: two-dimensional polyacrylamid gel electrophoresis (2D-PAGE) and mass spectometry (MALDI-TOF, ESI-MS/MS) (O'Farrell, 1975, Wendisch et al, 2006). Whereas 2D-PAGE is commonly applied for protein expression studies, MS is suitable for identification and quantification of translated proteins. Another method, the so called multidimensional protein identification technology (MudPIT), is based on liquid chromatography/mass spectrometry (LC/MS). The advantage of this approach is the possibility to analyze complex protein mixtures (e.g. whole cell lysates) without prior separation (Weckwerth, 2008).

All the procedures mentioned can be used for comparison of protein compositions. The decision depends on the certain set of conditions available.

1.1.4 Metabolomics

The metabolome comprises all metabolites present in the cell at a defined time and under controlled conditions. It is investigated in metabolomics studies. Like the transcriptome and the proteome the metabolome responds on changes in the genome or in the environment, and therefore it is not static. Consequently, a comprehensive analysis of the metabolome allows a highly sensible phenotype characterization.

The analysis of the metabolome belongs to the subject area of this thesis, and it is therefore described in more detail below (section 1.2).

1.2 Metabolomics in functional genomics

After decades of intensive but mostly independent research in the above described fields the focus started to shift towards functional genomics, to a post-genomic era. The aim is the analysis of genes and their products on a more functional level. For the study of complex biological systems the mentioned procedures and techniques are used complementary and in combination. The goal is to correlate the vast amount of data and

knowledge available in order to obtain a better understanding of regulatory mechanisms.
With the great progress in sequencing of organisms, for over 750 microorganisms a complete or nearly complete genome sequence is now available (NCBI). And currently, the identification of gene functions is in main focus. Therefore, multi-parallel analyses of transcriptomics and proteomics are often applied (Celis et al., 2000, Somerville et al., 1999). However, a direct connection of changes in mRNA and protein levels and a change in biological function can not often be revealed. In contrast, metabolome analysis offers the possibility for a direct correlation between a gene sequence and the function of the metabolic network (Fiehn et al., 2000, Weckwerth, 2003, Kell, 2004, Villas-Bôas et al., 2005). The creation of *in silico* models becomes possible (Sweetlove et al., 2003, Kell, 2006).

1.2.1 Methods in metabolome analysis

Methods in metabolome analysis have to meet certain requirements in order to be valuable in the field of functional genomics (Fiehn et al., 2000, Weckwerth, 2003). They have to be:

- reliable
- reproducible
- robust
- sensitive
- fast
- suitable for automation
- suitable for analysis of a significant number of metabolites.

Different approaches for metabolome analysis exist. The untargeted identification and quantification of all metabolites present in a biological sample under defined conditions is the overall goal. However, due to the high diversity of chemical properties as well as the different behavior of the individual compound classes most applications use the targeted approach instead (Weckwerth, 2003).
So far, no single method exists which covers all metabolites within a cell in one measurement. Differences are not only caused by varieties in chemical nature of the

substances but also due to the range of metabolite concentrations. It can vary over nine orders of magnitude (pM-mM) in a cell (Dunn et al., 2005). In addition, metabolome analysis in the field of plants (Fiehn et al., 2000a and Fiehn, 2002, Roessner et al., 2000 and 2001) and microorganisms (Fox, 1999, Buchholz et al., 2001, Raamsdonk et al., 2001, Strelkov et al., 2004, Ishii et al., 2005) is a still growing area of research. So far no complete network of all metabolites for a single organism exists. Additionally bioinformatics approaches are used. Databases of biological data are searched (e.g. BRENDA (Schomburg et al., 2002)). Organism specific information is investigated in order to gain a new understanding of the metabolic network of a defined organism. The Pathway Hunter Tool is only one example for application (Rahman et al., 2005).

The most applicable methods for metabolome analysis are NMR spectroscopy (Raamsdonk et al., 2001) and mass spectrometry (MS) or tandem mass spectrometry (MS/MS) (Feng et al., 2008). They are suitable for detection of metabolites in complex matrices. The MS is used mostly coupled to gas chromatography (GC) (Fox, 1999, Fiehn et al., 2000a, Roessner et al., 2000, Strelkov et al., 2004, Börner et al., 2007) or GC-GC (Dunn, 2008), liquid chromatography (LC) (Buchholz et al., 2001 and 2002) or capillary electrophoresis (CE) (Soga et al., 2002 and 2003, Edwards et al., 2006). Figure 1 shows the different ways of mass spectrometric methods in metabolome analysis. The GC/MS approach is described in detail afterwards.

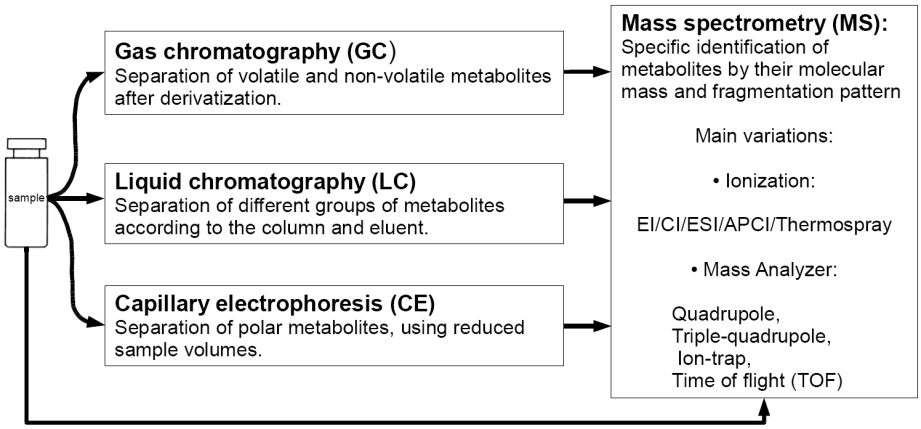

Figure 1. Possible ways of mass spectrometry analysis in metabolomics. The sample can either be directly analyzed or after separation (Villas-Bôas et al., 2005, modified).

Gas chromatography/mass spectrometry (GC/MS)

Gas chromatography coupled to mass spectrometry is a highly efficient approach in metabolome analyses in order to separate samples. It is suitable to resolve very complex biological compositions (Villas-Bôas et al., 2005). Applying GC/MS allows a fast analysis of volatile polar and lipophilic metabolites of low molecular mass to be performed in short time. The separation is caused by volatility, size and structure. Consequently, it is not suitable for organic diphosphates, cofactors, or metabolites larger than tri- to tetrasaccharides (Weckwerth, 2003). For analyzing such big and non volatile substances necessarily LC/MS has to be used. Small but non volatile compounds can be made available for GC/MS by derivatization (see section 1.2.2).

The complete assembly required for GC/MS analysis is shown in figure 2, and consists of three main parts: injector, gas chromatograph with a selected column that is suitable for the separation requirements of the sample, and detector, which is the mass spectrometer.

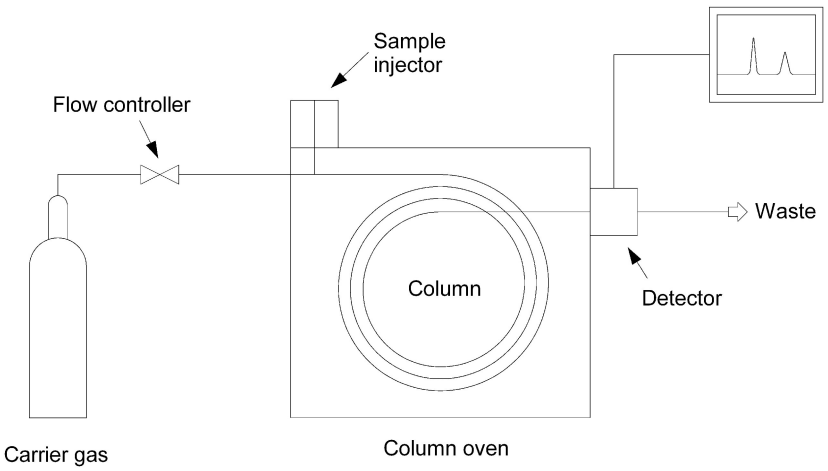

Figure 2. Assembly for a GC/MS analysis.

For analysis of cell extracts a *programmed temperature vaporizer* (PTV)-injector was used. The sample is indirectly injected onto the column. That means the sample is given into an evaporation chamber first and is transferred partly (split) or completely (splitless) onto the column afterwards. In figure 3 the scheme of a PTV-injector is shown.

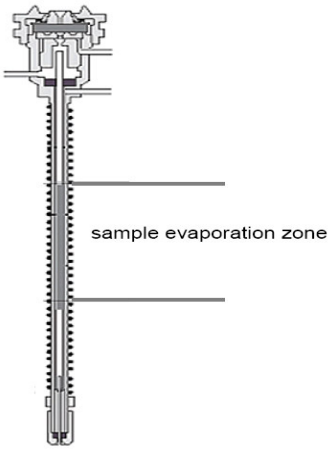

Figure 3. Scheme of a PTV-injector. The sample is indirectly transferred to the column.

In traditional techniques the sample is directly transferred to the column and vaporized at the same moment. In contrast, with PTV the sample is injected into a vaporizer chamber with a temperature below the boiling point. A temperature profile is applied afterwards to increase the temperature of the chamber very fast and to transfer the vaporized sample onto the column.

During gas chromatographic separation the analyte (sample extract) is carried with the mobile phase (carrier gas) over the stationary phase on the column. The eluting substances are detected and visualized as chromatographic peaks according to their retention time at the outlet. For the separation of sample extracts special columns are available. For the research underlying this thesis a DB-5MS column was used. It is a fused silica capillary with a coating of polyimide to increase flexibility and protect from chemical and mechanical influences. Inside there is a liquid, highly viscous polysiloxan (5 %-Phenyl)-dimethylpolysiloxan) (figure 4). The used column was 30 m in length, with an inner diameter of 0.25 mm, and the thickness of the stationary film was 0.25 µm.

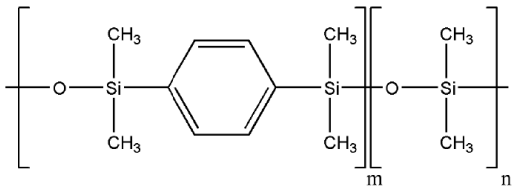

Figure 4. Chemical structure of Poly(dimethylsiloxy)poly(1,4-bis(dimethyl-siloxy)phenyl). In the used polymer, m has a value of 5%, n a value of 95%.

With such a DB-5MS column Strelkov et al. could demonstrate good results for analysis of cell extracts of *Corynebacterium glutamicum*. Around 1000 peaks were identified in the chromatograms (Strelkov et al., 2004). However, it is necessary to be very precise and careful choosing stationary phase and thickness and pay special attention to polarity and volatility of the compounds to be separated (Grob et al., 1993).

The mobile phase in such an approach is an inert gas. It must not interact with analyte or stationary phase. Therefore, helium, nitrogen or hydrogen are often used. Also very important issues are the flow properties of the carrier and the fact that it is not to viscous at high temperatures.

A chromatographic separation is caused by the retention. The retention time is specific for each substance. Compounds are transported over the separation distance by the mobile phase. During transport a substance can interact with the stationary phase and therefore stick to it. The retention behavior depends on the distribution coefficient K_D (equation 1.1). K_D is the ratio of the analyte concentration in liquid and gas phase. It depends on the analyte, the liquid phase and the temperature. The time needed from the moment of injection till the maximum of intensity of the eluting peak is the gross retention time t_R, which describes the overall time of a substance on the column.

$$K_D = \frac{concentration\ per\ volume\ unit\ liquid\ \ phase}{concentration\ per\ volume\ unit\ gas\ phase} \tag{1.1}$$

The efficiency of a separation is defined by the peak enlarging (e.g. by diffusion) and the relation of the retention times. The number of effective theoretical plates N_{eff} describes this efficiency (equation 1.2), with H_{eff} giving the height of effective theoretical plates and L giving the length of the column in mm. If the column is quite long, the number of effective theoretical plates is high. The smaller the diameter of the column, the less the height of effective theoretical plates. Efficiency of separation is increased with decreasing H_{eff} and increasing N_{eff}.

$$N_{eff} = \frac{L}{H_{eff}} = 5.54\left(\frac{t_S}{b_{0.5}}\right)^2 \tag{1.2}$$

The number of effective theoretical plates can also be calculated using the net retention time t_S and the width of the peak in half of its height $b_{0.5}$ (see equation 1.2).
The net retention time is calculated from the gross retention time t_R diminished by the dead time t_T (equation 1.3). The dead time is the time needed by the carrier gas to get through the column.

$$t_S = t_R - t_T \tag{1.3}$$

In order to estimate the optimal height of effective theoretical plates the Van-Deemter-estimation can be used (equation 1.4). It describes the connection between H_{eff}, the diffusion A, which displays the influence of the packing of the column on the width of the peak. However, because of the used capillary this term has to be neglected. Furthermore, the longitudinal diffusion B represents the diffusion of substances on their way through the column. Term C is the rate for reaching the equilibrium and u is the velocity of the carrier gas.

$$H_{eff} = A + \frac{B}{u} + Cu \tag{1.4}$$

The separation in gas chromatography is done in different dimensions. A vaporized mixture is introduced with the carrier into the temperature-regulated capillary. With increasing temperature of the column the equilibrium of the aggregate state of a substance is moved from the stationary phase to the mobile phase. Because of the applied temperature gradient, where the temperature is constantly increased, components with a low boiling point vaporize first and are carried over the column by the mobile phase. Substances with higher boiling points volatilize at a later moment. Therefore, the separation is due to the substance specific affinity to the stationary phase, but also according to the vapor pressure.
To perform a quantitative analysis with a GC/MS a calibration is necessary. A mixture of eight uniformly distributed alkanes was used. Because of their chemical nature alkanes are highly volatile and thus do not have to be derivatitized before measurement. Each alkane has a defined retention index (RI). The number of carbon atoms multiplied by 100 is equivalent to RI. When a substance is identified it is also given a retention index which is

calculated using the Kovàts' equation (see equation 1.5) and related to the RI values of the alkanes (Kovàts, 1956). The calculation according to equation 1.5 is suitable for compounds separated with the help of a temperature gradient. The advantage of applying retention indices rather than using the retention times is the possible compensation of shiftings in retention times. Such kinds of offsets might occur after routinely maintenance performances. Another advantage of using the retention index is the high reproducibility, and moreover the index only depends on dimensions of the column, liquid phase and temperature.

$$RI^{(T)} = 100[(y-x)\frac{t_i - t_x}{t_y - t_x} + x] \qquad (1.5)$$

containing:

	RI	retention index
	T	temperature
	x	number of carbon atoms in the alkane eluting before elution of the unknown substance
	y	number of carbon atoms in the alkane eluting after elution of the unknown substance
	t_i	retention time of the unknown substance
	t_x	retention time of the alkane eluting before the elution of the unknown substance
	t_y	retention time of the alkane eluting after the elution of the unknown substance

The intersection between gas chromatograph and mass spectrometer is a special interface. It permits the transfer of the analyte from atmospheric pressure to high vacuum (10^{-4} Pa). The ionization caused by electron impact as well as the mass separation are only possible at pressures below 10^{-2} Pa (Hübschmann, 2001).

The ionization process takes place in the EI (electron ionization) source. The assembly of such an EI source is shown in figure 5. Electrons are emitted from a filament into the electric field with a potential difference of 70 eV. Furthermore, the electrons are accelerated and hit the molecules of the sample which enter the ion volume.

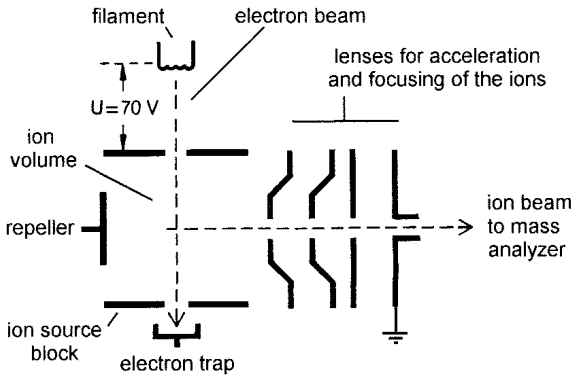

Figure 5. Schematic layout of an electron impact source (EI) (Gross, 2004)

The voltage is high enough to produce a high-energy radical cation. But due to the overrun of energy the cation resolves into smaller, charged and characteristic mass fragments (reaction 1.6).

$$AB \xrightarrow{e^-} AB^{+\circ} \longrightarrow A^+ + B^\circ \qquad (1.6)$$

The energy for ionization of 70 eV is chosen, because the yield of ions is high and stable even if the voltage varies slightly. Afterwards, the ionized fragments are continuously pushed by the repeller (see figure 5).

Ions generated in the ion source are focused to form an almost parallel ion beam and are introduced into the analyzer (in this case an *AccuTOF* machine was used). In the ion acceleration unit, the so called launcher (figure 6), they are brought to the pusher plate. The applied pulse voltages (7 kV) to the pusher plate and a stack of multiple electrodes with different voltage cause a change of the direction of the ions. They are pushed orthogonally into the flight tube. At the beginning ions are constantly accelerated but when they reach the flight tube they are in free flight with constant velocity. The ions fly at a speed depending on their mass because all of them got the same kinetic energy. The separation of the ions is according to their mass to charge ratio (m/z) (Gross, 2004, Jeol Instructions).

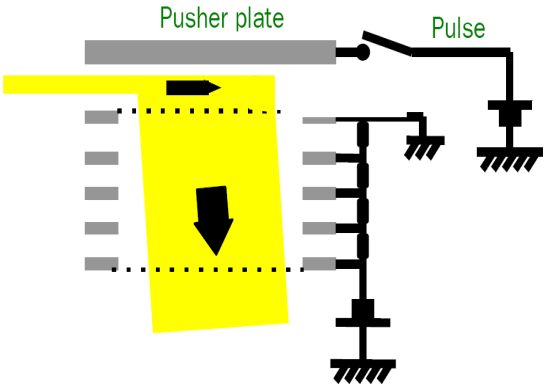

Figure 6. The Jeol *AccuTOF* launcher (Jeol Instructions, modified).

After acceleration with a defined voltage U all ions have the same kinetic energy E_{kin} which can be calculated using equation 1.7 (Gross, 2004).

$$E_{kin} = \frac{1}{2} m v^2 = zeU \qquad (1.7)$$

containing:

	m	mass of the ion
	v	velocity of the ion after acceleration
	z	ion charge
	e	unit charge
	U	acceleration voltage

The velocity of an ion after acceleration v can be calculated from the length of the flight tube l and the time t needed till ion reaches the detector (see equation 1.8) (Gross, 2004).

$$v = \frac{l}{t} \qquad (1.8)$$

The combination of both equations 1.7 and 1.8 leads to the flight time t as function of the mass (see equation 1.9). Furthermore, the mass to charge ratio is proportional to the square of the flight time (Gross, 2004, Jeol Instructions).

$$\frac{m}{z} = \frac{2eU}{l^2} t^2 \qquad (1.9)$$

The conversion of flight time into the depending mass to charge ratio is done by a special hardware called *fast flight*.

Time of flight spectrometer have the advantage of high mass resolution. The used Jeol *AccuTOF* provides an accuracy of four decimal places. The ion kinetic energy in the beam after the ion source is only slightly varying in a range of 10...100 eV. Consequently, even ions with identical mass are differing slightly in their velocity. This affects the width of the peaks. A compensation of these energy differences can be done with a reflector composed of several reflector lenses (see figure 7). Focusing is achieved, because ions with higher kinetic energy submerge deeper into the area of the reflector than those of same mass but lower energy. Thereby, all ions with the same mass can reach the detector almost at the same time resulting in an increased peak sharpness.

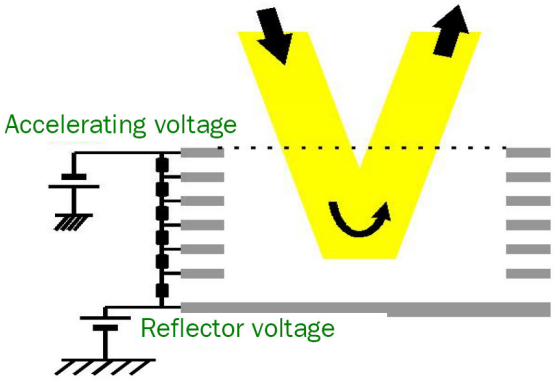

Figure 7. The scheme of the reflector of the Jeol *AccuTOF* (Jeol Instructions).

The detector of the *AccuTOF* consists of micro channel plate (MCP) detector, impedance converter, and preamplifier. The MCP detector is a unit comprising the secondary electron multiplier (dynode, MCP) and the electrode anode which detects the electrons (see figure 8).

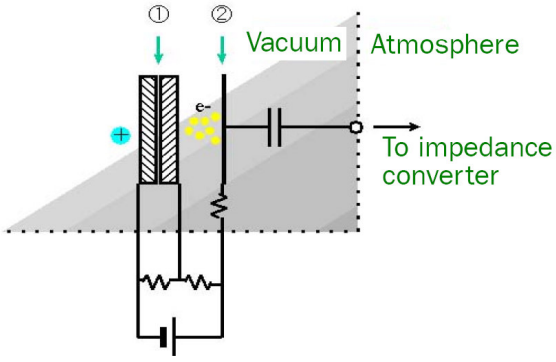

Figure 8. The operational principle of the MCP detector of the Jeol *AccuTOF* (Jeol Instructions). **1** is the MCP and **2** is the anode.

Arriving ions collide with the inside wall of a micro channel on surface of the MCP and generate secondary electrons. Because of the strong electric field applied to the MCP the generated electrons are accelerated and collide again with the micro channels. Due to the repetition of acceleration and collision the number of secondary ions increases. Afterwards, these ions pass the MCP and collide with the anode. The anode sends the current pulse signals to the impedance converter. The introduced electrical signal is converted into a voltage, the measurement variable which is sent to the preamplifier. Signals are amplified and transmitted to the *fast flight* (a continuous averager) afterwards. The amplification factor is a constant value of 5. Data acquisition protocol of the system applies the ADC (analog to digital conversion) method. Reconstruction of the intensities of all signals is done from the TIC (total ion current). Applying these technique allows the detection even of low ion currents.

Advantages of using GC/MS for metabolome analysis are a high reproducibility of measurement and a precise identification by deconvolution of overlapping chromatographic peaks (Villas-Bôas et al., 2005). This can be done for example with an automated mass spectral deconvolution and identification system (AMDIS) (Stein et al., 1999). Furthermore, data resulting from GC/MS not only provide the required quality but also allow quantification when applying compound specific calibration curves. Spectra (from 70 eV standard ionization energy) can be collected in databases, for example NIST (National Institute of Standards and Technology), and are available for identification of substances (Schauer et al., 2005).

1.2.2 Pre-analytical sample preparation for metabolome analysis with Gas Chromatography/Mass Spectrometry

An important prerequisite for representative and reliable metabolome analysis is a strict protocol. In microbial metabolomics the sample size is quite small, and only low amounts of metabolites (3 to 5% cell dry weight) are present within a cell (Neidhardt et al., 1996, Wendisch et al, 2006). Also important is to work with replicates, because biological and analytical variations have to be incorporated and assessed. Generally, differences between samples of the same biological origin (biological variance) can be expected as significantly greater than those from multiple analyses of the same sample (analytical variance) (Dunn et al., 2005).

Quenching of microorganisms

The sampling stage has to be fast and reproducible. Additionally, it is very important that the inherent enzymatic activity is stopped rapidly. Otherwise the metabolome would continuously change during sample preparation, leading to a metabolic profile not representative for the moment of harvesting. Therefore methods like immediate freezing in liquid nitrogen (Buziol et al., 2002, Mashego et al., 2003) or acidic treatments using nitric or perchloric acid (Larsson et al., 1996, Weuster-Botz, 1997) as well as alkali treatments are used. The most important problem of acidic treatments are difficulties that arise in the analytical methods following afterwards (Fiehn, 2002).

The basic requirement for a reliable quenching method is that no cell leakage should occur or if leakage occurs, the leaked metabolites should be quantifiable (Mashego et al., 2007). The currently most common method is quenching with cold methanol solution (de Koning et al., 1992, Schäfer et al., 1999, Jensen et al., 1999, Moritz et al., 2000, Villas-Bôas et al., 2005a, Loret et al., 2007). This protocol was first developed for yeast by de Koning (de Koning et al, 1992). Until today this method had been tested for many different microorganisms, generally resulting in different behavior of prokaryotes and eukaryotes. Prokaryotic cells tend to leak intracellular metabolites. This observation is now well known as “cold-shock” and was first described for *Corynebacterium glutamicum* by Wittmann (Wittmann et al., 2004), but similar results were obtained for *Escherichia coli* (Winder et al., 2008). Additionally, even for yeast the results are controvers. Whereas in some studies

cell leakage was detected (Maharjan et al., 2003, Villas-Bôas et al., 2005a) others could not approve this (Loret et al., 2007).

However, due to extensive research on this field a variety of methods exist. But so far none of them achieved satisfying results for different microorganisms. Published methods are, for example: quenching with boiling absolute ethanol (90°C) (Winder et al., 2008), cold pure methanol (Hans et al., 2001, Castrillo et al., 2003, Dunn et al, 2005, Canelas et al., 2008) or the use of a cold glycerol saline solution (Villas-Bôas et al., 2007).

Also, fast filtration often is applied to separate supernatant and cells. But sampling time in this approach takes several seconds. Therefore it is only suitable for metabolites with high intracellular levels and low turnover. Another method used nowadays is whole broth quenching. In this method cells and supernatant are not separated but prepared together (Canelas et al., 2008). The huge problem regarding this technique is the differentiation between intra- and extracellular metabolites. Additionally, the assumption that metabolites of central pathways are exclusively present inside the cells is not true and will lead to large errors (Bolten et al., 2007).

Extraction of metabolites

Whereas the analysis of the exometabolome (excreted metabolites into the growth medium) does not need any additionally extraction, this step is necessary for analysis of the endometabolome (metabolites inside the cells). The aim is to extract the maximum number of metabolites from different chemical classes in a quantitative way and minimize any loss (Dunn et al., 2005). When working with microorganisms it is necessary to disrupt the cell wall (lysation) to release internal metabolites.

A big difficulty is the extraction of phosphorylated compounds. Reasons are cleavage of phosphate groups in highly aqueous environments, interactions with phospholipids in the cell, and hydrolysis of triphosphates (Garcia et al., 2008).

Mostly organic solvents like methanol and ethanol, pure or diluted in water are used for metabolite extraction (Gonzalez et al., 1997, Fiehn et al., 2002). Performances with perchloric acid (Buchholz, et al., 2002) or potassium hydroxide also exist (Maharjan et al., 2003, Mashego et al., 2007). Furthermore, an additional step is performed adding a non-polar solvent (e.g. chloroform) to extract lipophilic components. Often efficiency is enhanced by applying additional energy (e.g. heat, sonication, microwave techniques)

(Fiehn et al., 2002). A comparison of different methods is mostly done for a defined organism only (e.g. Winder et al., 2008, Villas-Bôas et al., 2002).

Derivatization of compounds

In order to analyze semi- and non-volatile metabolites with gas chromatography coupled to mass spectrometry, substances have to be derivatized to improve volatility and thermal stability. A properly working reaction is the prerequisite but not always easy to achieve. Sterical hindrance can lead to mixtures of fully and partially derivatized analytes (Halket et al., 2005). Furthermore, a derivatization method has to be simple, efficient and fast (Villas-Bôas et al., 2005).

The cell extract of a microorganism contains several sugars. These sugars have different isomers. If each isomer is derivatized this will increase the complexity of the chromatogram dramatically. To reduce the complexity a reaction of sugar, precisely the carbonyl group, with methoxyamin is often performed as first step in derivatization protocol (see figure 9). With this oximation the open-chain form is stabilized (Adams et al., 1999). Oximation is done with aldehyd and keto groups (Halket et al., 2005).

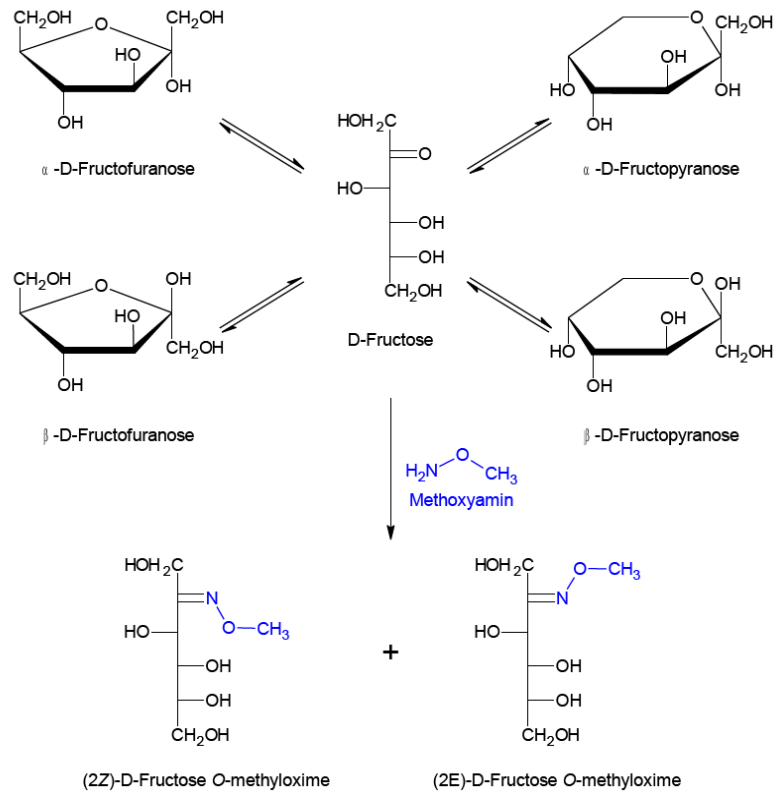

Figure 9. Reactions of D-fructose with methoxyamin (Thielen, 2007)

Often a silylation reaction with MSTFA (N-methyl-N-trimethylsilyltrifluoroacetamid), BSA (N,O-bis(trimethylsilyl)acetamid) or BSTFA (N,O-bis(trimethylsilyl)trifuoracetamid) is performed. This reaction takes place in pyridine under anhydrous conditions and heating. During silylation a silyl group is introduced into the molecule through substitution of active hydrogen. This hydrogen was part of a hydroxyl, thiol, amino or carboxylic acid group. An alkyl-silyl group (e.g. trimethylsilyl (TMS)) is introduced instead (Villas-Bôas et al., 2005) (see example for glycine, figure 10). The most important metabolites derivatized by silylation are sugars and sugar derivatives, e.g. sugar alcohols, phosphorylated sugars and amino sugars. The advantage of silylation is its efficiency and the production of stable derivatives as well as its high reproducibility. A critical fact is the performance under anhydrous conditions which requires the complete removal of water.

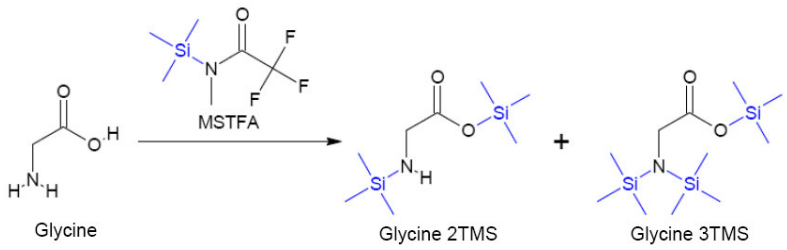

Figure 10. Trimethylsilylation of glycine (Thielen, 2007, modified)

Besides silylation alkylation or esterification are also derivatization techniques. With the use of chloroformate derivatives, polyfunctional amines and organic acids are derivatized. The reaction can be done in aqueous solutions at room temperature. Alkylation can also be performed using diazomethane. The disadvantage of this method is the smaller applicability (Villas-Bôas et al., 2003).

Another problem that might occur besides the formation of byproducts is the possible conversion of analytes. For example arginine can be converted to ornithine or the final product can degrade, e.g. the hydrolysis of trimethylsilyl derivatives (Garcia et al., 2008).

Some samples show ongoing reactions or even instabilities during longer time periods. Consequently, differences in the time needed from the end of derivatization till measurement are problematic for samples of a set. Therefore, “just-in-time” sample preparation is advantageous (Dunn, 2008).

1.2.3 High-throughput performances in metabolome analysis

So far, the understanding of high-throughput in metabolome analysis is always limited to a certain part of the performance. There was no complete high-throughput method available before this work. Nevertheless, small-scale cultivations of microorganisms could be found in literature (e.g. Zimmermann et al., 2003, Kumar et al., 2004, Duetz et al., 2000 and 2004) but only few examples for the use in metabolome analysis (e.g. Wittmann et al., 2004a). The problem is the limited cell mass after cultivation in micro titer plates. Furthermore, good aeration and agitation has to be assured to obtain equal growth in all wells and no well specific limitations.

High-throughput in metabolome studies is mostly regarded to the high amount of produced samples. Also often designated as high-throughput is the measurement performance itself and the high number of revealed metabolites.

1.2.4 Transposon mutagenesis and the construction of a mutant bank

Besides the traditional methods of random or targeted mutagenesis followed by screening for the development and identification of mutants with desired properties another technique rose attention. Transposon mutagenesis is now a well established approach (Grindley et al., 1985, Vertès et al., 1994, Hamer et al., 2001) for the generation of large mutant banks (Mormann et al., 2006, Suzuki et al., 2006). Especially since the first complete genome sequences were available, transposon mutagenesis became an advantageous tool for functional genome analysis (Hayes, 2003). The principle of this type of mutagenesis is based on the random integration of a mobile transposon element. A loss of gene function can be caused, but only in cases where a gene itself or its control sequence is affected. If - statistically seen - enough mutants are produced (depending on the number of genes annotated for the organism), every open reading frame can be effected by a gene knock-out (Ross-Macdonald et al., 1999).

For this study a transposon mutant bank of *Corynebacterium glutamicum* was used. This mutant bank was developed using the IS*6100* transposon element of the plasmid pAT6100 (figure 11). Insertion sequences are the simplest transposable elements. They only consist

of a gene for transposition which is bounded by inverted repeat sequences (Hayes, 2003). The element IS*6100* belongs to the IS6 family which is exclusively integrated by a cointegrative mechanism forming two directly repeated IS copies. It was naturally found in the chromosome of *Mycobacterium fortuitum* and is 880 bp in length (Mahillo et al., 1998). It could be demonstrated that this insertion sequence is able to randomly integrate into the genome of different organisms, e.g. *Corynebacterium glutamicum*. For the development of the transposon mutant bank for *C. glutamicum* the restriction deficient mutant res$^-$ 167 of the wild type strain ATCC 13032 was used. So, enzymatic cleavage during conjugation could be avoided (Tauch et al., 2002).

The plasmid pAT6100 (see figure 11) was generated by cloning a copy of IS*6100* into the vector pK18*mob2*. With a size of 4,516 bp it consists of the mobilizable (RP4*mob*) cloning vector pK18*mob2*, a kanamycin resistance marker (Kan^R), an origin of replication in *Escherichia coli* (ori), the IS*6100* element as well as several restriction sites for transposases. The kanamycin resistance can be used for selection.

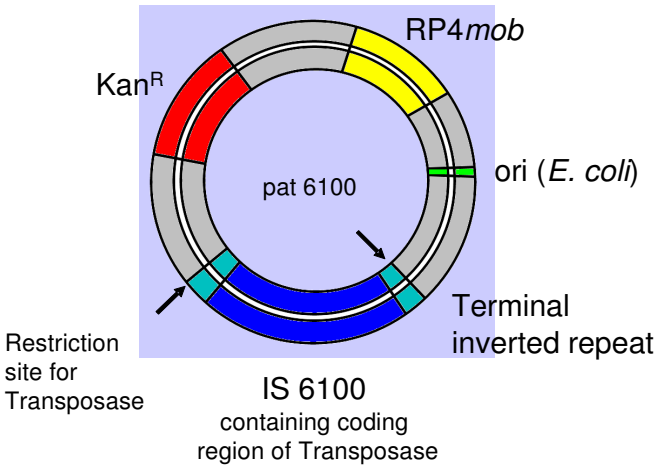

Figure 11. Plasmid pAT6100 used for transposon mutagenesis, and containing the mobilizable (RP4*mob*) cloning vector, the IS*6100* transposon element as well as an origin for replication in *E. coli* (ori), a kanamycin resistance marker (Kan^R) and several restriction sites for transposases (Tauch et al., 2002, modified).

Transposon mutants were generated by conjugation of *Corynebacterium glutamicum* and *Escherichia coli S17-1* (donor). The plasmid was transferred to *C. glutamicum* by RP4-mediated high frequency conjugation (Schäfer et al., 1990 and 1994). pAT6100 is unable to replicate in its new host, due to a missing origin of replication in this organism. A

kanamycin resistant phenotype of *C. glutamicum* is only possible when transposition of the vector into the chromosome took place (Tauch et al., 2002).

For identification of insertion sites the *plasmid rescue* technique can be used (Tauch et al., 1995). Knowledge about the affected gene is necessary to establish a connection between the loss of a gene function and changes in the phenotype (Bailey et al., 2002). Furthermore, it enables the identification of novel gene functions.

The genomic DNA is cleaved by restriction enzymes (e.g. *Eco*RI, *Xba*I). The cleavage sites are on the inserted plasmid and in the genome. For example, a cleavage site for *Eco*RI in the genome of *C. glutamicum* can be statistically found every 4^6 bases. The resulting DNA fragment contains the part of the plasmid with the kanamycin resistance marker and the replication of origin for *E. coli* as well as the part of the genomic DNA which was located next to the plasmid. This fragment can be ligated using the cleavage sites and augmented in *E. coli*. Afterwards, cells containing the circular plasmid can be selected via kanamycin resistance. Sequencing of the plasmid and a search in the genome sequence of *C. glutamicum* leads to the identification of the affected gene.

1.3 Model organisms

For this comprehensive study in the field of metabolomics three different microorganisms were used. However, main focus was put on the Gram-positive prokaryote *Corynebacterium glutamicum*. This bacterium was the model organism in the high-throughput and the quenching studies. Furthermore, for a comprehensive analysis of quenching of microorganisms the Gram-negative prokaryote *Escherichia coli* and the eukaryote *Saccharomyces cerevisiae* were investigated as well.

1.3.1 Corynebacterium glutamicum

Corynebacterium glutamicum is a Gram-positive, fast growing, aerobic soil bacterium. It belongs to the Actinomycetales (Liebl, 2005). The bacterium has a clubbed morphology (*coryne*, Greek for club). Furthermore, it forms irregular, non sporulating rods (figure 12).

Cells have a width between 0.7 µm and 1.0 µm and a length of 1.0 µm to 3.0 µm. *C. glutamicum* is non pathogen but related to several pathogen organisms (e.g. *Corynebacterium diphtheriae, Mycobacterium tuberculosis, Mycobacterium leprae*).

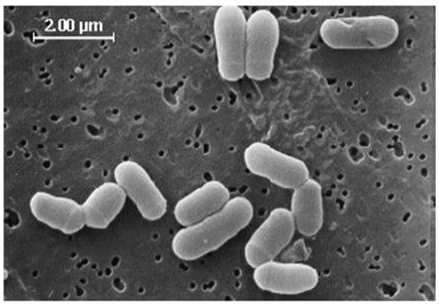

Figure 12. *Corynebacterium glutamicum*, cells viewed by scanning electron microscopy (Liebl, 2005)

C. glutamicum was first detected in the year 1956 by a Japanese working group during a research program aiming to obtain glutamic acid producing microorganisms (Abe et al., 1967, Kinoshita, 2005). Because of its capability to produce amino acids, vitamins and nucleotides, its industrial relevance became more and more important. The amino acids L-glutamic acid (flavor enhancer) and L-lysine (feed additive) are the substances with the highest production yields from fermentations with *C. glutamicum* (Eggeling et al., 2001, Glazer et al., 2007).

In the year 2002, a strategy for genome sequencing of *C. glutamicum* ATCC 13032 was published (Tauch et al., 2002a). One year later, two independent groups completely sequenced the genome of the wild type strain ATCC 13032 (Kalinowski et al., 2003, Ikeda et al., 2003). Both revealed a total genome size of approximately 3.3 Mb (see figure 13) with around 3000 protein coding genes as well as a high G+C content of 53.8%. Therewith they could correct the size which was published some years before by Bathe et al. (Bathe et al., 1996). For about 83% of the genes a function could be assigned, mostly from homology studies to known proteins. Nevertheless, some of the functions can only be assumed rather than definitely proved. For 8% of the genes similarities to conserved hypothetical proteins in other organisms could be found (Kalinowski et al., 2003).

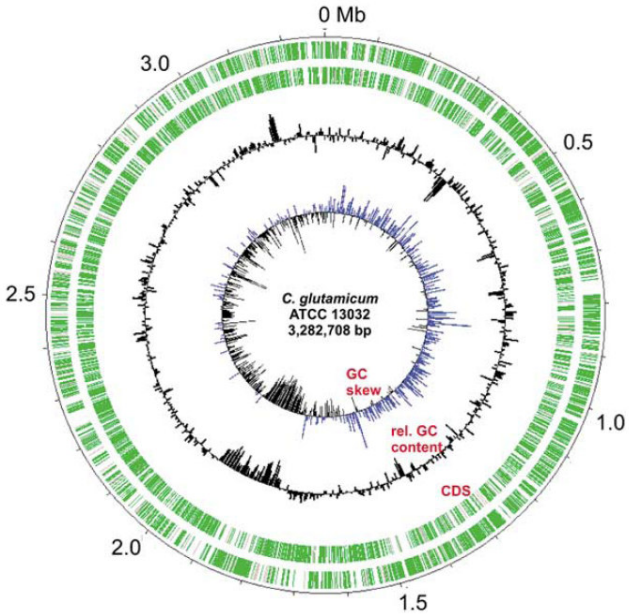

Figure 13. Chromosome of the *Corynebacterium glutamicum* wild type strain ATCC 13032 (Kalinowski et al., 2003)

1.3.2 Escherichia coli

Escherichia coli is a motile, facultative anaerobe and non sporulating Gram-negative bacterium. It's a rod-like organism with peritrichous flagella (figure 14). With a size of 0.5 µm x 1.5 µm it is a rather small microbe. *E. coli* is a γ-Proteobacteria from the Enterobacteriaceae family. As non pathogen organism its native habitat is the intestinal tract of humans and animals. Nevertheless, some strains can cause diarrhea because of their enterotoxins.

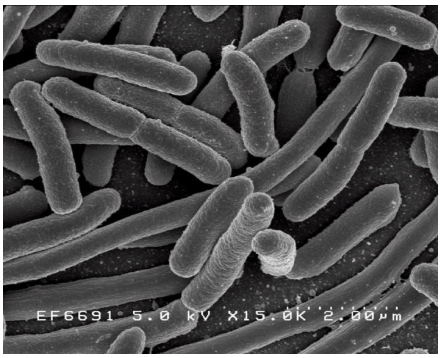

Figure 14. *Escherichia coli* (http://www3.niaid.nih.gov/.../e_coli.jpg)

E. coli is able to grow chemo-organotroph. Consequently, it can produce energy through respiration but also by mixed acid fermentation. During this fermentation process significant amounts of formic acid, acetic acid, lactic acid as well as succinic acid are formed as byproducts.

Furthermore, *E. coli* is the standard model organism in microbiological research. This is because of its genetic accessibility, the short generation interval (20 minutes when cultivated aerobically on complex medium) as well as its ability to grow on minimal medium. It is industrially used especially for the production of recombinant insulin (Goeddel, et al. 1979) and recombinant proteins (e.g. Derynck, et al. 1980) as well as amino acids (Ikeda, 2003a).

1.3.3 Saccharomyces cerevisiae

The eukaryote *Saccharomyces cerevisiae* belongs to the class of the Ascomyceta. Cells are round or oval with a size between 5 µm and 10 µm (see figure 15). It is an intensively used microorganism and important for the economy. This is among other things due to its bi-phaseal metabolism. If it is grown on carbon sources, *S. cerevisiae* produces large amounts of ethanol. When this source is consumed the eukaryote can use the produced ethanol for farther growing (Dickinson et al., 1999).

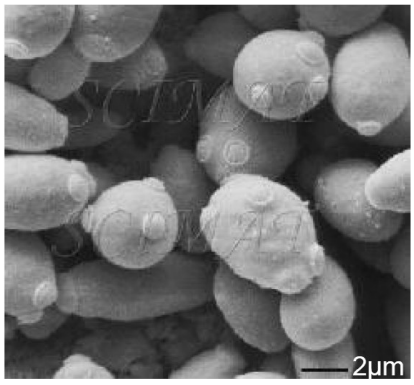

Figure 15. *Saccharomyces cerevisiae* (http://www.magma.ca/.../ Yeast-2m.jpg, modified)

Furthermore, *S. cerevisiae* is a well established model organism for research. In the year 1996, Goffeau et al. published the first complete sequence of a yeast strain (Goffeau et al.,

1996). The yeast has 16 chromosomes with approximately 6200 genes. It can exist in stable form in the diploid as well as in the haploid state. Today research is focused on gene annotation and the identification of the functions to achieve a complete understanding of the metabolic network.

Due to its robustness and its advantageous in genetic manipulation performances yeast is an often used model organism. For example, a lot of studies in the field of quenching of microorganisms have been done with *S. cerevisiae* (e.g. de Koning et al., 1992, Loret et al., 2007). Furthermore, a lot of principle mechanisms of transcriptional and translational control of gene expression, growth control, signal transduction as well as the metabolism are transferable to higher eukaryotes (Peterson et al., 1992, Tamkun et al., 1992).

1.4 Thesis aims

A *Corynebacterium glutamicum* transposon mutant bank had already been in construction by Chatterjee at the beginning of this work.

Metabolome analysis of a high number of mutants was not realizable with our standard performance established by Stelkov et al. (Strelkov et al., 2004). For this reason, the first part of this thesis was the development of a high-throughput protocol for metabolome analysis. This included the following sub tasks: The culture size had to be miniaturized and the cultivation done in parallel. Some pre-analytical parts had to be automated and the time required for measurement performance with the gas chromatograph/mass spectrometer had to be shortened.

After the successful development of the high-throughput method, the second part of work started which is to be considered a pilot project. The aim of this part was to analyze a representative amount of transposon mutants. Criteria for the identification of interesting mutants had to be developed. The major difficulty was the differentiation between biological and environmental variations and variations caused by the introduced genetic perturbation.

In the third part of this thesis a suitable quenching method for different microorganisms was developed. Whereas for a mutant screening with the semi-automated, fast high-throughput method the quenching of the organism could be neglected, it is essential to stop the organism in the moment of harvesting when desired states and times had to be investigated and compared. The interesting genetic modifications would overwhelm other changes during such a screening. But quenched samples are a prerequisite for a comparative metabolome analysis, for example of different phases of an organism.

For the evaluation of the developed method it was compared to our unquenched method as well as to two published quenching protocols. Furthermore, the prokaryotes *Corynebacterium glutamicum*, *Escherichia coli* as well as the eukaryote *Saccharomyces cerevisiae* were used as model organisms.

2 Material & Methods

In the following, all used chemicals, machines etc. are listed. Furthermore, the standard operation protocols for all applied solutions and methods are specified.

1.5 Used chemicals and machines

Table 1. Manufacturer's list of chemicals

Name	Purity	Manufacturer
α-D(+)-Glucose monohydrate	99.5%	Carl Roth, Karlsruhe, D
Adonit/Ribitol	≥ 99.0%	Carl Roth, Karlsruhe, D
Agar-Agar		Carl Roth, Karlsruhe, D
Agarose NEEO ultra-quality		Carl Roth, Karlsruhe, D
Ammonium sulfate	≥ 99.5%	Carl Roth, Karlsruhe, D
Biotin	> 98.0%	Serva, Heidelberg, D
Boric acid		Carl Roth, Karlsruhe, D
Brain Heart Infusion		Sigma-Aldrich, Steinheim, D
Calcium chloride dihydrate	≥ 99.0%	Carl Roth, Karlsruhe, D
Calcium pantothenate		Sigma-Aldrich, Steinheim, D
Caseinhydrolysate (Casamino acids)		Carl Roth, Karlsruhe, D
Chloroform		Fisher Scientific, Schwerte, D
Cobalt(II)-chloride hexahydrate	≥ 99.0%	Carl Roth, Karlsruhe, D
Cupric sulfate pentahydrate	≥ 99.5%	Carl Roth, Karlsruhe, D
Cyclohexane		Fisher Scientific, Schwerte, D
Decane	> 98.0%	Carl Roth, Karlsruhe, D
Di-Potassium hydrogen phosphate	≥ 99.0%	Carl Roth, Karlsruhe, D
DNA Ladder Mix Fermentas		St. Leon-Rot, D
Docosane	99.0%	Sigma-Aldrich, Steinheim, D
Dodecane		Carl Roth, Karlsruhe, D
Dotriacontane	97.0%	Sigma-Aldrich, Steinheim, D
*Eco*RI (100.000 U/ml)		NEB, Frankfurt, D
*Eco*RI buffer		NEB, Frankfurt, D

Name	Purity	Manufacturer
EDTA		Serva, Heidelberg, D
Ethanol	HPLC	Carl Roth, Karlsruhe, D
Ethidium bromide		Carl Roth, Karlsruhe, D
Ferric chloride hexahydrate		Fluka Sigma-Aldrich, Steinheim, D
Ferrous sulfate heptahydrate	≥ 99.0%	Carl Roth, Karlsruhe, D
Folic acid		Sigma-Aldrich, Steinheim, D
Glycerol		Zentrales Lager für Chemikalien TU-Braunschweig, D
Hexatriacontane	98.0%	Sigma-Aldrich, Steinheim, D
Hydrochloric acid	37,0 %	Honeywell, Seelze, D
(myo-) Inisitol	≥ 99.0%	Sigma-Aldrich, Steinheim, D
Kanamycinsulfate		Carl Roth, Karlsruhe, D
Loading Dye Solution Fermentas		St. Leon-Rot , D
Lysozyme		Carl Roth, Karlsruhe, D
Magnesium chloride hexahydrate		Carl Roth, Karlsruhe, D
Magnesium sulfate		Zentrales Lager für Chemikalien TU-Braunschweig, D
Magnesium sulfate heptahydrate	≥ 99.0%	Carl Roth, Karlsruhe, D
Manganese sulfate monohydrate	≥ 99.0%	Carl Roth, Karlsruhe, D
Methanol		Fisher Scientific, Schwerte, D
Methoxyamine hydrochloride	≥ 98.0%	Sigma-Aldrich, Steinheim, D
MSTFA		CS-Chromatographie, Langerwehe, D
Niacine (Nicotinic acid)	≥ 98.0%	Sigma-Aldrich, Steinheim, D
Nickel(II)-chloride hexahydrate	≥ 98.0%	Carl Roth, Karlsruhe, D
Nonadecane		Carl Roth, Karlsruhe, D
Octacosane	> 98.0%	Carl Roth, Karlsruhe, D
p-Amino-benzoic acid		Sigma-Aldrich, Steinheim, D
Pentadecane		Carl Roth, Karlsruhe, D
Peptone from Casein		Carl Roth, Karlsruhe, D
Phosphor pentoxide	≥ 98.5%	Carl Roth, Karlsruhe, D
Potassium aluminum sulfate dodecahydrate	≥ 98.0%	Carl Roth, Karlsruhe, D
Phenol		Sigma-Aldrich, Steinheim, D

Name	Purity	Manufacturer
Potassium di-hydrogen phoshpate	≥ 99.0%	Carl Roth, Karlsruhe, D
Potassium hydroxide		Zentrales Lager für Chemikalien TU-Braunschweig, D
Potassium iodide		Merck KGaA, Darmstadt, D
Proteinase K		Sigma-Aldrich, Steinheim, D
Pyridine	≥ 99.5%	Carl Roth, Karlsruhe, D
Pyridoxine hypochloride		Sigma-Aldrich, Steinheim, D
Riboflavin		Sigma-Aldrich, Steinheim, D
RNase A		Roche, Mannheim, D
Sodium acetate	≥ 99.0%	Carl Roth, Karlsruhe, D
Sodium dodecyl sulfate		Carl Roth, Karlsruhe, D
Sodium chloride	≥ 99.5%	Carl Roth, Karlsruhe, D
Sodium hydroxide	≥ 99.0%	Carl Roth, Karlsruhe, D
Sodium molybdate dihydrate	≥ 99.5%	Carl Roth, Karlsruhe, D
Sulfuric acid	≥ 96.0%	Carl Roth, Karlsruhe, D
T4-DNA-ligase (400.00 U/ml)		NEB, Frankfurt, D
Thiamine hypochloride		Sigma-Aldrich, Steinheim, D
Tris	≥ 99.0%	Carl Roth, Karlsruhe, D
Tryptone from Casein		Carl Roth, Karlsruhe, D
Urea	≥ 99.7%	Carl Roth, Karlsruhe, D
Yeast extract		Serva, Heidelberg, D
Zinc sulfate heptahydrate	≥ 99.5%	Carl Roth, Karlsruhe, D

Table 2. List of equipment

Equipment	Manufacturer
GC System	
6890N Network GC System	Agilent Technologies Sales & Services, Waldbronn, D
Multi Purpose Sampler MPS2-Twister	Gerstel, Mülheim an der Ruhr, D
Mass Spectrometer	
AccuTOF GC JMS-T100GC	Jeol (Deutschland), Eching, D

Equipment	Manufacturer
Shaker for incubation	
Certomat BS-1 (orbit: 50 mm)	Sartorius Biotech,Göttingen, D
Certomat SII (orbit: 25 mm)	Sartorius Biotech,Göttingen, D
TiMix 5, TH15 (orbit: 3 mm)	Edmund Bühler, Tübingen, D
Centrifuges	
Centrifuge 5810R	Eppendorf, Hamburg, D
Centrifuge 5424	Eppendorf, Hamburg, D
Primo R Benchtop Centrifuge	Fisher Scientific, Schwerte, D
Mikro 22 R	Hettich, Tuttlingen, D
Z 300 K	Hermle, Wehingen, D
Others	
Electroporater 2510	Eppendorf, Hamburg, D
G:BOX	Syngene, Cambridge, UK
Mix Mate	Eppendorf, Hamburg, D
Sonorex Digitec UW 2070	Bandelin Electronic, Berlin, D
Sonorex Digitec DT 255H	Bandelin Electronic, Berlin, D
Spectral photometer Genesys 6	Sysmex Digitana, Horgen, D
Speed Vac Concentrator 5301	Eppendorf, Hamburg, D
Sunrise-Basic	Tecan Deutschland GmbH, Crailsheim, D
Thermo mixer Comfort	Eppendorf, Hamburg, D

Table 3. Applied materials

Material	Manufacturer
GC column	
DB-5MS (30 m * 0.25 mm * 0.25 µm)	Agilent (J & W Scientific), Folsom, USA
GC glass liner	
71*2 mm glass liner	Gerstel, Mülheim an der Ruhr, D
Filter	
Fiber glass filter GF/F, 0.7 µm	Whatman, Dassel, D
Nitrocellulose filter MCE-MF, 0.22 µm	Millipore, Schwalbach, D
Others	
Adhesive foil, polyolefin	Nunc, Wiesbaden, D

Material	Manufacturer
AeraSeal™, foil	Excel Scientific Inc., Wrightwood, USA; Sigma-Aldrich, München D
Bottle R1 s, clear	CS-Chromatographie, Langerwehe, D
Bottle 1.1 ml, flange, clear	IVA Analysentechnik, Meerbusch, D
BreathEasy™, foil; T093.1	Diversified Biotech, Boston, USA; Carl Roth, Karlsruhe, D
Cuvette for electroporation (1 mm)	Eppendorf, Hamburg, D
Cuvette from silica glass, 10 mm	Carl Roth, Karlsruhe, D
F96 MicroWell™ plate, PS	Nunc, Wiesbaden, D
Flanging pliers	CS-Chromatographie, Langerwehe, D
Glass wool	Restek, Bad Homburg, D
Magnetic flanging cap R11-Silicon, red/white	CS-Chromatographie, Langerwehe, D
Micro insert G30s	CS-Chromatographie, Langerwehe, D
Screw cap 8-SCJ	Chromacol, Herts, UK; Kupfer Pfungstadt, D
Septa 8 ST 101	Chromacol, Herts, UK; Kupfer Pfungstadt, D
Silicon mat	Nunc, Wiesbaden, D
U96 DeepWell™ plate, PP	Nunc, Wiesbaden, D
U96 MicroWell™ plate, PP	Nunc, Wiesbaden, D

1.6 Software and libraries

Table 4. Applied software

Software	Description
AMDIS 32, Version 2.64 (http://chemdata.nist.gov/mass-spc/amdis/)	Automated Mass Spectral Deconvolution and Identification System, Analysis of GC/MS data
BLAST, NCBI (http://www.ncbi.nlm.nih.gov/blast/Blast.cgi)	Comparison of DNA sequences with genome annotation data
CUMETA	Calculation of correlation values (Pearson and Spearman correlation)

Software	Description
Excel 2007	Microsoft spreadsheet and data reporting
Gerstel Maestro 1, version 1.1.4.18 (http://www.gerstel.com)	Control software for the MPS2 twister autosampler and the PTV injector
LER Auswertung	Tool for analysis and comparison of GC/MS data
Macro3	Macro (Excel) for standardization of peak areas to peak area of the ribitol
Mass Center Main, Version 2.3.0.1	Control software for the GC/MS system
Processing4_3	Processing of results from AMDIS for usage in XCalibur
Scatter plot beta7	Programmed Excel sheet for generation of scatter plots for comparison of GC/MS data
XCalibur 1.4	Analysis of GC/MS data

Table 5. Applied libraries

Database	Description
NIST Mass Spectral Database (http://www.nist.gov/)	Library and program for analysis of GC/MS spectra
Library 3.4.0	Internal mass spectra database with defined parameters for identification
KEGG Encyclopedia (http://www.genome.jp/kegg/)	Collection of pathways for different organism
PubMed (http://www.ncbi.nlm.nih.gov/pubmed)	Literature research

1.7 Used bacteria strains

Table 6. Bacteria strains

Strain	Origin	Reference
Corynebacterium glutamicum		
ATCC 13032	American Type Culture Collection, Wesel, D	Kalinowski et al., 2003 Abe et al., 1967
res$^-$ 167, ATCC 13032 Delta (*cgllMcgllR-cglllR*) (restriction deficient)	Prof. Krämer, Universität zu Köln, D	Cleas et al., 2002
Transposon mutants	Prof. Schomburg, Technische Universität Braunschweig, D	Chatterjee, unpulished Mormann et al., 2006
Escherichia coli		
DSM 498	DSMZ, Braunschweig, D	Castellani et al., 1919
DH5α (mcr)	Prof. Waffenschmidt, Univesität zu Köln, D	Hanahan, 1983
Saccharomyces cerevisiae		
CEN.PK 113-7D	Dr. Kötter, Universität Frankfurt (Main), D	Villas-Bôas et al., 2005a

1.8 Applied kits

Table 7. List of applied kits

Name	Application	Origin
Wizard Plus SV Minipreps DNA Purification System	Plasmid preparation out of *E. coli*	Promega,Mannheim, D
peqGOLD Plasmid Miniprep Kit I	Plasmid preparation out of *E. coli*	Peqlab, Erlangen, D
Phase lock-test tubes	Preparation of genomic DNA out of *C. glutamicum*	Eppendorf, Hamburg, D

1.9 Statistic and calculation of errors

The arithmetic average was calculated from a series of *n* different measurements. The mean value $\bar{x}$ (equation 2.1) represents the supposable value of the series.

$$\bar{x} = \frac{1}{n} \sum_{i=1}^{n} x_i \qquad (2.1)$$

The standard deviation *s* (equation 2.2) describes the variation of each single measurement x_i compared to the mean value $\bar{x}$. It is the mean error of the single measurement.

$$s = \pm \sqrt{\frac{1}{(n-1)} \sum_{i=1}^{n} (\bar{x} - x_i)} \qquad (2.2)$$

In most cases the accuracy of the mean value is important. The standard error of the mean value $s_{\bar{x}}$ (equation 2.3) differs from the standard deviation *s* by the factor $1/\sqrt{n}$. It describes the interval around the mean value, where the true value can be expected.

$$s_{\bar{x}} = \pm \sqrt{\frac{1}{n(n-1)} \sum_{i=1}^{n} (\bar{x} - x_i)} = \frac{s}{\sqrt{n}} \qquad (2.3)$$

The important assumptions for these calculations are the independence of all values x_i and there similar accuracy.
The relative error s_{rel} (equation 2.4) represents the accuracy of the measurement procedure.

$$s_{rel} = \pm \frac{s_{\bar{x}}}{\bar{x}} * 100 \quad \% \qquad (2.4)$$

When comparing mean values the error propagation after Gauss was applied. If the ratio (equation 2.5) of two values x_1 and x_2, with associated standard errors $s_{\bar{x}_1}$ and $s_{\bar{x}_2}$ was calculated, the error s_f had to be calculated according to equation 2.6.

$$f(x_{1,}x_2)=\frac{x_1}{x_2} \tag{2.5}$$

$$s_f=\sqrt{(\frac{1}{x_2}*s_{\overline{x}_1})^2+(-\frac{x_1}{x_2{}^2}*s_{\overline{x}_2})^2} \tag{2.6}$$

If correlations were calculated the Pearson correlation was applied. Values were calculated using the logarithmic values of the relative concentration vectors.

1.10 Media, buffer and solutions

Brain heart infusion medium (BHI)

Brain Heart Infusion	37 g

BHI has to be filled up to 1 l with double distilled water and autoclaved afterwards.

Luria-Bertani medium (LB)

Peptone from Casein	10 g
Yeast extract	5 g
Sodium chloride	10 g

The compounds were dissolved in double distilled water, filled up to 1 l and autoclaved.

YPD medium

Yeast extract	10 g/l
Peptone from Casein	20 g/l
α-D(+)-Glucose monohydrate	20 g/l

Components were dissolved in double distilled water, filled up to 1 l and autoclaved.

Stock solution for minimal medium (MM1)

Ammonium sulfate	20.00 g
Urea	5.00 g
Di-Potassium hydrogen phosphate	1.53 g
Potassium di-hydrogen phoshpate	2.00 g

Substances were dissolved in 0.85 l double distilled water and the pH-value was adjusted with potassium hydroxide (c = 5 M) to 7. Afterwards the solution was filled up to 0.947 l with double distilled water and autoclaved.

Stock solution for minimal medium with amino acids

Ammonium sulfate	20.00 g
Urea	5.00 g
Di-Potassium hydrogen phosphate	1.53 g
Potassium di-hydrogen phoshpate	2.00 g

Substances were dissolved in 0.85 l double distilled water and the pH-value was adjusted with potassium hydroxide (c = 5 M) to 7. Afterwards the solution was filled up to 0.947 l with double distilled water and autoclaved.

Caseinhydrolysate (Casamino acids)	4.00 g

Caseinhydrolysate was dissolved in 20 ml sterile solution prepared before, sterilized by filtration and combined with the rest of the solution.

Stock solution of glucose (25 fold)

α-D(+)-Glucose monohydrate	550 g

Glucose had to be dissolved in 0.85 l double distilled water and filled up to 1 l before it was sterilized by filtration.

Stock solution of magnesium sulfate (100 fold)

Magnesium sulfate heptahydrat	25 g

Compound was dissolved in 0.85 l double distilled water, filled up to 1 l and autoclaved.

Stock solution of calcium chloride (1000 fold)

Calcium chloride dihydrat	10 g

Calcium chloride was dissolved in 0.85 l double distilled water and filled up to 1 l before it was autoclaved.

Stock solution of trace elements (1000 fold)

Ferrous sulfate heptahydrate	28.500 g
Manganese sulfate monohydrate	16.500 g
Zinc sulfate heptahydrate	6.400 g
Cupric sulfate pentahydrate	0.764 g
Cobalt(II)-chloride hexahydrate	0.128 g
Nickel(II)-chloride hexahydrate	0.044 g
Sodium molybdate dihydrate	0.064 g
Boric acid	0.048 g
Potassium aluminum sulfate dodecahydrate	0.028 g

Substances were dissolved in 0.85 l double distilled water and the pH-value was adjusted to 1 with sulfuric acid (c = 3 M). Afterwards the solution was filled up to 1 l with double distilled water and sterilized by filtration.

Stock solution of biotin (1000 fold)

Biotin	20 g
Sodium hydroxide solution (c = 1 M)	3 drops

Biotin was dissolved in 80 ml double distilled water via supplementation of sodium hydroxide solution. The solution was filled up to 100 ml with double distilled water, sterilized by filtration, divided into aliquot parts and stored at -20°C.

Minimal medium (MM1)

Table 8. Composition of different volumes MM1

Component	Volume for 100 ml	Volume for 20 ml
stock solution for minimal medium	94.7 ml	18.94 ml
stock solution of magnesium sulfate	1.0 ml	0.20 ml
stock solution of calcium chloride	0.1 ml	0.02 ml
stock solution of glucose	4.0 ml	0.80 ml
stock solution of biotin	0.1 ml	0.02 ml
stock solution of trace elements	0.1 ml	0.02 ml

MM1 was always freshly prepared prior to usage.

Basic medium

Calcium chloride dihydrate	0.132 g
Sodium chloride	0.100 g
Magnesium sulfate	0.500 g
Potassium di-hydrogen phosphate	1.000 g
Ammonium sulfate	5.000 g

Compounds were dissolved in 1 l double distilled water and autoclaved.

Stock solution of vitamins (1000 fold)

Biotin	1 mg
Calcium pantothenate	200 mg
Folic acid	1 mg
Inositol	1000 mg
Niacine	200 mg
p-Amino-benzoic acid	100 mg
Pyridoxine hypochloride	200 mg
Riboflavin	100 mg
Thiamine hypochloride	200 mg

Substances were dissolved in 1 l double distilled water and sterilized by filtration.

Stock solution of trace metals (1000 fold)

Boric acid	500 mg
Cupric sulfate pentahydrate	40 mg
Potassium iodide	100 mg
Ferric chloride hexahydrate	200 mg
Manganese sulfate monohydrate	400 mg
Sodium molybdate dihydrate	200 mg

Substances were dissolved in 1 l double distilled water and sterilized by filtration.

Minimal medium for yeast

Table 9. Composition of the minimal medium for yeast

Component	Volume for 1 l
basic medium	973 ml
stock solution of glucose	25 ml
stock solution of vitamins	1 ml
stock solution of trace metals	1 ml

Nutrient agar plates

For BHI-, LB-, YPD- as well as MM1-agar plates, 15 g agar-agar had to be added to 1 l of the media and autoclaved. Possibly, a sterile antibiotic was added to the medium before preparing the agar plates. Plates were stored at 4°C.

Stock solution of ribitol

Ribitol (Adonit) 0.2 g

Ribitol was dissolved in 1 l double distilled water. The solution was sterilized by filtration, divided into aliquot parts and stored at -20°C.

Ethanol-ribitol-solution

Ethanol 10.0 ml
Stock solution of ribitol 0.4 ml

Solutions were combined prior to usage.

SOC medium

Tryptone from casein	20.0 g
Yeast extract	5.0 g
Sodium chloride	0.5 g

Substances were dissolved in 0.98 ml double distilled water.

Potassium chloride solution	250 mM

10 ml of the potassium chloride solution were added to the dissolved substances. Afterwards the pH-value was adjusted to 7 with sodium hydroxide solution (c = 5 M) and autoclaved.

Magnesium chloride solution	2 M
α-D(+)-Glucose monohydrate	1 M

A magnesium chloride solution was autoclaved separately. A glucose solution was sterilized by filtration. 5 ml of the magnesium chloride solution and 20 ml of the glucose solution were added to the before prepared solution.

TE-buffer (Tris-EDTA-buffer)

Tris	10 mM
EDTA	1 mM

The prepared solution was filled up to 1 l with double distilled water and the pH-value was adjusted to 7.5 with a hydrochloric acid solution.

TAE-buffer (Tris-Acetate-EDTA-buffer, 50 fold)

Tris	2 M
Acetic acid	1 M
EDTA (pH 8)	50 mM

Components were combined and solution was filled up to 1 l with double distilled water.

Stock solutions of antibiotics

Kanamycin I	25 mg/ml
Kanamycin II	50 mg/ml

Stock solutions were prepared with double distilled water. Solutions were sterilized by filtration, divided into aliquot parts and stored at -20°C.

B1-solution

Tris/HCl (pH 8)	25 mM
EDTA (pH 8)	10 mM
α-D(+)-Glucose monohydrate	50 mM

Components were combined and a B1-stock solution prepared. As solvent double distilled water was used. Stock solution was stored at room temperature.

Lysozyme	20 mg/ml
RNase A	100 µg/ml

Both stocks were prepared with double distilled water, sterilized by filtration, divided into aliquot parts and stored at -20°C. Lysozyme and RNase A were always given to the B1-stock solution prior to usage.

Proteinase K

Proteinase K	20mg/ml

Stock solution was prepared with double distilled water, sterilized by filtration, divided into aliquot parts and stored at -20°C.

ATP solution

ATP	10 mM

Stock solution was prepared with double distilled water, sterilized by filtration, divided into aliquot parts and stored at -20°C.

RNase A

RNase A	10 mg/ml
Sodium acetate solution (pH 5.2)	10 mmol/l

RNase A was dissolved in sodium acetate solution and incubated at 100°C for 15 minutes. Afterwards the solution cooled down to room temperature.

Tris/HCl solution (pH 7.5)	1 mol/l

100 µl of the Tris/HCl solution were given to 1 ml of the before prepared solution, sterilized by filtration, divided into aliquot parts and stored at -20°C.

Sodium chloride solution

Sodium chloride (0.9% w/v)	9.0 g/l

The sodium chloride solution was prepared with double distilled water and stored at 4°C.

Quenching solutions

Ethanol quenching solution

Ethanol (I...III)	40% v/v
Sodium chloride solution I	0.5% w/v
Sodium chloride solution II	0.8% w/v
Sodium chloride solution III	1.5% w/v

Ethanol quenching solutions I, II and III were prepared with double distilled water, divided into aliquot parts and stored at -20°C. Ethanol was always combined with a sodium chloride solution (I...III) to obtain the end concentration stated earlier.

Methanol quenching solution

Methanol	60% v/v

Methanol quenching solution was prepared with double distilled water, divided into aliquot parts and stored at -80°C.

Cold glycerol saline quenching solution

Glycerol	pure
Sodium chloride solution	13.5 g/l

Glycerol and the sodium chloride solution were mixed 3:2 v/v, divided into aliquot parts and stored at -20°C.

Cold glycerol saline washing solution

Glycerol	pure
Sodium chloride solution	13.5 g/l

Glycerol and sodium chloride solution were mixed 1:1 v/v, divided into aliquot parts and

stored at -20°C.

Methoxyamine-pyridine-solution (reagent for derivatization)

Methoxyamine hydrochloride	20 mg
Pyridine	1 ml

Solution was freshly prepared prior to usage.

Quality control solution

Pentadecane	0.4 g

Pentadecane was dissolved in 0.85 l cyclohexane and filled up to 1 l with cyclohexane afterwards. Solution was stored at 4°C.

Time standard solution

Decane	17.12 µl
Dodecane	16.67 µl
Pentadecane	16.23 µl
Nonadecane	12.50 mg
Docosan	12.50 mg
Octocosane	12.50 mg
Dotriacontane	12.50 mg
Hexatriacontane	12.50 mg

Substances were dissolved in 20 ml cyclohexane and filled up to 25 ml with cyclohexane afterwards. Solution was stored at room temperature.

1.11 Standard metabolome analysis

In the following part all necessary steps for the standard metabolome analysis (Strelkov et al., 2004) are described in detail.

1.11.1 Cultivation in shaking flasks

Strains were routinely stored as glycerol stocks at -80°C. For metabolome analysis stocks were taken and streaked out on agar plates containing a complex medium. After incubation at organism-specific temperatures plates were sealed with parafilm and stored at 4°C.

Cultivation of Corynebacterium glutamicum

C. glutamicum was raised on BHI as complex medium. After incubation on BHI-plates at 30°C for around one day, a single colony was transferred to 5 ml fresh BHI medium in a test tube. Incubation was done at 30°C, 180 rpm for 7 hours. Afterwards 0.5 ml of this pre-culture was transferred to 20 ml freshly prepared MM1 medium in a 100 ml-shaking flask and incubated at 30°C, 180 rpm over night (~16 h). The main culture was prepared in a 500 ml-shaking flask containing fresh MM1. The culture was inoculated with the over night culture to a starting OD_{600} of 1. Cells grew for 7 hours, at 30°C and 180 rpm.
If a mutant was raised, kanamycin was added to pre-culture and overnight culture to obtain a concentration in the medium of 25 µg/ml.

Cultivation of Saccharomyces cerevisiae

S. cerevisiae was streaked out from glycerol stocks on YPD-agar plates and incubated at 30°C for three days. For the inoculation of the pre-culture several colonies were taken and transferred to 20 ml YPD in a 100 ml-buffled shaking flask and incubated at 30°C, 200 rpm for 9 hours. 20 ml fresh minimal medium for yeast was prepared in a 100 ml-buffled shaking flask and inoculated with 2.2 ml of the pre-culture. The over night culture was incubated at 30°C, 200 rpm for 14...16 hours. For the main culture 50 ml minimal medium were freshly prepared in a 250 ml-buffled shaking flask and inoculated with the over night

culture to a start OD_{600} of 2.5 and incubated at 30°C and 200 rpm for 5 hours.

Cultivation of Escherichia coli

E. coli was handled differently, compared to both other organisms. Cells were streaked out from a glycerol stock on MM1-agar plates. After incubation at 37°C for at least one day a single colony was transferred to 5 ml freshly prepared MM1 medium in a test tube. The cultures were incubated over night at 37°C and 220 rpm (~16 h). The cultivation of *E. coli* was done without pre-culture. 100 ml main culture (MM1) was inoculated with the over night culture in a 500 ml-shaking flask to a starting OD_{600} of 0.03...0.05. Again, incubation was done at 37°C and 220 rpm for 7 hours.

1.11.2 Pre-analytical sample preparation

For metabolome analysis samples were prepared routinely using a standard protocol (Strelkov et al., 2004). The workflow is shown in figure 16. The pre-analytical preparation starts after cultivation with the harvesting of the cells. Time for harvesting is specific for each organism, but is performed always in the middle of the exponential growth phase. For reason of comparison the ratio of cell number and volume has to be stable. Consequently, the volume for harvesting was always calculated according to the optical density of the main culture. Because of the different morphology of the analyzed cells, for each microorganism an equation was determined, related to their cell dry mass.

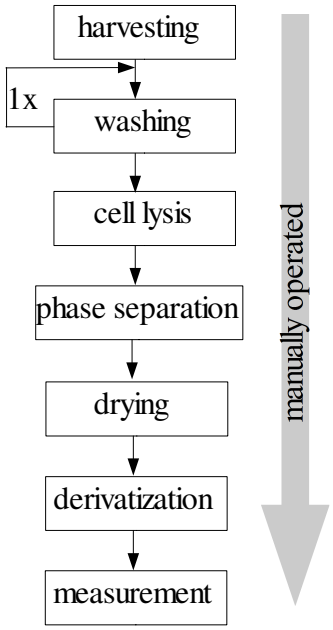

Figure 16. Workflow of the standard protocol for metabolome analysis.

Equation 2.7 describes the calculation of the harvesting volume for *C. glutamicum* and *S. cerevisiae* and equation 2.8 for *E. coli* (Jäger, 2007).

$$V_{harvesting} = \frac{50}{OD_{600}} \tag{2.7}$$

$$V_{harvesting} = \frac{48}{OD_{600}} \tag{2.8}$$

After harvesting, the cells were centrifuged at 4°C and 3904 g for 3 minutes. The supernatants were discarded and pellets washed with 20 ml of sodium chloride solution (0.9% w/v and a temperature of 4°C). Resuspended cells were centrifuged under the same conditions and the whole washing step was repeated one time. Afterwards, pellets were resuspended in 1.5 ml of the ethanol-ribitol-solution and cell lysis was performed in the ultrasonic bath at 70°C for 15 min. Then the samples were cooled on ice for 2 min. 1 ml double distilled water was added. After intense mixing for around 1 min 0.75 ml chloroform was added and the mixing was repeated. For phase separation samples were centrifuged at 4°C and 3904 g for 5 minutes. Afterwards, 1 ml of the upper polar phase

could be removed and transferred to a fresh 2 ml-tube and dried over night in the speed vac. The first hour was performed with rotation to avoid any delay in boiling and the remaining time without rotation.

Extract of the samples had to be derivatized before measurement. This was done in two steps. At first 20 µl methoxyamine-pyridine-solution was added, intensely mixed for 1 min and incubated in a thermo mixer for 90 min at 30 °C and 600 rpm. Subsequently, 32 µl MSTFA were added, intensely mixed for 1 min and incubated for 30 min at 37°C and for further 2 h at 25°C each time at 600 rpm.

Derivatized samples were centrifuged for 3 min and 10,000 g and the clear supernatants were transferred to glass vials containing micro inserts.

1.11.3 GC/MS analysis and data processing

Measurement was done with a fast GC coupled to a TOF-MS. Analyses were performed over 60 minutes. Electron impact mode at 70 eV was used for ionization with a source temperature adjusted to 200°C. The detector voltage was set to 2100 V and the emission current to 300 µA. Mass spectra were acquired in full scan mode from 40 to 800 m/z with a scan rate of 2/s and a solvent delay time of 6 min.

Chromatography was performed with a flow rate of 1 ml/min. For measurement 2 µl of the sample were injected in split mode with a split ratio of 1/25 into the PTV-injector which had a temperature of 70°C. Injector temperature was increased to 280°C with a rate of 12 K/s for transferring the sample onto the column. The oven temperature had 70°C at the beginning and was held at 70°C for 1 min. Afterwards it was increased to 76°C with 1 K/min, and further to 325°C with 6 K/min. This temperature was held for 10 min.

At the beginning of each data collection one sample (2 µl, split ratio 1/25) containing the time standard (mix of 50 µl MSTFA and 4 µl time standard) was injected. Furthermore - after six samples - pure MSTFA was injected for rinsing the column and after around 12 samples the quality control was injected to check the performance of the mass spectrometer.

After measurement samples had to be converted three times. Because acquired mass spectra were recorded continuously they had to be made centroid. Furthermore, data were

converted into net-cdf-files. These net-cdf-files had to be transformed into raw-files and could be used for standard data processing afterwards.
The first step of the data processing was the identification of the retention times of the alkane series in AMDIS. Afterwards the information of retention time and corresponding retention index was used and data were deconvoluted, and peaks identified applying our internal library. The results were rewritten using Processing4_3 to receive data adaptable for XCalibur. In XCalibur the in AMDIS identified substances were related to pre-defined quantification ions and the intensity of these peaks were determined. Afterwards the results of the data set were exported to Excel where they were rewritten in a result list using the Macro3. During rewriting process two additional steps were performed: all intensities were related to the intensity of the internal standard ribitol, and derivatives of the same metabolite were combined.

1.12 High-throughput metabolome analysis

In the following part all necessary steps for the high-throughput metabolome analysis (Börner et al., 2007) are described in detail. Data processing was done according to the performance in the standard protocol (see part 2.7.3).

1.12.1 Cultivation in micro titer plates

If only the wild type had to be raised, the first steps till over night culture were done according to the standard cultivation in part 2.7.1. For the over night culture 150 µl fresh MM1 was prepared per well and each well except for two blanks was inoculated with 10 µl of the pre-culture. Incubation was done at 30°C and 1050 rpm over night (~16 h). 25 µl of the over night culture per well were used to inoculate 400 µl fresh MM1 of the main culture. Incubation was done at 30°C and 1050 rpm for 7 h.
Working in micro titer plates required certain preconditions: the plates had to be closed using a combination of two foils in order to assure sufficient oxygen supply. Therefore, the plates were sealed with the AeraSeal foil first and the BreathEasy foil on top.

Transposon mutants were always stored as glycerol stocks in micro titer plates at -80°C. For cultivation they had to be streaked out on BHI-kanamycin plates (25 µg/ml) using a replicator. Incubation was done at 30°C for one day. Pre-cultures contained 150 µl BHI-kanamycin-solution (25 µg/ml) per well and were inoculated with colonies from the plate. Colonies were transferred to the wells with the replicator. Pre-culture was incubated at 30°C and 1050 rpm for 7 h. 150 µl fresh MM1 containing kanamycin (25 µg/ml) was prepared for each well of the over night culture. This culture was inoculated with 10 µl of the pre-culture and incubated over night (~16 h) at 30°C and 1050 rpm. Starting with the over night culture, every mutant was "raised three times". In other words, three consecutive wells of this plate were inoculated with the same pre-culture. Furthermore, six wells (two separated triplicates) contained MM1 without kanamycin and were inoculated with 10 µl of a separately prepared pre-culture of the wild type. Three wells of the plate remained not inoculated as blanks.

Main culture was raised in 96deepwell plates. 400 µl MM1 were prepared for each well and inoculated with 25 µl of the over night culture. Inoculation was done at 30°C and 1050 rpm for 7 hours.

1.12.2 Semi-automatic sample preparation

Sample preparation for the high-throughput analysis was adapted from the standard performance (see part 2.7.2) but performed in a micro titer plate. The workflow is shown in figure 17. For harvesting the whole micro titer plate was centrifuged at 4°C and 3220 g for 3 min. Afterwards cells were washed with 400 µl cold sodium chloride solution (4°C, 0.9% w/v). For resuspension the plate was sealed with a silicon mat and mixed on a shaker for micro titer plates ("mix mate"). Subsequently, the plate was centrifuged again and the washing step was repeated one time. Afterwards, pellets were resuspended in 400 µl ethanol-ribitol-solution, and cell lysis was performed at 70°C in an ultrasonic bath for 15 min. For the lysis micro titer plate had to be covered with a special foil (adhesive foil) and a metal brace. The plate with the metal brace had to be cooled after lysis for around 10 min on ice. After adding 400 µl double distilled water to each well and mixing for 1 min on the mix mate, 250 µl chloroform were added, mixed for 1 min again, and then the plate

was centrifuged to separate the polar and the apolar phase.

Up to this each step was performed manually. All following steps were done automated using the MPS2 twister autosampler. Equipped with a 1 ml syringe, around 600 µl of the upper aqueous phase were transferred from each well into a tapered glass vial (filling speed 40 µl/s and depth of immersion 30 mm). All samples were dried over night in a desiccator using phosphor pentoxide as desiccant under vacuum. Glass vials were closed with magnetic caps the next day. Afterwards, the dried samples were derivatized automated with the MPS2 twister autosampler equipped with a 10 µl syringe. Therefore the autosampler was also filled with vials containing pure MSTFA and methoxyamine-pyridine-solution.

Derivatization was done in two steps. First 20 µl methoxyamine-pyridine-solution were added to the sample. The whole vial was shaken for 2 min at 750 rpm. Incubation was done for 125 min at around 37°C. Then 32 µl MSTFA were added and the whole vial was shaken again. Incubation was repeated under same conditions.

Each sample was freshly prepared before measurement. For the measurement of the time standard, 4 µl alkane mix was transferred to a tapered glass vial, closed with a magnetic cap and prepared together with the other samples.

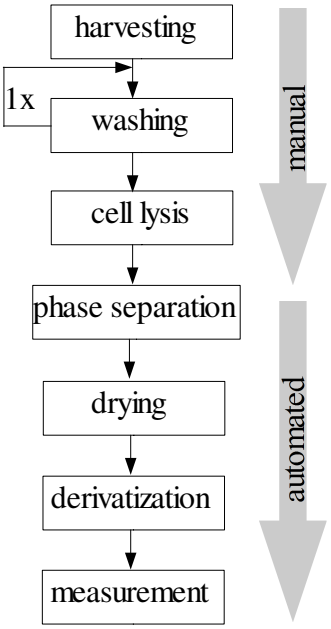

Figure 17. Workflow of the pre-analytical parts of the high-throughput performance.

1.12.3 GC/MS analysis and data processing

Measurement was done with a fast GC coupled to a TOF-MS over 18 minutes. Electron impact mode at 70 eV was use for ionization with a source temperature adjusted to 200°C. The detector voltage was set to 2100 V and the emission current to 300 µA. Mass spectra were acquired in full scan mode from 40 to 800 m/z with a scan rate of 5/s and a solvent delay time of 3.9 min.

Chromatography was performed with a flow rate of 1 ml/min. 2 µl of the sample were injected in split mode with a split ratio of 1/10 into the PTV-injector which had a temperature of 70°C. The temperature was increased to 280°C with 12 K/s transferring the sample onto the column. The oven temperature had 70°C and was held at 70°C for 1 min. Afterwards, it was increased to 76°C at 4 K/min, to 325°C with 24 K/min and was held at this temperature for 6 min.

Retention times were determined and rinsing of the column with pure MSTFA was done as described before (see part 2.7.3). Data conversion and data processing were performed as characterized in detail for 60-min-measurements in part 2.7.3.

1.13 Quenching of microorganisms

The following part describes the applied quenching methods. In order to provide a comparison, our standard method (unquenched method, see part 2.7) was also used. In all protocols a temperature reduction was applied to achieve a complete stop of metabolism. Table 10 gives an overview about the tested quenching methods. In all cases the methods were handled in parallel and the samples (at least triplicates) were strictly derived from the same cultivation. The way how the different organisms were cultivated was already described in detail in part 2.7.1. Thus, the following part specifies the steps starting from harvesting.

Table 10. Quenching methods: unquenched standard method UQ, ethanol quenching EQ, methanol quenching MQ, cold glycerol saline quenching GSQ

Method	Quenching solution	Temperature of quenching solution	Mixing: parts of cell suspension and quenching solution	Centrifugation
UQ	-	-	-	4°C, 3904 g
EQ	40% ethanol, 0.8% NaCl (w/v)	-20°C	1+1	-16°C, 3940 g
MQ	60% methanol-solution	-60°C	1+2	-9°C, 10,000 g
GSQ	60% glycerol, 0.54% NaCl (w/v)	-20°C	1+4	-9°C, 18,000 g

For all methods the same extraction protocol was applied. Because the aim of the study was to examine the quenching step, extraction was performed according to our standard protocol (see part 2.7.2). Samples were dried over night in the speed vac and derivatization as well as measurement were done automated according to our high-throughput protocol (see part 2.8.2).

The sample volume was calculated according to the equations 2.7 and 2.8, with the difference that only half of the volume was taken for *E. coli* and *S. cerevisiae*. In table 11 the sample volume and the corresponding amounts of ethanol-ribitol-solution for metabolite extraction and water are summarized.

Table 11. Used volumes during extraction for quenching experiments of the different organisms

Organism	Sample volume	Volume of ethanol-ribitol-solution	Volume of double distilled water
C. glutamicum	5 ml	1.50 ml	1.50 ml
E. coli	16 ml	0.75 ml	0.75 ml
S. cerevisiae	10 ml	0.75 ml	0.75 ml

1.13.1 Ethanol quenching (EQ)

An ethanol-sodium chloride-solution (40% v/v ethanol and 0.8% w/v sodium chloride) was parted into aliquots and stored in falcon tubes at -20°C. For each organism the defined amount of quenching solution (1+1, see table 11 for the volume) was provided. The detailed workflow is shown in figure 18.

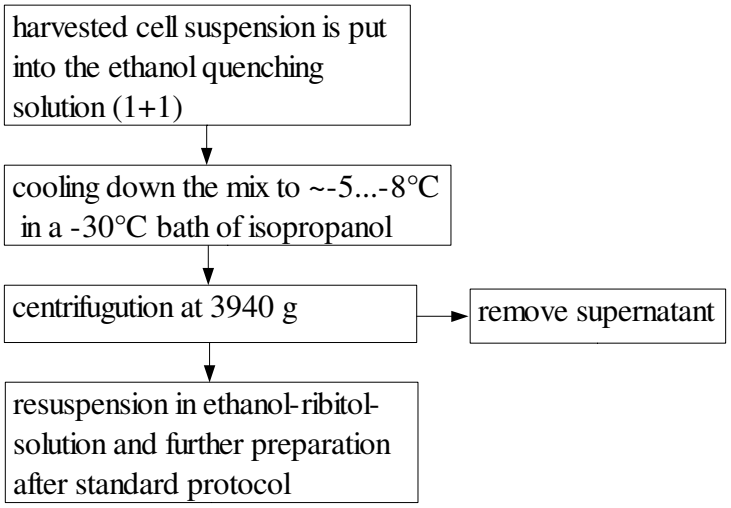

Figure 18. Workflow of the ethanol quenching performance

Cooling time and centrifugation time were determined for each organism and are listed in table 12.

Table 12. Organism specific cooling and centrifugation times.

Organism	Cooling time	Centrifugation time
C. glutamicum	1.0 min	5 min
E. coli	1.5 min	7 min
S. cerevisiae	1.0 min	5 min

1.13.2 Methanol quenching (MQ)

A 60% methanol solution with double distilled water as solvent was parted into aliquots and stored in falcon tubes at -80°C. When removing the tubes from the freezer, solution heats up and thaws immediately and reaches a temperature of around -60°C prior to usage. For each organism the defined amount of quenching solution (1+2, see table 11 for the volume) was provided. The detailed workflow is shown in figure 19.

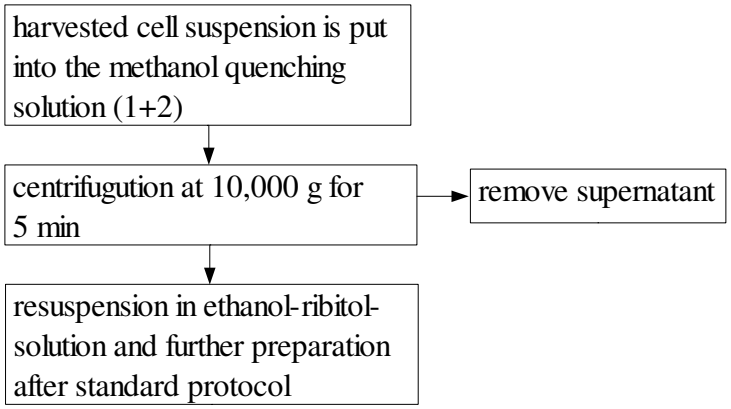

Figure 19. Workflow of the methanol quenching performance

1.13.3 Cold glycerol saline quenching (GSQ)

A 60% glycerol solution was prepared using a 1.35% (w/v) sodium chloride solution. The obtained quenching solution showed a salt concentration of 0.54%. Solution was parted into aliquots and stored in falcon tubes at -20°C. Additionally, a washing solution was prepared containing 50% glycerol and 0.675% (w/v) sodium chloride, and stored at -20°C. For each organism the defined amount of quenching solution (1+4, see table 11 for the volume) was provided. The detailed workflow is shown in figure 20.

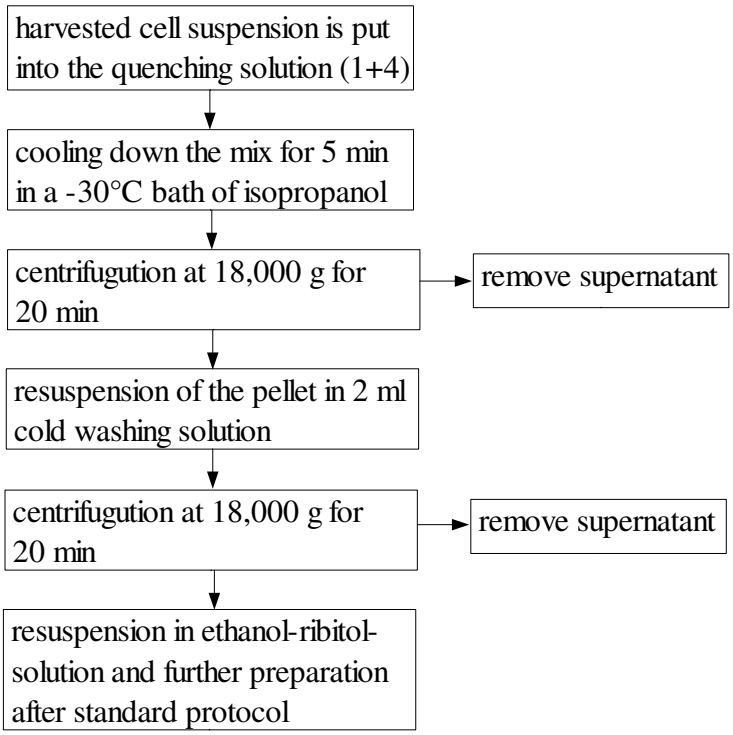

Figure 20. Workflow of the cold glycerol saline quenching performance

1.14 Plasmid rescue technique

The insertion site of the plasmid in the genome of *Corynebacterium glutamicum* mutant was identified using the plasmid rescue technique (Tauch et al., 1995). Figure 21 gives an overview over the method which is described in detail afterwards.

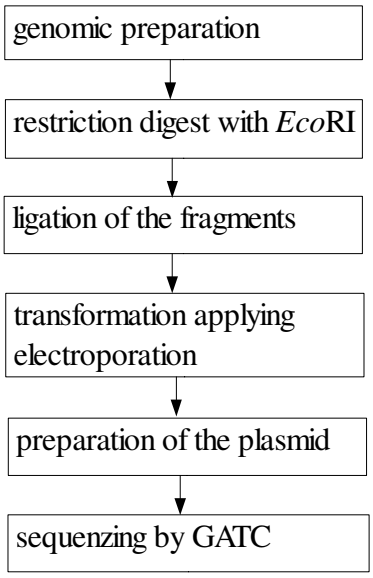

Figure 21. Overview over the plasmid rescue technique

Genomic preparation

For the genomic preparation a single colony of a *C. glutamicum* transposon mutant was inoculated in 5 ml BHI-Kanamycin (25 µg/ml) in a test tube over night at 30°C and 180 rpm. Culture was harvested by centrifugation at 3220 g and 4°C for 15 min the next day. After discarding of the supernatant the pellet was resuspended in 500 µl B1 and incubated for 1 h at 37°C and 220 rpm. Afterwards, 60 µl of a 10% sodium dodecyl sulfate solution were added and mixed, 250 µl proteinase K added, again mixed and incubated for 1 h at 37°C and 220 rpm.

For the preparation of the DNA phase lock-test tubes were prepared. Tubes were centrifuged for 1 min and 10,000 g to spin down the gel and stored at 4°C until use. 800 µl of the cell lysat and 800 µl of a phenol-chloroform-solution (25:24, v/v) were transferred into the phase lock-test tubes. Tubes were intensely mixed for 2 seconds and incubated for 5 minutes at room temperature before they were centrifuged at 12,000 g and 4°C for 5 minutes. The clear supernatant was transferred into a fresh 2 ml-tube. 1250 µl pure ethanol (~100%) and 50 µl sodium acetate solution (3 M) were added and the tube was reversed for mixing. After 10 minutes of incubation at room temperature the sample was centrifuged at 14,000 g and 4°C for 15 minutes. The supernatant was discarded afterwards, the pellet was washed with 1 ml ethanol solution (70%) and the sample was centrifuged at

14,000 g and 4°C for 15 minutes. The washing step was repeated one time. The DNA pellet was then dried and dissolved in 105 µl sterilized double distilled water.
To remove the RNA 100 µl of the prepared sample were incubated with 5 µl RNase A for 60 minutes in the thermo mixer at 37°C and 400 rpm.
The remaining 5 µl sample was analyzed on an agarose gel.

Restriction digest of genomic DNA

For the restriction digest 90 µl of the genomic DNA, 11 µl *Eco*RI buffer (10 fold), 4 µl *Eco*RI and 1 µl RNase A were mixed. Incubation was done over night in a thermo mixer at 37°C and 400 rpm.

Ligation of the fragments

After cleavage the samples were heated to 70°C and held at this temperature for 20 min to denature the restriction enzyme. Samples were cooled to room temperature afterwards and 5 µl were analyzed on an agarose gel.
For ligation 85 µl restricted DNA, 10 µl ATP solution and 5 µl T4-DNA-ligase were mixed and incubated over night in a thermo mixer at 16°C and 300 rpm.

Transformation by electroporation

For electroporation electro competent *E. coli* (DH5α mcr) cells had to be prepared. *E. coli* was stored as glycerol stock at -80°C. Cells were streaked out on LB-plates and incubated at 37°C for one day. One colony was picked and transferred to 25 ml LB medium in a 100 ml-shaking flask. Incubation was performed over night at 37°C and 220 rpm. One milliliter of the over night culture was used for inoculation of 250 ml fresh LB in a 1000 ml-shaking flask. *E. coli* was raised to an optical density at 600 nm of 0.5...0.7 at 37°C and 220 rpm. Afterwards, the culture was left on ice for 15 min before centrifugation at 1000 g and 4°C was done for 15 min. The supernatant was discarded and the pellet resuspended in 500 ml sterile, cold (4°C) double distilled water and centrifuged under the same conditions for 20 min. The washing step was repeated one time. After decantation of the supernatant the pellet was resuspended in 10 ml sterile, ice cold, 10% glycerol solution and centrifuged for 20 min again. The supernatant had to be carefully decanted one more

time and the pellet resuspended in 1 ml sterile, ice cold, 10% glycerol solution. Cell suspension was divided into aliquot parts of 40 µl and frozen in liquid nitrogen before it was stored at -80°C.

For the transformation an aliquot for each sample had to be removed from the freezer and hold on ice. 20 µl of ligated DNA was dialyzed for 10 minutes against double distilled water. Additionally, 2 µl of the pure plasmid was prepared this way, too. It was used as positive control. Pure SOC medium was used as negative control to see, whether transformation worked properly. 10 µl of the dialyzed DNA as well as 1 µl of the controls were transferred to an aliquot electro competent cells. Mixture was transferred into a cuvette for electroporation and placed in a electroporation machine at 1700 V for around 5 ms. Afterwards, the sample was mixed with 1 ml SOC, transferred to a sterile tube and incubated for ~45 min at 37°C and 600 rpm. Subsequently, 300 µl and 700 µl of each sample were streaked out on LB-kanamycin-plates (50 µg/ml) and incubated at 37°C over night.

Preparation of the plasmid

Colonies of the successfully transformed mutants were transferred to 5 ml LB-kanamycin (50 µg/ml) in a test tube and incubated at 37°C and 220 rpm over night. Cells were harvested by centrifugation at 4000 g and 4°C for 10 min. All applied solutions as well as the used protocol were derived from the *Wizard Plus SV Minipreps DNA Purification System* from Promega or the *peqGOLD Plasmid Miniprep Kit I* from Peqlab.

After discarding of the supernatant the pellet was resuspended in 250 µl cell lysis solution and mixed by reversion. 3 min incubation at room temperature followed. 10 µl alkaline protease solution were added, mixed and incubated for 5 min again. Afterwards, 350 µl neutralization solution was given to the sample and the tube was mixed at 14,000 g for 10 min. The supernatant was transferred to a spin column and centrifuged for 1 min under the same conditions as before. Spin column was washed with 750 µl column wash solution followed by centrifugation, washed again with 250 µl column wash solution and centrifuged one more time. 50 µl nuclease-free water was transferred to the spin column and incubated for 2 min at room temperature before centrifugation was repeated for 1 min. During this step the plasmid eluted from the column in the tube. 5 µl of the solution were analyzed on an agarose gel. The plasmid was stored at -20°C.

Agarose gel electrophoresis

The agarose gels were prepared with 1% agarose diluted in TAE-buffer (1 fold). 1 fold TAE-buffer was also used as running buffer during electrophoresis. 5 µl of the sample was mixed with 1 µl 6x loading dye solution (purchased from Fermentas together with the DNA ladder mix). One lane of the gel was used for the marker, which was a DNA ladder mix.

Electrophoresis was performed at 100 V for 50 minutes. The gel was incubated in an ethidium bromide bath for 15 min afterwards. Analysis of the gel was performed using a gel documentation system (G:BOX) where the DNA could be made visible due to trans-illumination using UV light.

Photometric determination of the DNA concentration

DNA concentration of the samples was determined photometrically. 2 µl of the sample were diluted in 498 µl double distilled water. Using a cuvette of silica glass the absorption at 260 nm was determined. An absorption of 1 correlates with 50 µg/ml double-strand DNA.

Additionally, the absorption at 280 nm was measured to identify the protein level (aromatic amino acids). The ratio of both absorptions (A_{260}/A_{280}) is a representative value for the purity of the sample. The value should be in the range of 1.8 to 2.0.

Sequencing and analysis of the insertion site

Sequencing was performed by GATC-Biotech. DNA concentration of the samples was diluted to 75 ng/µl and an aliquot of 30 µl was used for sequencing. As primer the "vorIS"-primer 5'-CTGCACCAATCTCGACTATGCTCAATAC-3' (Feldhaus, 2005) was used.

For further analysis the obtained DNA sequence was converted to the fasta-formate and could be used for Blast analysis on the NCBI web page (http://www.ncbi.nlm.nih.gov/sutils/genom_table.cgi). Search was done against both annotations (Bielefeld and Japan) for the *Corynebacterium glutamicum* wild type strain ATCC 13032 (Kalinowski et al., 2003, Ikeda et al., 2003).

3 Results & Discussion

The first part of this thesis deals with the development of a high-throughput method for metabolome analysis using gas chromatography/mass spectrometry.
In the second part this method was applied to analyze a high number of transposon mutants and also to establish a screening performance in order to find suitable criteria for comparison and selection.
In the third part different quenching methods were compared whereas two of these methods base on results of other research groups and the third one was established in this working group and optimized during this study. Investigations were performed with three different microorganisms.

3.1 Development of a high-throughput method for metabolome analysis

If a high number of samples has to be investigate in a suitable time frame a method like our standard method (Strelkov et al., 2004, see also part 2.7) is not applicable. Therefore, on the basis of this standard method a high-throughput method had to be developed.

3.1.1 Method development

The standard method from our lab was analyzed in detail to find possible starting points for designing a high-throughput method. Figure 22 shows the main parts of the standard method and the selected points for method improvement. The applied changes are described in detail afterwards. With the parallel processing of 96 samples a time reduction by a factor larger than 15, compared to the standard method, was achieved. The procedure is described in detail in chapter 2.8.

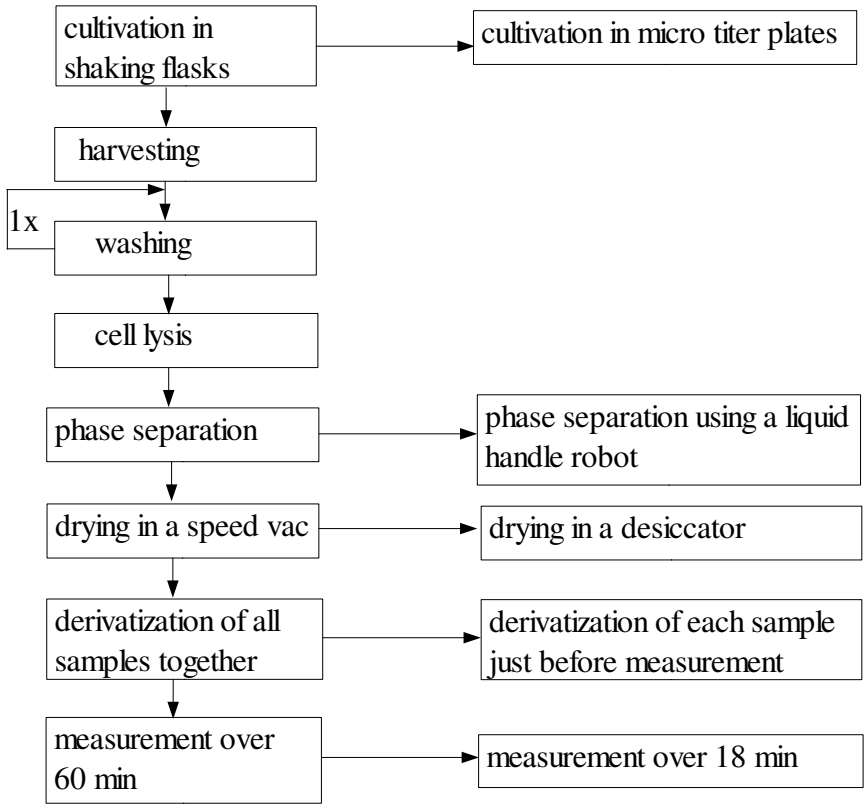

Figure 22. Selected starting points for changes of the standard performance in order to establish a high-throughput method.

The change of the cultivation vessel

In order to handle a high number of samples in parallel the cultivation vessel was changed. Instead of commonly used shaking flasks, cultivation was performed in micro titer plates. Experiments were performed with plates filled only with wild type samples (*Corynebacterium glutamicum* ATCC 13032) to establish the method. And there was a number of questions that had to be investigated:

- Is enough oxygen supplied in micro titer plates?
- How can cross contamination be avoided?
- Are cells growing similarly in each well of the micro titer plate or are there any limitations on some places?
- Is enough cell dry mass produced for metabolome analysis?

Foils as coverage during cultivation

For a good growth of the cells in the 96deepwell plates different foils were tested. The BreathEasy foil which was routinely used in our lab caused some problems. During cultivation some of the water of the medium evaporated. Because the foil is not water permeable droplets were formed on the inner surface of the foil and the foil was dragged into the wells. Consequently, oxygen supply was limited and thus cells showed low growth rates (OD_{595}) of 4.1 ± 0.3 (see figure 23). And furthermore, problems occurred during sample transfer. Because the foil can not be penetrated by tip, it had to be removed. Because of the droplets on the inner surface of the foil, removing of the foil caused sputtering which led to cross contaminations observable in the blank wells.

Problems with foils were already mentioned in literature (Zimmermann et al., 2003) and no single foil was mentioned to overcome all difficulties. Nevertheless, another foil, AeraSeal, was tested. This foil had a completely different structure. None of the above described problems occurred. Because the foil was not dragged into the wells it could be removed easily without causing cross contaminations. But due to the vapor permeability of this foil after 17 h of cultivation, approximately 12% of the medium were evaporated whereas with the BreathEasy foil only half the amount was gone. The cell concentration had been higher after cultivation with this foil because of the loss of water. With the AeraSeal foil cells grew to nearly two times higher optical densities measured at 595 nm of 7.8 ± 1.2 compared to the other foil (see figure 23). Nevertheless, the OD_{595} of the different wells was quite variant.

In order to overcome the difficulties of both foils, they were combined. The AeraSeal foil was placed on the micro titer plate and the BreathEasy foil on top of it. With this combination the advantages of both foils could be combined and the disadvantages could be reduced to almost nothing. Only 5% of the medium were lost after 17 h of cultivation. Furthermore, cells grew to high average optical densities of around 8.1 ± 0.8 (see figure 23). The variation between the wells could also be reduced. Both foils can be removed together without causing any cross contamination.

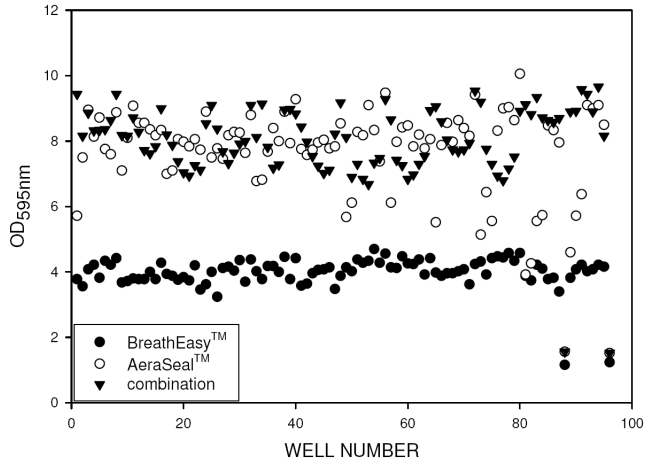

Figure 23. Comparison of the growth of *C. glutamicum* wild type samples in a 96deepwell plate covered with different foils or foil combination (Börner et al., 2007).

Evaluation of the growth in micro titer plates

A complete 96deepwell plate was inoculated with wild type colonies, leaving only two wells not inoculated as blanks. Cultures were always covered with the combination of the above described foils. The main culture was inoculated with the corresponding well of the over night culture (see part 2.8.1 for details). Each well of the over night culture was independent from the others and used for inoculation of a main culture. Again, each well represented an independent main culture. This was a huge contrast to the standard method where three samples are taken from one main culture inoculated from one over night culture. Nevertheless, the average starting OD_{595} in each well was very similar (1.4 ± 0.2) (figure 24). After 7 h of growth the average optical density was 7.4 ± 0.5 (figure 24). No limitation could be found, confirming that the bacteria have the same growth conditions in each well of a 96deepwell plate. Additionally, no change in optical densities of the blank wells was observed. Thus, cross contamination had not occurred.

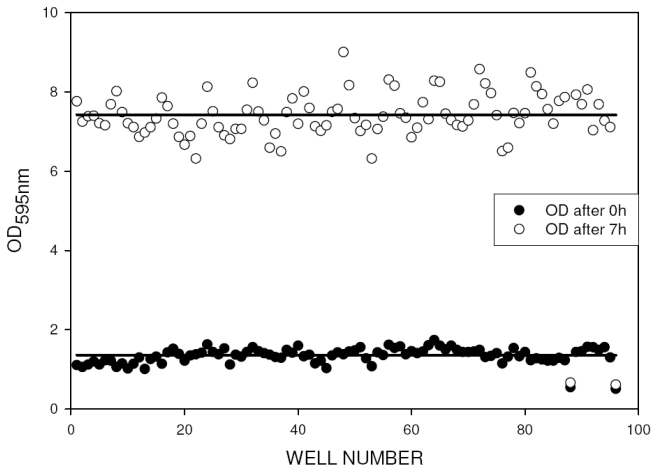

Figure 24. Example for an equal growth of wild type samples cultivated in a 96deepwell plate covered with the two combined foils. No cross contamination occurred (Börner et al., 2007, modified).

Calculation of the available amount of cell dry weight

It could be demonstrated so far, that wild type cultures grow to high optical densities in all wells of a plate. In order to find out whether this growth rate is sufficient for a metabolome analysis with GC/MS, the OD_{595} was correlated to the cell dry weight (CDW). This correlation was determined from two experiments shown in figure 25. In the first part the optical densities of the photometer (600 nm) and the tecan reader for micro titer plates (595 nm) were compared (figure 25A). As blank pure minimal medium (MM1) was used. In contrast to the photometer it was not possible to set a reference value at the tecan reader. Consequently, there is always a shift of the zero-value along the ordinate, which was estimated to be constant around 0.032 ± 0.001.

Additionally, for the OD_{600} the corresponding cell dry weight was determined (figure 25B). Using both established correlations an equation for the calculation of the cell dry weight from OD_{595} values was established (equation 3.1).

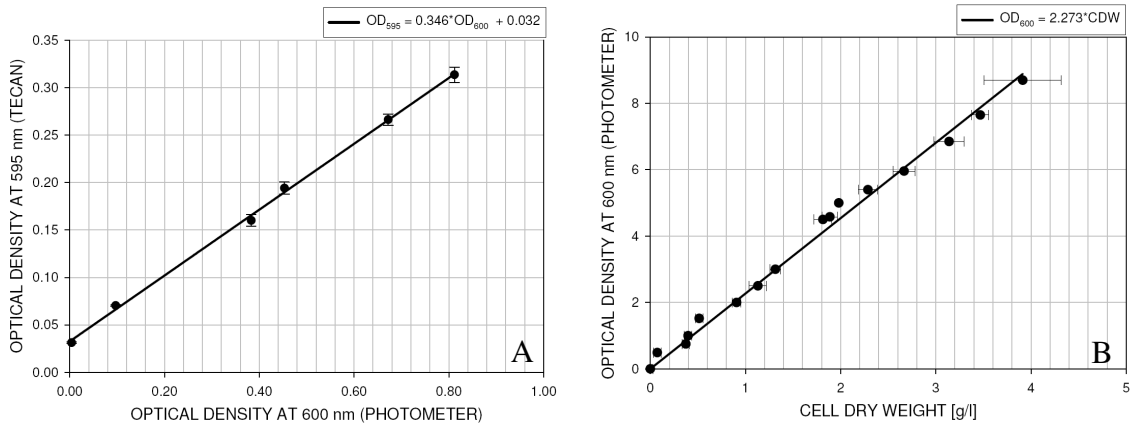

Figure 25. **A** Correlation of the optical densities of the photometer (600 nm) and the tecan reader (595 nm). **B** Relation of the cell dry weight and the OD_{600}.

$$CDW[g/l] = 1.272 * OD_{595} - 0.041 \qquad (3.1)$$

With the equation (3.1) the average amount of cell dry weight was calculated - which was 3.9 mg. The volume in each well was assumed to be 415 µl (400 µl MM1 + 25 µl over night culture - 2*5 µl sample for OD_{595} measurement). Compared to the standard method in which around 22 mg were harvested, a reduction of cell mass by a factor of 5.6 was calculated.

It was necessary to determine whether the extracted sample amount from 3.9 mg cells would be enough for metabolome analysis, and the results hereto will be described and discussed in detail in part 3.1.2.

Automated phase separation

Cells were harvested by centrifugation of the whole micro titer plate. Also the washing steps were performed in the plate. During these parts, the 96deepwell plate had to be covered with a silicon mat. For cell lysis in the ultrasonic bath at 70°C the whole plate had to be closed with an adhesive foil and a metal brace. This foil was temperature stable as well as solvent resistant. The metal brace was necessary to assure a tight closure, to avoid any vapor leakage. Because of the metal brace, the cooling step had to be extended.

A liquid handle robot, the MPS2 twister autosampler, was used to remove the upper aqueous phase from 94 samples during phase separation. The machine was equipped with a

1 ml syringe. In order to avoid any contamination with the apolar phase the depth of immersion had to be estimated carefully. It was adjusted to 30 mm. Additionally, filling speed of the syringe had to be optimized. If the syringe is filled too fast, the apolar phase would be drawn in, too. The filling speed was set to 40 µl/s. After evaluation of these two parameters they could be used for all experiments. Approximately 580 µl (±20 µl) of the upper aqueous phase could be removed this way and were transferred into tapered glass vials.

Drying of the samples

A desiccator with phosphor pentoxide as desiccant and a vacuum pump were used for drying of up to 150 samples at a time. The normally used speed vac which is only capable of drying 72 samples at a time was replaced. With this change more than twice the number of samples could be prepared together.
The pressure had to be reduced carefully in order to avoid a delay in boiling. This was done for duration of one hour. Afterwards the samples were hold nearly under vacuum over night.

Automated sample derivatization

The glass vials with the dried samples were sealed with magnetic caps and placed in the autosampler of the GC/MS system. Of the high number of so far prepared samples 96 could be placed in the autosampler at a time. The remaining ones were stored at 4°C. Before using the stored samples, they had to be placed in the desiccator for at least one hour again to remove condensed water.
Derivatization was performed automatically from the autosampler (with a 10 µl syringe) sample by sample after a certain schedule. Because the syringe had to be used both for derivatization and for sample injection it was not possible to use a bigger one. Otherwise the reproducibility of injection of 2 µl sample would decrease.
The detailed workflow is described in chapter 2.8.2. Derivatization reagent is always given to one sample followed by mixing and incubation. Some minutes later the the next sample was prepared likewise and so on. This scheduled performance made sure that each sample was freshly prepared just before injection. The time shifts between sample preparations were calculated by the Maestro software of the autosampler. With this automated

derivatization any chemical conversions due to differences in standing times after completed derivatization till injection could be avoided.

Adapted GC/MS measurement and metabolite detection

The metabolome analysis was performed with a GC/*AccuTOF* in EI mode equipped with an autosampler. Samples were injected in a PTV injector and evaporated. A detailed comparison of the 60 min standard run and the adapted 18 min run is shown in table 13. In chapters 2.7.3 and 2.8.3 both GC/MS analyses are described in detail. The injector performance was not needed to be changed. For both run types the same schedule was used. To shorten the GC-run temperature rates were increased by a factor of four. The holding time at the end of the run was reduced from 10 min to 6 min. Due to the increased ramps the solvent delay could be reduced to 3.9 min.

Table 13. Parameters of 60 min GC-run and 18 min fast GC-run

Parameter	60 min run	18 min run
Injector		
Start temperature	70°C	
End temperature	280°C	
Rate	12 K/s	
GC		
Start temperature	70°C	
1st holding time	1 min	
1st rate	1 K/min	4 K/min
Temperature after 1st rate	76°C	
2nd rate	6 K/min	24 K/min
End temperature	325°C	
2nd holding time	10 min	6 min
Solvent delay	6 min	3.9 min

The settings of the mass spectrometer were the same for both GC-runs except for the scan rate. The spectrum recording time of course was adapted to the length of the runs. During 18 min of measurement the same information regarding the sample composition had to be handled as during 60 min runs. A more compact data amount in shorter time was the result

and the scan rate needed to be increased from 2 scans/s to 5 scans/s. With this higher scan rate a loss of information could be avoided.

Furthermore, to use the reduced, available cell dry weight after cultivation in micro titer plates (5.6 times lower mass compared to standard cultivations) for analyzable measurement the split ratio was changed from 1/25 to 1/10. This way a 2.5 times higher amount of sample was transferred to the GC-column and was analyzed. With it the lower biomass could be compensated.

After the GC/MS measurement the metabolite detection could be done according to the standard protocol. Our internal library could still be applied because of the use of retention indeces instead of retention times. The retention times of the alkane series in a 60 min run and in a 18 min run are summarized in table 14.

Table 14. Retention times and indices of the alkanes in 60 min runs and 18 min runs

Alkane	~RT in 60 min run	~RT in 18 min run	RI
Decane	7 min	4.5 min	1000
Dodecane	13 min	6 min	1200
Pentadecane	20.5 min	8 min	1500
Nonadecane	28 min	10 min	1900
Docosane	33 min	11 min	2200
Octacosane	41 min	13 min	2800
Dotriacontane	46 min	14.5 min	3200
Hexatriacontane	49 min	17.5 min	3600

Nevertheless, RI-values of the identified derivatives after measurements over 18 min were investigated. Additionally, using the information derived from the alkane test (“time standard”), for all substances in our library the retention times could be estimated. This was done using the Kovàts equation (see part 1.2.1, equation 1.5) in the other direction. The majority of substances should demonstrate a linear behavior for the changed elution time. This results from the fact that only the temperature rates were increased, but the same column was used. The information from over 1000 measurements was also used to improve the retention indeces of the identified derivatives. An improved standard library for the 18 min runs was generated after combining the information from the measurements and the estimated RI-values. It was applied for further identifications afterwards. The

whole list of derivatives and the RIs is shown in table A in the appendix. Table 15 gives a short summary of the changes in the retention time. As assumed over 88% of the substances had changes in their RIs of less than 20 ($\Delta RI=|RI_{60}-RI_{18}|$). Less than 3% of the derivatives had significant changes over 100 (ΔRI).

Table 15. Overview to changes in retention index due to a changed temperature profile in the 18 min run.

Change in RI ($\Delta RI=\|RI_{60}-RI_{18}\|$)	Affected derivatives [%]
< 20	88.2
> 20, < 30	4.6
> 30, < 40	2.2
> 40, < 50	1.0
> 50, < 100	1.2
> 100, < 1000	2.8

The obtained result confirmed the assumption that most of the substances had only slight changes in their RI-values according to the increased temperature ramp. Only few derivatives changed dramatically in their retention behavior, eluting earlier or later compared to the long measurements. A positive effect was the possible separation of substances coeluting in a 60 min run. On the other hand, it was also possible that some derivatives, which eluted separately in the long term run, now in the 18 min run appear unseparated. An example is shown in figure 26. Alanine 3TMS is coeluting with fumaric acid 2TMS in the long term run. In contrast, it is found clearly separated as single peak in the short term run.

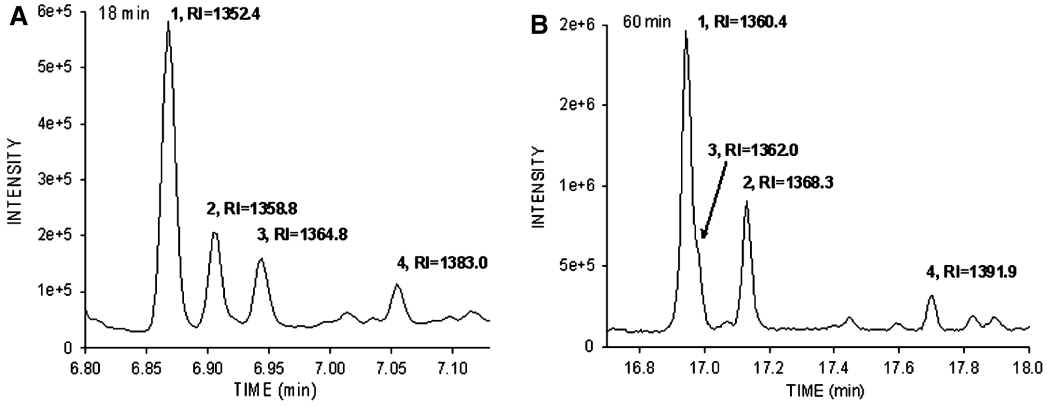

Figure 26. Example for a substance (**3** alanine 3TMS) which appeared separated in a 18 min run (**A**) but coeluting in a 60 min run (**B**). **1** fumaric acid 2TMS, **2** serine 3TMS, **4** threonine 3TMS (Börner et al., 2007, modified).

The identification of a compound was not only done according to its retention index. Additionally, the mass spectrum was used which is substance specific. Both information are combined in our internal standard library and had been applied. Mass spectra showed nearly no effects regarding the GC-run. Maybe some moieties of former or later eluting substances can be seen as minor mass lane(s). Still, if two substances coelute the single spectrum needs to be extracted. This could be done with the deconvolution algorithm of AMDIS.

Furthermore, our internal standard library was developed on a quadrupol MS with an EI-source. The mass spectra are independent of any detector (MS) if the same ionization method is used and thus they could be applied to the TOF MS with the EI-source without any problem.

3.1.2 Method evaluation

In order to evaluate the new high-throughput performance it was compared to the standard protocol. The major results are summarized in table 16. Obviously the reduction of biomass after cultivation in a 96well format and the measurement over 18 min reduced the number of detectable peaks (based on AMDIS) as well as the number of observable and quantifiable compounds. However, the reduction is still within tolerance range as only 15%

less peaks were detected and 7% less compounds were quantifiable. Applying our internal library, still 83% of the compounds were identified. Furthermore, with the high-throughput method the relative standard error could be highly reduced from 25% (standard performance) to 13%.

Table 16. Comparison of the developed high-throughput method and the standard method (Börner et al., 2007, modified).

	standard method	high-throughput method
Observable peaks	~1200	~1020
Quantifiable peaks	~700	~650
Library hits	~180	~150
Mean relative standard error [%]	~25	~13

The resulting total ion currents - both for 60 min run of a standard method (A) and 18 min run of a high-throughput method (B) - are shown in figure 27. They are the result of an analysis of a *C. glutamicum* wild type sample. The TICs are quite similar: the 18 min run represents the compressed profile of the 60 min run. The relative intensities are reduced in the shortened run by a factor of 100.

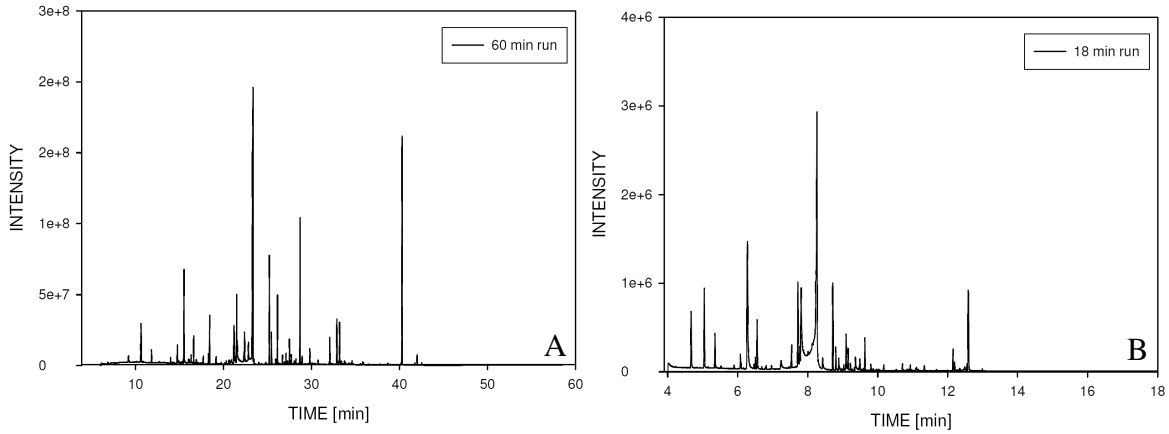

Figure 27. Total ion currents of a *C. glutamicum* wild type sample from the standard performance (**A**) and the high-throughput performance (**B**).

Additionally, triplicates from wild type samples raised at different positions on the same 96deepwell plate were compared and the Pearson correlation coefficient was calculated

using the logarithmic values of the relative concentration vectors. An example is shown in figure 28. The average correlation gave a high value of 0.99 ± 0.01.

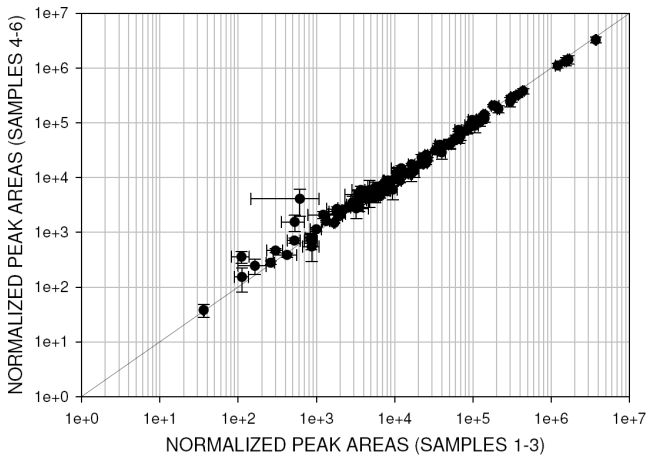

Figure 28. Example for a comparison of triplicates of wild type samples cultivated in different wells of the same micro titer plate (Börner et al., 2007).

The here presented evaluation criteria show clearly that the high-throughput performance revealed satisfying results and hence this method can be used for reliable metabolome analyses.

3.2 Screening of transposon mutants

After the development of a well performing high-throughput protocol, the method was used to start screening of the *Corynebacterium glutamicum* transposon bank. Because the analysis of more than 10,000 mutants is still very time consuming, a pilot project started. More than 300 randomly selected mutants were investigated. The information from this research were then used to develop suitable screening criteria.

3.2.1 Growth of analyzed transposon mutants

Transposon mutants were always stored in micro titer plates as glycerol stocks. Cultures had to be transferred in first instance on agar plates (see chapter 2.8.1). This was done using a cryo replicator. Using this replicator the glycerol stocks remained frozen and only the surface thawed due to the contact with the warmer replicator. Cells could be transferred this way. The used device had been built at our institute and could be autoclaved.
In the first instance the growth behavior of 325 transposon mutants was investigated. Additionally, more than 150 wild type samples were examined and used for comparison purpose. The wild type samples showed an overall growth of 6.12 ± 0.90 when measuring the optical density at 595 nm. The mean value of all mutants was slightly lower and calculated with 5.24 ± 1.49. The distribution of the mutants according to their growth is shown in figure 29. In contrast to cultures raised in a shaking flask where the optical density is calculated as mean of three samples from one culture, the optical density of samples raised in plates was the mean of three independent wells and cultures of one mutant. Approximately 9% of the cultivated mutants revealed a growth decrease of more than 50% when compared to the mean optical density of the wild type. Furthermore, around 5% showed growth rates of only 50% to 75%. In short that means around 14% of 325 examined mutants were growth-deficient. According to the growth behavior of the chosen mutant set it could be assumed that these data were a representative quantity. Consequently, all following results could be assumed as representative for *C. glutamicum*.

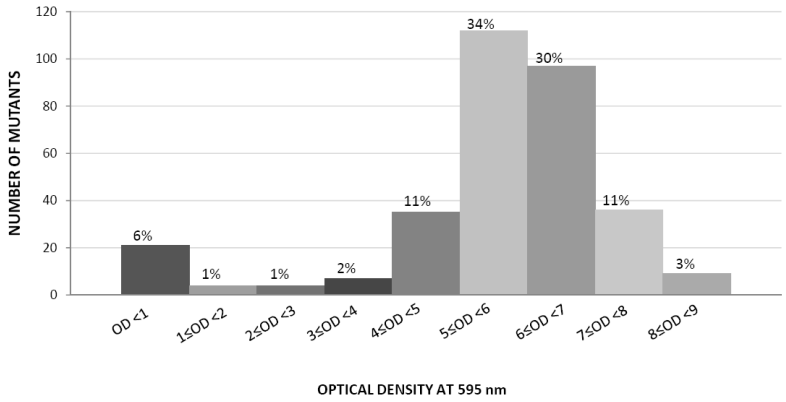

Figure 29. Distribution of 325 analyzed transposon mutants according to their growth after 7 h of inoculation.

For 318 transposon mutants a successful metabolome analysis was performed when applying our established high-throughput method. The metabolites could be identified using our internal standard library and the relative standard error for a mutant was calculated (from triplicates). The relation of the error according to the growth behavior of the mutants is displayed in figure 30. As expected, growth-deficient mutants often had an increased error due to the reduced cell mass available for metabolome analysis. Nevertheless, some mutants with reduced growth showed relatively low standard errors as well. The calculated mean of the relative standard error over all mutants was 17.4 ± 7.7. Approximately 64.5% of the growth-deficient mutants revealed an increased error.

Transposon mutants grown to higher optical densities are distributed cloud-like around the introduced line which represents the rough trend (figure 30). The increased error of some mutants with good growth behavior might be an indication for changes in metabolite levels due to genetic perturbation. Sample treatment and measurement were performed as routine procedures in complex sets, thus changes in triplicates were more likely the result of differences in the metabolome, resulting from variations due to transposon integration in the analyzed organism. The tested transposon mutants therefore could be used for identification of suitable screening criteria. Nevertheless, some mutants might have had increased errors due to problems during performance, especially after difficulties with the GC/MS-system (e.g. increased standing times because of system tuning).

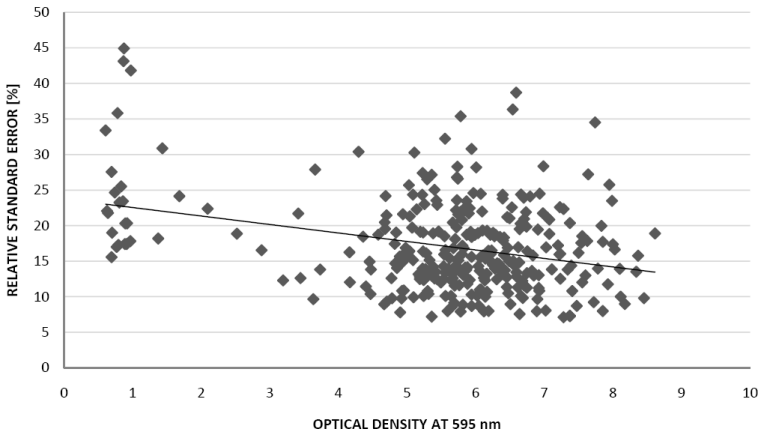

Figure 30. Spreading of the overall relative standard error [%] according to the corresponding optical density at 595 nm for tested transposon mutants. The black line describes the rough trend.

3.2.2 Development of suitable screening criteria

For a direct comparison of metabolic profiles, the wild type samples (2 independent triplicates) were always prepared together with the mutants on the same plate. Analysis of the wild type could therefore reveal systematic problems which possibly had occurred.

The Pearson correlation coefficient (r) was calculated using the logarithmic values of the relative concentration vectors of all determined metabolites. The reference was always the parallely handled wild type from the same cultivation. The distribution of the 318 investigated mutants according to the calculated correlations is shown in figure 31. Approximately 78% of all examined mutants revealed a very good correlation between 0.9...1. Altogether for around 89% a correlation value higher than 0.8 was calculated. Still around 11% of all tested transposon mutants displayed a low correlation when compared to the wild type what is obviously the result of the gene disruption. In comparison, the correlation coefficient of two triplicates of wild type samples on the same plate revealed values of 0.96 ± 0.02.

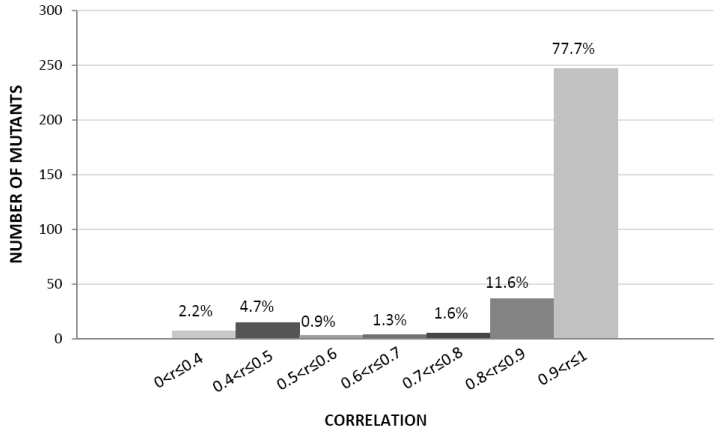

Figure 31. Distribution of the correlation values (r) of 318 transposon mutants related to the wild type raised on the same plate.

One reason for a reduced correlation coefficient had been growth-deficiency. In order to investigate this in detail, correlation and growth were related. The result is displayed in figure 32. The distribution clearly indicated two groups. The first group of mutants was the growth-deficient one. These mutants were located in the left part of the plot showing a linear behavior between correlation and optical density. For these mutants the low correlation to the wild type was the consequence of the reduced growth and the resulting decrease in cell mass. An increase in the amount of analyzed cells could possibly compensate this effect.

The second group was found in the right part of the plot in figure 32. Mutants with good growth were distributed around an average correlation of 0.93 ± 0.10. However, some mutants with reduced correlation coefficient but good growth values were also visible. These transposon mutants possess changes in their phenotype and are therefore interesting for further investigations.

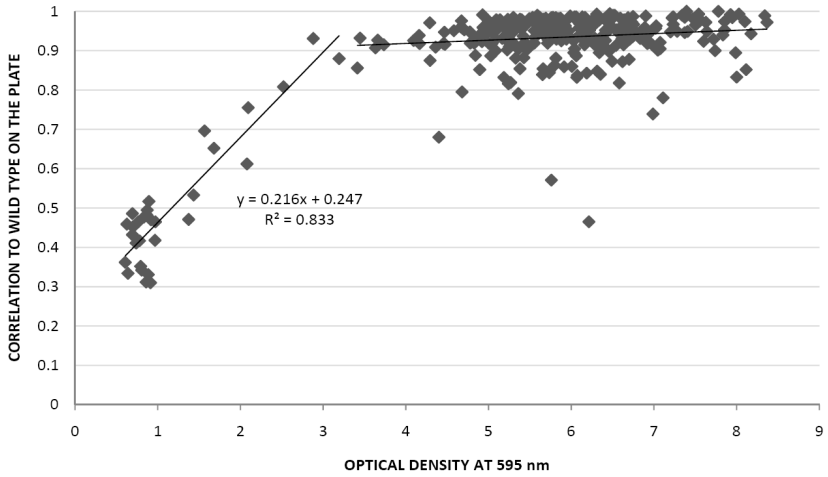

Figure 32. Interrelation of the calculated correlation values of 318 analyzed mutants and their growth values.

In order to have a representative wild type data set more than 150 examined wild type samples were combined and a reference list was created. A comparison to this native state could reveal important variations, not only of the mutants but also of the wild type samples raised together with the mutants. The samples used for this reference list were derived from different and independent cultivations, which had been performed by two operators. The correlation coefficient between independent operators calculated from logarithmic mean values of all identified metabolites derived from all wild type samples was 0.94. This demonstrates the high reproducibility of the method - not only if the test is performed on different testing days, but also if it is performed by different users.

All metabolites that had been identified so far in more than 150 wild type samples were combined and summarized as a reference list with currently 216 different metabolites (structurally characterized but also structurally unidentified ones - so called “unknowns”). This list comprises the mean of the relative concentrations normalized to ribitol, the standard errors and the relative errors as well as the occurrences in the analyzed samples. This reference list which is extended continually represents in an excellent way the phenotype of the wild type.

An overview of the distribution of the metabolites according to their relative standard errors is shown in figure 33. Around 73% of the substances revealed an error lower than 20%. For example most of the phosphorylated compounds, for example, were found to have errors between 20% and 30%. The relative standard error of most alcoholic

compounds was quite high - more than 40%. Besides these compounds, substances with more than 50% error were often structurally unidentified ("unknowns").

A critical fact is that the number of identified metabolites varied among analyses. This happened despite standardized cultivation performance, harvesting, sample preparation and measurement procedures. Mostly this came from variations of the sensitivity of the used *AccuTOF*-MS due to independent manual tunings and the high sample throughput. Consequently, average relative standard errors of some metabolites were reduced due to their high occurrence. Nevertheless, the high reproducibility of the performance was obvious. The overall relative standard error was calculated to be 16.2% on average.

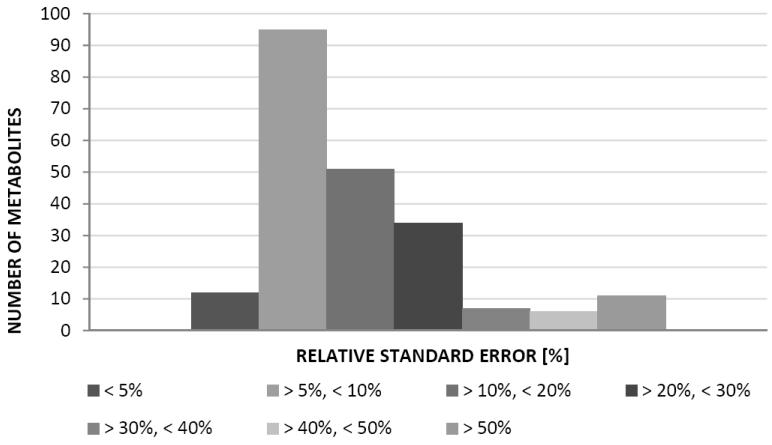

Figure 33. Distribution of 216 different reproducible metabolites, combined on a wild type reference list, according to their relative standard errors.

When applying this reference list on mutant samples, metabolites with higher relative standard error occurred more often to have changed than those with smaller errors. But due to the higher variance of these metabolites changes were not likely to be the result of gene disruption in every case. To circumvent this difficulty a threshold for each metabolite (T_{Met}) was considered. Using the information from the derived wild type list a metabolite was regarded as significantly changed if the absolute value of the difference between the relative concentration values of this compound on the reference list (Ref) and in the mutant sample (MT) related to the relative standard error of this metabolite on the reference list ($Error_{Ref}$) exceeded the factor six (equation 3.2). After tests this factor was chosen, because it led to results which were a good compromise between sensitivity and number of

identified differences. A change of the factor led to more (reduced value) or less (increased value) sensitive thresholds which corresponded to a higher or a lower number of identified differences. With the application of this equation the metabolites with changed levels due to the genetic perturbation were identified. The whole reference list is summarized in table B of the appendix.

$$T_{Met} \cdot \left| \frac{(Ref - MT)}{Error_{Ref}} \right| > 6 \qquad (3.2)$$

A representative overview of the different classes of identified metabolites, their relative errors and their occurrences in the wild type samples (details from the reference list, see also table B in the appendix) is summarized in table 17. The above described threshold was applied on each wild type sample and mutant. The frequency of each metabolite as variant in these samples is also displayed. Metabolites which were found to be changed very often - in the wild type samples - had to be regarded as less specific. Variances of that kind might result from biological and environmental changes. The metabolites tryptophan and 2-hydroxyglutaric acid were identified in changed levels in around 15% of the wild types. That means, both variated quite much. Consequently, they were also found to be changed in around 80% of the mutants. These changes surely were only in a few cases the result of the genetic perturbation, but more often it was the biological or environmental variance of the compound itself. In the case of tryptophan these observation might be due to the low solubility in polar solvents. Thus, measurement with the applied protocol is difficult.

The metabolites AMP, 5-oxoproline, aspartic acid, gamma-glutamylleucine, serine, maltose and trehalose, 2,6-diaminopimelic acid, hexadecanoic acid, pyrophosphoric acid, pyruvic acid as well as quinic acid were identified as changed in more than 60% of the analyzed mutants. In wild type samples up to 14% variation was observed for these compounds which is quite high compared to other metabolites. Identification of these 12 metabolites as changed in a sample has therefore to be regarded as less specific. For example pyruvic acid and AMP are both involved in many different pathways. Consequently, it was not very surprising that these compounds often pertained to changes.

On the other hand, malonic acid and hydroxylamine had been very often identified in the samples. But the first of them was only found changed in less than one percent of the wild

type and around 3% of the mutant samples. Therefore, changes might come from genetic perturbation. The compound itself did not seem to be affected by biological or environmental variations. Hydroxylamine was identified as varying in only nine percent of wild type and 24% of mutant samples. But these compound is often an artifact introduced by the derivatization reagents (Herebian et al., 2007).

Table 17. Representative overview of identified metabolites, their relative standard errors and occurrences in more than 150 analyzed wild type samples as well as the number of changed ones in wild type samples and mutants.

Amino acids	Relative error [%]	Occurrence [%]	Number of changes in wild type	Number of changes in mutants	Amino acids	Relative error [%]	Occurrence [%]	Number of changes in wild type	Number of changes in mutants
2-Aminobutyric acid	4.12	80.1	9	127	Leucine	7.29	84.6	11	134
5-Oxoproline	6.03	100.0	17	195	Lysine	5.15	98.1	8	118
Alanine	6.20	100.0	12	138	Methionine	18.46	69.2	5	52
Aspartic acid	9.19	98.7	17	234	N-Acetyl-L-glutamic acid	5.38	98.1	9	100
beta-Alanine	5.79	99.4	13	144	N-Acetyl-L-glutamine	7.54	88.5	17	176
Cycloleucine	5.26	67.9	7	72	O-Acetyl-serine	11.29	71.2	12	133
gamma-Glutamylleucine	7.71	87.2	15	208	Phenylalanine	5.23	98.1	10	139
gamma-Glutamylvaline	13.63	90.4	13	138	Proline	7.06	96.2	17	183
Glutamic acid	6.28	99.4	15	163	Serine	6.58	99.4	16	197
Glutamine	8.41	91.7	17	170	Threonine	7.46	98.7	16	180
Glycine	12.71	98.1	11	177	Tryptophan	6.85	93.6	23	242
Homoserine	6.02	94.9	13	170	Tyrosine	6.81	98.1	7	133
Isoleucine	6.51	95.5	8	142	Valine	5.42	99.4	10	125
Organic acids	Relative error [%]	Occurrence [%]	Number of changes in wild type	Number of changes in mutants	Organic acids	Relative error [%]	Occurrence [%]	Number of changes in wild type	Number of changes in mutants
2,6-Diaminopimelic acid	10.50	78.8	16	211	Hexadecanoic acid	6.29	96.8	17	196
2-Hydroxybutanoic acid	10.36	67.9	12	131	Lactic acid	6.02	99.4	8	187
2-Hydroxyglutaric acid	6.86	96.2	24	282	Lactyllactate	6.80	48.1	2	45
2-Phosphoglyceric acid	11.17	50.6	11	135	Malic acid	5.90	98.7	12	145

Organic acids	Relative error [%]	Occurrence [%]	Number of changes in wild type	Number of changes in mutants	Organic acids	Relative error [%]	Occurrence [%]	Number of changes in wild type	Number of changes in mutants
3-Hydroxy-2-tetradecyl-octanoic acid	6.14	64.7	8	86	Malonic acid	17.33	87.8	1	10
3-Phosphoglyceric acid	5.01	98.1	13	137	Nicotinic acid	21.31	66.0	5	51
alpha-Ketoglutaric acid	7.72	98.7	23	186	Oxalic acid	22.24	12.2	1	6
Benzoic acid	19.63	98.1	1	3	Phosphoenolpyruvic acid	6.08	98.1	10	150
Citric acid	7.26	97.4	14	168	Pyrophosphoric acid	6.89	96.2	12	212
Fumaric acid	5.03	98.7	14	184	Pyruvic acid	5.16	98.1	10	192
Glyceric acid	7.33	95.5	15	177	Quinic acid	6.53	98.1	17	212
Glycolic acid	35.13	85.3	2	21	Succinic acid	5.34	99.4	17	116
Phosphorylated compounds	Relative error [%]	Occurrence [%]	Number of changes in wild type	Number of changes in mutants	Phosphorylated compounds	Relative error [%]	Occurrence [%]	Number of changes in wild type	Number of changes in mutants
2-Deoxyribose-5-phosphate	28.90	35.3	2	30	Glucose-6-phosphate	19.29	84.6	6	62
6-Phosphogluconate	28.02	78.2	5	61	Glycerol-3-phosphate	5.82	98.7	11	180
AMP	6.29	89.1	15	193	Mannose-6-phosphate	24.35	78.8	4	64
Erythrose-4-phosphate	23.89	26.3	3	26	Ribose-5-phosphate	31.28	31.4	3	58
Fructose-1,6-biphosphate	12.60	73.7	8	76	Ribulose-5-phosphate	22.59	75.6	6	64
Fructose-6-phosphate	30.19	33.3	3	40	Uridine-5'-monophosphate	6.92	76.3	10	116
Glucosamine-6-phosphate	24.15	78.8	4	49	Xylulose-5-phosphate	23.73	35.9	2	13
Alcohols	Relative error [%]	Occurrence [%]	Number of changes in wild type	Number of changes in mutants	Alcohols	Relative error [%]	Occurrence [%]	Number of changes in wild type	Number of changes in mutants
1-Monooleoylglycerol	23.59	53.8	3	39	Glycerol	5.35	99.4	16	124
1-Monopalmitoylglycerol	11.71	71.8	9	117	Hexadecanol	16.22	76.9	3	56

Alcohols	Relative error [%]	Occurrence [%]	Number of changes in wild type	Number of changes in mutants	Alcohols	Relative error [%]	Occurrence [%]	Number of changes in wild type	Number of changes in mutants
Diethyleneglycol	9.49	54.5	2	21	Mannitol	2.67	75.0	7	100
Erythritol	25.80	34.6	4	45	Tetradecanol	45.68	65.4	0	0
Sugars	Relative error [%]	Occurrence [%]	Number of changes in wild type	Number of changes in mutants	Sugars	Relative error [%]	Occurrence [%]	Number of changes in wild type	Number of changes in mutants
Fructose	18.29	34.0	2	23	Mannose	10.80	89.7	9	132
Glucose	9.90	99.4	17	142	Sucrose	18.62	57.7	4	56
Isomaltose	20.97	72.4	9	86	Trehalose	4.41	98.7	18	252
Lactose	7.14	76.9	13	164	Xylulose	14.35	53.2	3	27
Maltose	5.16	99.4	21	260					
Others	Relative error [%]	Occurrence [%]	Number of changes in wild type	Number of changes in mutants	Others	Relative error [%]	Occurrence [%]	Number of changes in wild type	Number of changes in mutants
5-Deoxy-5-Methylthioadenosine	6.03	77.6	15	223	Succinic acid monomethylester	4.76	78.2	13	153
Adenine	6.89	88.5	12	138	Thymine	6.89	71.2	7	70
Adenosine	6.62	91.7	15	145	Uracil	8.56	91.0	11	152
Cytosin	4.37	55.8	6	74	Urea	22.45	98.1	3	33
Hydroxylamine	13.54	95.5	13	76	Uridine	6.83	98.7	17	184
Nicotinamide	7.25	94.9	9	105					

The wild type reference list, representing a kind of native wild type state, was afterwards applied on all mutants. As described before a correlation coefficient was calculated for each mutant. However, this time mutants were correlated to this reference list. The distribution of the calculated correlation values according to the optical density of each mutant after 7 h of inoculation is shown in figure 34. A similar picture as before (see figure 32, correlation of the mutants to the wild type from the same plate) was revealed. Again mutants with growth-deficiencies revealed a decreased correlation coefficient. A linear interrelation of correlation and optical density was found. Therefore, the reduced correlation values were due to the reduced growth and the low corresponding cell mass. But the picture for mutants grown to higher optical densities looked different from the one seen in figure 32. The average correlation coefficient of these mutants was 0.75 ± 0.09. The mutants were spread like a big cloud around the mean value (the trend is indicated as black line in figure 34). Mutants with high growth values but reduced correlations were the most interesting ones. They were found below the trend line in the right part of the plot. The high number of changes in the metabolome of these mutants resulted in decreased correlation values. These huge differences are likely the result of an important genetic perturbation leading to a changed phenotype.

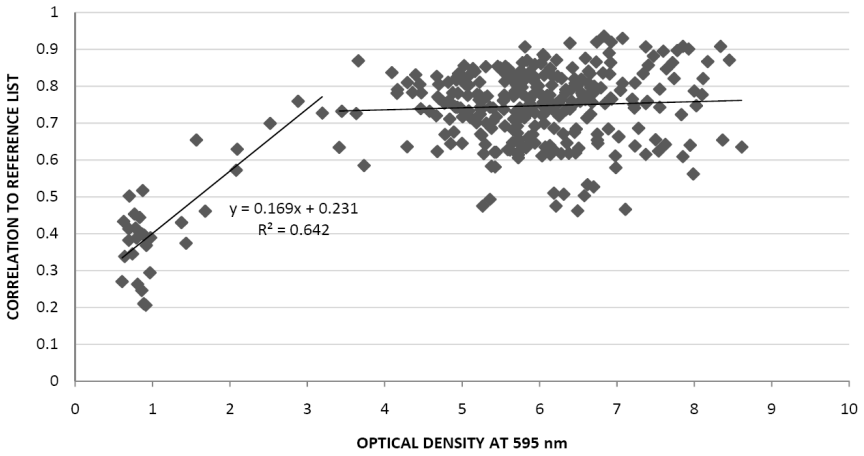

Figure 34. Distribution of the analyzed transposon mutants. Their correlation coefficients were calculated to the reference list and the results were related to the growth values of each mutant after 7 h of inoculation.

The information from the wild type reference list could be used for further procedures. Additionally the metabolite specific thresholds had been applied and thus changes in the

metabolome of the 318 analyzed mutants were revealed. The observations are shown in figure 35. The mutants are plotted against the rate of changed metabolites. Obviously the majority of tested mutants (65%) had variations in 25%...50% of their identified metabolites. Furthermore, 72% of all transposon mutants had changes in less than 50% of their detected components. In only 28% of the randomly selected samples more than half of the metabolites were different when compared to the wild type reference list. And only 1.3% of the mutants revealed dramatic differences in more than 75% of the identified compounds. Especially these mutants had a rigorously changed phenotype. Again the reason for this was limited growth which led to a reduced amount of biomass available for metabolome analysis. The analysis of the mutants with changes in more than 75% of the identified metabolites proved that they all were growth-deficient with optical densities below 1.

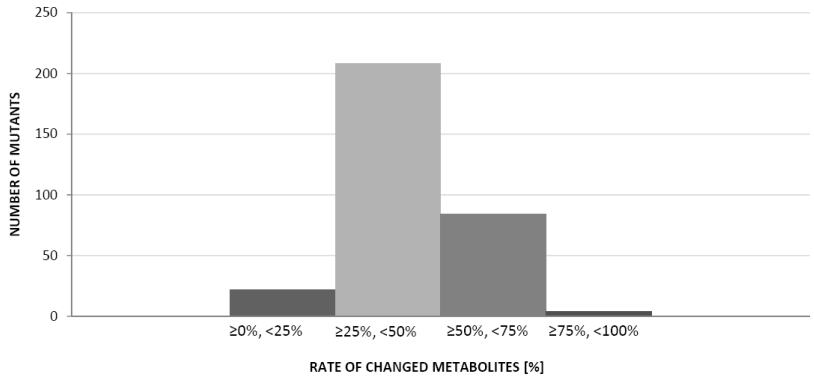

Figure 35. Distribution of the analyzed mutants according to the rate of changed metabolites identified when applying the reference list and the metabolite specific thresholds.

Also the mutants with changes in 50%...75% of the metabolites (see figure 35) were further investigated. Again, a lot of growth-deficient mutants could be identified, but also some mutants which showed a normal growth. When the investigation was concentrated on samples which revealed changes of more than 60% but less than 75%, most of the mutants also could be specified as growth-deficient. In this analysis it was very interesting that besides these growth-deficient ones also mutants with high growth rates were found. These mutants were from plate 21 (B2P21, one mutant), plate 19 (B2P19, one mutant) and from

plate 7 (B2P7, eight mutants). The high number of samples (eight mutants) on the same plate (B2P7) was very surprising and hence it was decided to perform a further investigation which is described later on.
Mutants with changes in 50%...60% could not only be related to reduced growth values: some mutants with slightly limited growth were found, but also mutants with high growth values. For the last mentioned mutants a variant phenotype due to the transposon integration is most likely the reason for the high number of changes.

To gain a better understanding about the necessity of correct wild type reference further analyses were performed. In the first step the correlation coefficients calculated for each transposon mutant to the wild type raised together was related to the calculated number of changed metabolites after application of the reference list and the metabolite specific thresholds. The result is shown in figure 36. The majority of mutants could be found at very high correlations and till around 75 changed metabolites (of the average 135 quantifiable metabolites). Nevertheless, already in this part some mutants with decreased correlations could be revealed. These mutants would be chosen for further investigations.
For values higher than 75 changed metabolites, the correlation values decreased in an almost linear way with an increasing number of changed metabolites. These were again the growth-deficient mutants. But additionally, a small group of nine mutants could be seen with high correlations but also a high number of changes, an occurrence which normally should not be possible (labeled group in figure 36).

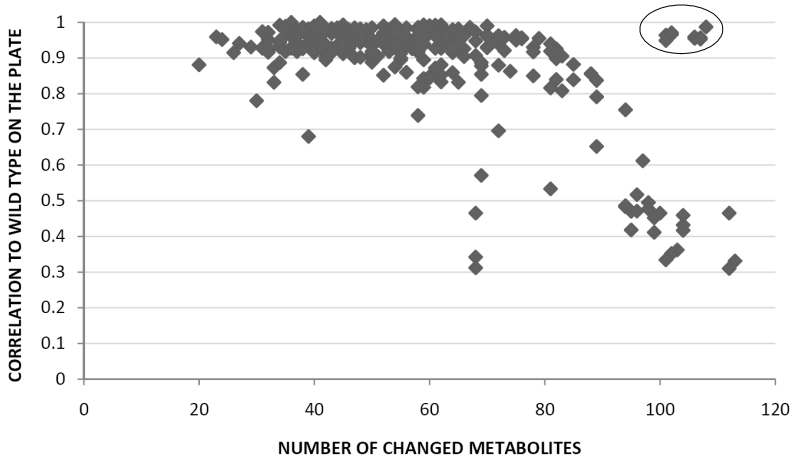

Figure 36. Relation of the correlation values calculated for each mutant to the wild type cultivated together to the revealed number of changed metabolites after application of the reference list and the thresholds for each metabolite. A small group of nine mutants of outstanding occurrence is labeled.

In order to understand the reason why some mutants had a high correlation value to the wild type from the same plate but also a high number of changed metabolites, the same picture was generated applying the correlations to the reference list. The plot is shown in figure 37. The distribution looked different. The whole plot revealed a linear tendency. With increasing number of changed metabolites the correlation decreased. Nevertheless, the majority of mutants again could be found at quite high correlations and changes in less than 75 metabolites (compare figure 36). The same mutants revealed decreased correlations and only few variant compounds. The variant metabolites were specific and not identical in these mentioned mutants. Moreover, these variant compounds were from different chemical classes.

Also growth-deficient mutants could be found on the right side of the plot with low correlations and high number of changes. But in contrast to figure 36, the group of the nine mutants (labeled in figure 37) now clearly showed decreased correlation values. Again they were found at the right side because of the high number of changed metabolites at correlation values that were a little bit higher compared to the mutants with growth limitations.

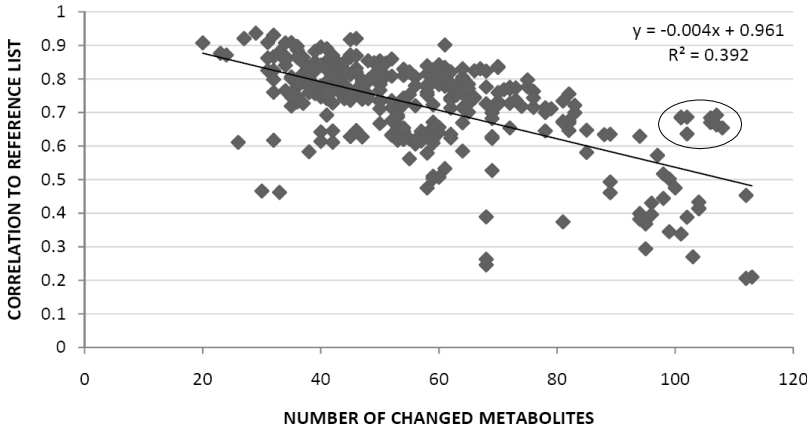

Figure 37. Relation of the correlation values calculated for each mutant to the wild type reference list to the revealed number of changed metabolites after application of this list and the thresholds for each metabolite. The nine mutants which had been of outstanding occurrence in figure 36 are again labeled.

The different picture for the nine noticeable mutants in figure 37 compared to figure 36 is only due to the comparison to the wild type reference list instead of using the wild type grown on the same plate. Therefore, the used wild types raised on the different plates were further analyzed. All these wild type samples were correlated with the wild type reference list. Furthermore, the reference list and the threshold specified for each metabolite were applied and the number of varying metabolites determined. The resulting plot is shown in figure 38. The average correlation coefficient was 0.70 ± 0.08 and around 55 ± 10 metabolites were mostly varying when applying the above described threshold with the factor 6 (equation 3.2). A higher factor would of course decrease the number of differing metabolites but would also reduce the sensitivity of the threshold.

Only one wild type sample was very different. The correlation value was only slightly reduced, but the number of changed metabolites was nearly twice the average value.

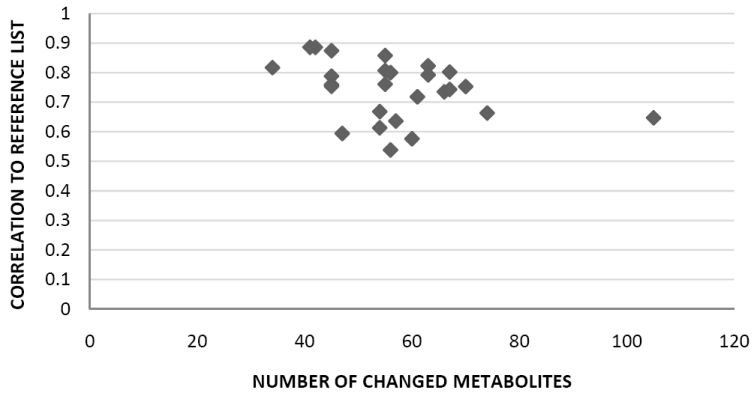

Figure 38. Application of the reference list and the metabolite specific thresholds on the wild type samples that where raised together with mutants on different plates. The revealed correlation coefficient was related to the number of changed metabolites.

The differing wild type was from plate 7 (B2P7). This wild type had been used to calculate the correlation of the eight varying mutants found and described before (see figure 35 and 36). The high number of changed metabolites was the same for the mutants as for the wild type. Consequently, they were very much differing although the correlation to the wild type of the same plate was quite high. The reason for this was found in the cultivation. Because of a mistake the medium volume had been twice as much as normal in these wells. The calculated optical density was of course lower as result of the dilution in the higher medium volume. A correction of the OD-values (a multiplication by two) during data processing would compensate this problem.

This mistake was shown because it is a good example to demonstrate why it is very important to have a reliable reference list. The wild type prepared together with the mutants might be used as first comparison value. But it does not prevent the necessary application of an independent and reliable reference. Only with the use of the reference list and the identification of variant metabolites with the metabolite specific thresholds, problems like the above described one can be revealed easily.

Additionally, the two other mentioned mutants: the one from plate 19 (see figure 35 and labeled group in figures 36 and 37) and the one from plate 21 (see figure 35) were also further investigated. For the mutant from plate 19 the reason for the differing behavior was a systematic shift of all metabolites due to a wrong identified ribitol value. With the correction of this value the number of varying compounds was decreased.

The reason for the distinctive feature of the mutant from plate B2P21 might come from a

problem during data acquisition. Although the samples were raised to high densities, only a small number of metabolites was identified. To further investigate this problem it is probably recommended to repeat cultivation and metabolome analysis for this mutant.
In summary it can be said that mutants which revealed a change in more than 60% of the detected metabolites (see figure 35) were mostly growth-deficient. The few others revealed variations resulting from problems during data acquisition or systematic errors or even differences in cultivation. Thus, the first interesting mutants which had normal growth values and hence enough cell mass for metabolome analysis had changes in maximum 60% of the metabolites. A differentiation between changes caused by biological or environmental variations and the desired changes after genetic modification was done. The latter should be chosen for further investigation.

3.2.3 Hierarchical clustering of the growth-deficient mutants

Cluster analysis is a useful tool for the analysis of large data sets. This data-mining tool is well established for the interpretation of DNA microarray data (Celis et al., 2000). Furthermore, Roessner et al. could demonstrate the usefulness for metabolic profiling studies in plant systems (Roessner et al., 2001). In this study hierarchical cluster analysis was applied to investigate the growth-deficient mutants. A program which uses emergent self organizing maps (ESOMs) for this clustering was applied (Hiller, personal communication). This program does not only arrange data in clusters but also can give further information about the metabolites responsible for the clustering. A test was also performed to cluster around 250 mutants. Mutants mostly clustered according to the plate and date of preparation. This was expected because the high-throughput method with its several automated steps still is affected by changes due to biological and environmental variations. On the other hand, some differences caused by the introduced genetic perturbation might just lead to minor changes. Nevertheless, some mutants clustered separately (see figure A in the appendix) and mutants from different plates clustered together. These are the interesting ones because the genetic perturbation in such cases outweighed changes due to biological or environmental variations.
It were the growth-deficient mutants that appeared to be clearly separated. They were

found in two clearly separated groups (see appendix figure A) on top and at the bottom of the dendrogram. Due to this observation only the mutants with growth limitations (optical densities below 2, see figure 29) were again clustered (figure 39). In this process five clusters were formed. The metabolites causing the separation were identified as hydroxylamine and urea for cluster three. Possibly, the reason for deficiencies in growth might come from problems in nitrogen usage.

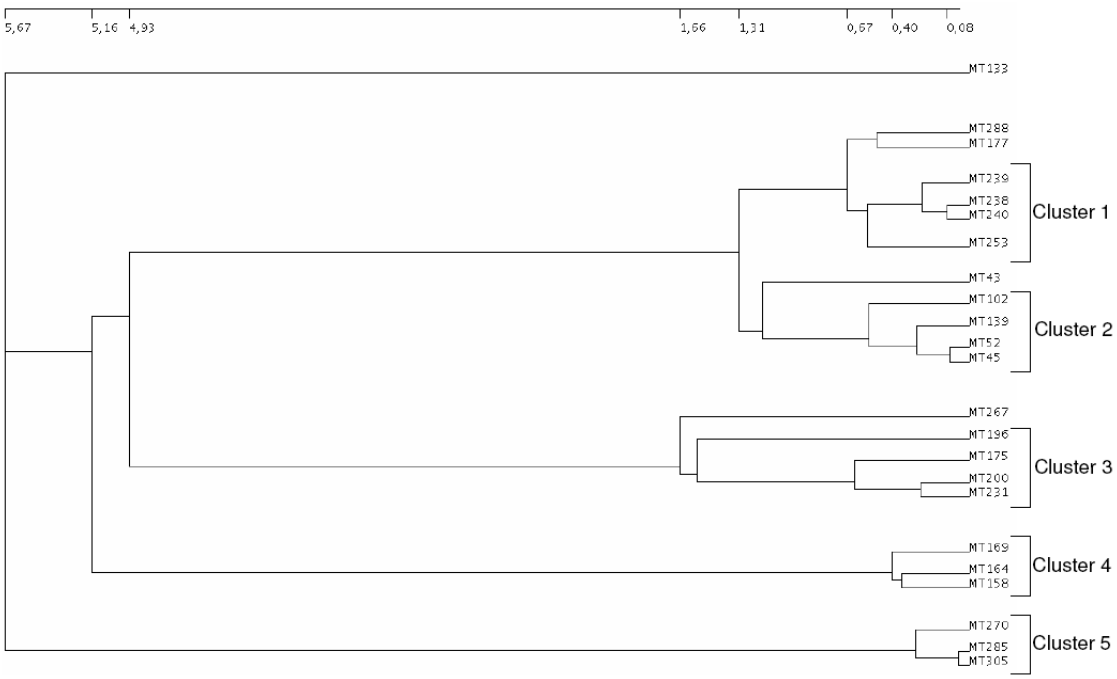

Figure 39. Hierarchical cluster from 23 growth-deficient mutants using ESOMs.

With the use of hierarchical cluster analysis for one separate cluster a hint for the reason for growth-deficiency of the mutants could possibly be found. The information about the metabolites responsible for the other clusters did not lead to further indication. Nevertheless, these mutants could be separated in groups of mutants with similar metabolome. Detailed investigation of such small groups might lead to further information.

3.2.4 Investigation of changes in metabolite levels

The analysis of ten up to twenty most intensive compounds of a sample is a very common method to investigate changes in metabolite levels. It can give further indications for interesting changes in the phenotype of a mutant. Possibly, affected pathways or bottlenecks can be found. In table 18 the metabolites which were identified as most intensive in over 50% of the tested mutants are shown. A complete list, containing additional information, for example about the pathways, is located in the appendix (table C). Ribitol is used as added internal standard. Beside the sugars trehalose and maltose which are very hard to differentiate, because they are isomers, five amino acids were found mostly in high relative concentrations. Except lysine, all of these amino acids are built directly from intermediates of the central pathways or at least close to these pathways. Trehalose is a compatible solute in microorganisms.
5-oxoproline is formed by cyclization of glutamic acid. This reaction continuous with extended standing times of the samples after derivatization before measurement. Phosphoric acid was detected in nearly all samples in high concentration. Furthermore, adenosine-5'-monophosphate and glycerol-3-phosphate as phosphorylated compounds were often identified and succinic acid as well as lactic acid from the central pathways.

Table 18. Summary showing the most intensive metabolites in over 50% of the investigated transposon mutants.

Metabolite	Most intensive compound [%]
Phosphoric acid	99.69
Ribitol	95.31
Trehalose	93.13
Glutamic acid	95.94
Lysine	85.63
Maltose	85.00
Alanine	82.81
Lactic acid	81.88
Glycerol-3-phosphate	80.00
Serine	63.13
Succinic acid	63.13
Aspartic acid	61.56

Metabolite	Most intensive compound [%]
Adenosine-5'-monophosphate	55.31
5-Oxoproline	53.75

The information about these most intensive metabolites was analyzed for 318 mutants as well as for the wild type reference list and a second list which was created after combining all mutant samples. The reference list revealed all metabolites listed in table 18 (except for 5-oxoproline) as the most intensive compounds. Additionally, the amino acids glutamine, proline and cycloleucine were found in very high concentrations. For the wild type of *C. glutamicum*, a bacterium which is often used for amino acid production - a fact that is not really surprising. For the list of all mutants again the majority of the compounds listed in table 18 were found as most intensive compounds. Nevertheless, serine, succinic acid and 5-oxoproline were not among the twenty highest substances. The phosphorylated compounds glucose-6-phosphate and fructose-1,6-biphosphate as well as cycloleucine and gamma-glutamylvaline were found in the highest amounts instead.

Out of the 318 analyzed transposon mutants 19 growth-deficient mutants were further investigated and interesting findings could be revealed. These 19 mutants comprised those which did not grow higher than an optical density of 2 (compare figure 29). Again, 12 of the 14 metabolites in table 18 that had been identified as most intensive compounds were found. However, adenosine-5'-monophosphate and succinic acid were not present. Furthermore, only phosphoric acid, maltose and trehalose, ribitol, alanine and lactic acid occurred in the majority of the growth-deficient mutants. The others were only found in a low number of samples. In contrast, some sugars and sugar alcohols, like glucose, mannose (isomers) as well as mannitol and erythritol, were found in a lot of samples. Most of them are metabolites of the sugar metabolism. An assumption could be that the mutants increased their performance in this part of the metabolism to regulate their energy source but were still not able to compensate the mutation.

Other metabolites which often occurred in the analyzed mutants (see table 19) were hexadecanoic acid and octadecanoic acid from the fatty acid metabolism as well as glycerol from the glycerolipid metabolism. Their levels were increased compared to mutants without growht-deficiencies. Possibly, such mutants had problems in the formation of membranes which limited their growth.

Urea and hydroxylamine, important for the nitrogen metabolism, were found increased in

some mutants as well (compare results from part 3.2.3). Probably such mutants had difficulties in the nitrogen usage. Nitrogen is one of the important compounds for the formation of biomolecules, e.g amino acids, and thus could cause growth-deficiencies.
2-hydroxypyridine was also found. This was a residue derived from the derivatization compound. It was present in higher concentration in samples derived from growth-deficient mutants, in which less metabolites were extracted and thus the derivatization reagent is present in excess. In samples of mutants and wild type which revealed no growth limitation all of the derivatization reagent is used and 2-hydroxypyridine is not present.

Table 19. Metabolites identified as most intensive compounds in the 19 analyzed mutants with growth-deficiencies.

Metabolite	Occurrence [%]	Metabolite	Occurrence [%]
Hexadecanoic acid	100	Malonic acid	21
Ribitol	100	Lysine	21
Octadecanoic acid	95	Aspartic acid	16
Carbonic acid	95	beta-Alanine	16
Phosphoric acid	95	Glucono lactone	16
Trehalose	95	Valine	16
Glycerol	84	Glycolic acid	16
Maltose	84	Serine	11
Alanine	84	Xylulose	11
Mannose	68	2-Hydroxybutanoic acid	11
Lactic acid	79	2-Hydroxyglutaric acid	11
Glucose	79	Benzoic acid	11
Erythritol	63	Glyceraldehyde	11
Mannitol	53	Norvaline	11
Urea	53	Glycerol-3-phosphate	5
Glutamic acid	42	3-OH-2-tetradecyl-octanoic acid	5
Hydroxylamine	42	Fructose-1,6-biphosphate	5
5-Oxoproline	37	gamma-Glutamylvaline	5
Dodecanol	32	Glucose-6-phosphate	5
2-Hydroxypyridine	26	Glutamine	5
Cycloleucine	26		

Another important observation regarding table 19 was the presence of compounds from the glycolysis - glucose-6-phosphate and fructose-1,6-biphosphate were identified. On the other side, the amino acids which were found in high intensities in the majority of mutants (see table 18) and which are located near the tricarboxylic acid cycle were only rarely found. Normally these phosphorylated compounds from the first steps of glycolysis are not accumulated, but underlie a quick and ongoing conversion. Possibly, such an accumulation is a hint that the mutation affects enzymes of the glycolysis itself or the tricarboxylic acid cycle. The latter is the most important pathway in an organism and mutations inside or near it surely could lead to severe problems - for example in growth.

However, in addition to the 19 analyzed growth-deficient transposon mutants some randomly selected mutants with good growth rates were further investigated. An interesting finding was that very often compounds from the glycolysis, pentose phosphate pathway and the tricarboxylic acid cycle were found in high levels. For example fumaric acid and malic acid were detected. Also glucose-6-phosphate, fructose-1,6-biphosphate, 6-phosphogluconate and 3-phosphoglyceric acid were often found. Although these mutants had limitations in the central pathways they still grew to high optical densities. It can not surely be said that the bottlenecks are directly located in these pathways, but due to the effort of the bacterium to overcome them - in that way it overproduces these important metabolites which can not be used completely and hence they are found accumulated in the metabolome.

3.2.5 Identification of the transposon insertion site of some mutants

A complete list of the transposon mutants analyzed in this study is shown in table D in the appendix. The important characteristics are summarized. The identification of the insertion site of the transposon was done for ten selected mutants during this study. An overview is given in table 20. The mutants printed in fat writing had already been described by Reimer (Reimer, 2008). For half of the mutants only a hypothetical protein could be identified as affected. One of these was a hypothetical membrane protein and another one was identified as UDP-N-acetylenolpyruvoylglucosamine reductase hypothetical protein. The analysis of the metabolic profile did not lead to an indication for affected pathways.

Table 20. Transposon mutants and the identified affected enzyme.

Number	Mutant	Affected enzyme (gene)
MT63	**A2_B2P7**	para-aminobenzoat synthase (*pabAB, cgl0997*)
MT88	**C3_B2P7**	hypothetical membrane protein (*cg0879*)
MT91	C6_B2P7	pseudouridine synthase (*rluD, cgl2138*)
MT92	C7_B2P7	hypothetical protein (*cgl0592*)
MT107	**E1_B2P7**	glutamate-ammonia-ligase adenyltransferase (*glnE*)
MT122	**F2_B2P7**	hypothetical protein (*cg0858*)
MT147	H4_B2P7	UDP-N-acetylenolpyruvoylglucosamine reductase (*murB*)
MT161	A6_B2P8	hypothetical protein (*cgl1708*)
MT165	B1_B2P8	aminopeptidase N (*pepN, cgl2426*)
MT168	B4_B2P8	citrate-transporter/symporter (*citP, cgl0067*)

The growth behavior of mutant 63 was described in detail by Reimer (Reimer, 2008). This mutant was growth-deficient. It hardly grew on minimal medium. The additional supply of amino acids in the minimal medium could improve the growth, but a complete compensation was not possible. The affected gene (*cgl0997* annotation Kyowa, *pabAB* annotation Bielefeld) is coding for a subunit of the para-aminobenzoat synthase which is involved in the tyrosine, phenylalanine and tryptophan biosynthesis. However, the supplementation of these amino acids alone did not improve the growth behavior. This enzyme is responsible for the conversion of chorismate into anthranilate which is than further converted to tryptophan. Furthermore, this enzyme is involved in the folate biosynthesis where it is responsible for the conversion of chorismate into 4-amino-4-deoxychorismate. The enzyme is also part of a two-component system responsible for the regulation of the biosynthesis of tryptophan.

Mutant 107 was analyzed and the affected gene (*glnE* annotation Bielefeld) was identified encoding for a glutamate-ammonia-ligase adenyltransferase. This gene is regulating the glutaminsynthase I, which is involved in the nitrogen metabolism. Glutamine and proline were found in increased levels in this mutant. Normally the glutaminsynthase I catalyzes the fixation of nitrogen via glutamine in case of a lack in nitrogen supply. Due to the gene knock-out in this mutant the regulation of the glutaminsynthase I by the glutamate-ammonia-ligase adenyltransferase is missing. Therefore, glutamine was found in increased

levels because the described path for the nitrogen fixation was active although no limitation existed. Furthermore, in case of nitrogen abundance, proline is one of the substances synthesized as protectant for osmotic stress. The increased level of this amino acid could be an indicator for such an abundance of nitrogen, with further influence on regulations dependent on the nitrogen supply (Reimer, 2008).

In mutant 91 the affected gene (*rluD, cgl2138*) was identified to code for a pseudouridine synthase. This enzyme works as catalyst for the reaction of uridine to pseudouridine. In the metabolic profile of the mutant a reduced amount of uridine was found. Pseudouridine is not included in our internal library. Therefore, no information about that compound was available. Additionally, a decrease in the uridine-5'-monophosphate and uracil and most of the amino acids like tyrosine, threonine, thymine, isoleucine and phenylalanine were detected. Uridine is part of the RNA. It is built from the base uracil and the pentose ribose. The knock-out of the enzyme seems to have an effect on the formation of a lot of compounds. The changed uridine level has a direct influence on the uracil level. Because this base is responsible for the amino acid formation, the value of the base was reduced as well.

Mutant 147 had the transposon integration in the gene (*murB*) coding for an UDP-N-acetylenolpyruvoylglucosamine reductase. This enzyme is involved in the amino sugars metabolism. It converts the second part of the reaction of UDP-N-acetyl-D-glucosamine into UDP-N-acetyl-3-O-(1-carboxyvinyl)-D-glucosamine and further into UDP-N-acetyl-muramate. In the metabolic profile the phosphorylated compounds glucose-, mannose- and glucosamine-6-phosphate were increased in this mutant. Ribose-5-phosphate as well as fructose-6-phosphate were only identified in the mutant but not in the wild type. These raised levels seemed to be the direct result of the mutation. Because a conversion to UDP-N-acetylmuramate was not possible, the level of UDP-N-acetyl-D-glucosamine might be high (not identified because not in our library). Possibly an accumulation of this compound led to an increased formation of such phosphorylated sugars because glucosamine-6-phosphate and fructose-6-phosphate are directly built from UDP-N-acetyl-D-glucosamine.

The gene (*pepN, cgl2426*) coding for an aminopeptidase N was identified to be disrupted in mutant 165. This enzyme is involved in the glutathione metabolism where it converts the formation of glycine. The metabolic profile did not show many differences. That means, the mutation did not have much influence on the whole metabolism. The knock-out of this

specific enzyme rather impacts only the mentioned reaction. Consequently, glycine was found in reduced concentration.

Mutant 168 had the mutation in the gene (*citP, cgl0067*) coding for a citrate-transporter/symporter. The mutant was grown on glucose as carbon source. Consequently, the mutation in the citrate-transporter did not lead to any changes of the phenotype. The citric acid concentration was identical to the one of the wild type.

3.3 Comparison of different quenching methods

In the scientific literature available up to now, different quenching methods exist. Mostly the methods were developed and optimized especially for one organism. The adaptation of a protocol from one microorganism to another was often unsatisfactory and could only be regarded as a compromise.

In this study (together with Reimer (Reimer, 2008)) different quenching methods were tested on three different organisms. Additionally, our standard protocol was used as unquenched method for comparison. Two methods from literature were applied: quenching with methanol and a cold glycerol saline quenching. Furthermore, an ethanol quenching method was tested. This one had been developed in our working group and was further improved during this study.

3.3.1 Refinement of the ethanol quenching method

First experiments using an ethanol solution for quenching were done in our lab by Buchinger. During this study the method was refined and evaluated, using a 40% ethanol sodium chloride solution as basis. The whole method is shown in chapter 2.9.1. Background for the development of a quenching method with an alcoholic solution was the methanol method (see part 2.9.2) which is the quenching performance for microorganism most often used. Nevertheless, Wittmann et al. described so called cold-shock phenomenons during quenching of *C. glutamicum* (Wittmann et al., 2004). The idea was to use a reduced alcoholic solution and ethanol instead of methanol in order to reduce negative impacts of the high alcohol concentration on the cell membrane. Furthermore, the temperature of the solution was increased from -50°C to -20°C to reduce stress caused by the temperature drop but still to be able to stop the metabolism. Additionally, after optimization the quenching solution was prepared with a physiological salt concentration in order to avoid osmotic stress.

In first tests the ethanol quenching solution was made with a 0.5% (w/v) sodium chloride end concentration. This solution revealed good results for the organisms *C. glutamicum* and *S. cerevisiae* but for *E. coli* dramatic losses were found compared to our unquenched

standard method. Probably stress caused by the change in osmolarity and the alcohol caused this effect in the Gram-negative organism. Because of its special morphology with a relatively thin cell wall *E. coli* was the only of the tested three organisms responding to this stress. To optimize the performance different salt concentrations were tested. The sodium chloride concentration in the ethanol quenching solution was adjusted to a physiological concentration of 0.8% (w/v) and for comparison to 1.5% (w/v). Tests were prepared with *E. coli*. Figure 40 shows the results. The different identified metabolites for each quenching performance were compared to each other.

In figure 40A the comparison of the quenching solution with 0.5% (w/v) sodium chloride to the solution with 0.8% (w/v) is shown. A lot of metabolites were spread around the 45-degree line but closer shifted to the abscissa. Some of the amino acids were even missing in the 0.5%-solution but detectable when quenched with the physiological solution (0.8% w/v).

The comparison of the quenching solution with 1.5% (w/v) sodium chloride to the solution containing 0.8% (w/v) is shown in figure 40B. The result is very similar to the one in figure 40A. Again the majority of metabolites is spread around the 45-degree line. The tendency was shifted to the abscissa. Nevertheless, a lot of substances had only been detectable in the physiological solution. Again some amino acids were missing after quenching with the 1.5%-solution.

In figure 40C the results for quenching with the 0.5%-solution and the 1.5%-solution are plotted against each other. The identified metabolites showed a cloud-like distribution around the 45-degree line. Some of the substances were only found after quenching with the 0.5% (w/v) quenching solution and can be seen in the plot on the abscissa whereas others were only detectable after quenching with the 1.5% (w/v) quenching solution (on the ordinate). Altogether, the result for these two solutions was quite different.

Overall, the physiological solution with 0.8% (w/v) sodium chloride revealed the best result for *E. coli*. This solution was used for further experiments with the other organisms, too. Although, first results with the 0.5%-solution had not revealed such an influence on these microorganisms, stress caused by the change in osmolarity was avoided this way. One further result of this study is that one statement from literature could be disapproved - namely that a salt concentration above the physiological one would be the best and the one preferred to a physiological concentration (Bolten et al., 2007).

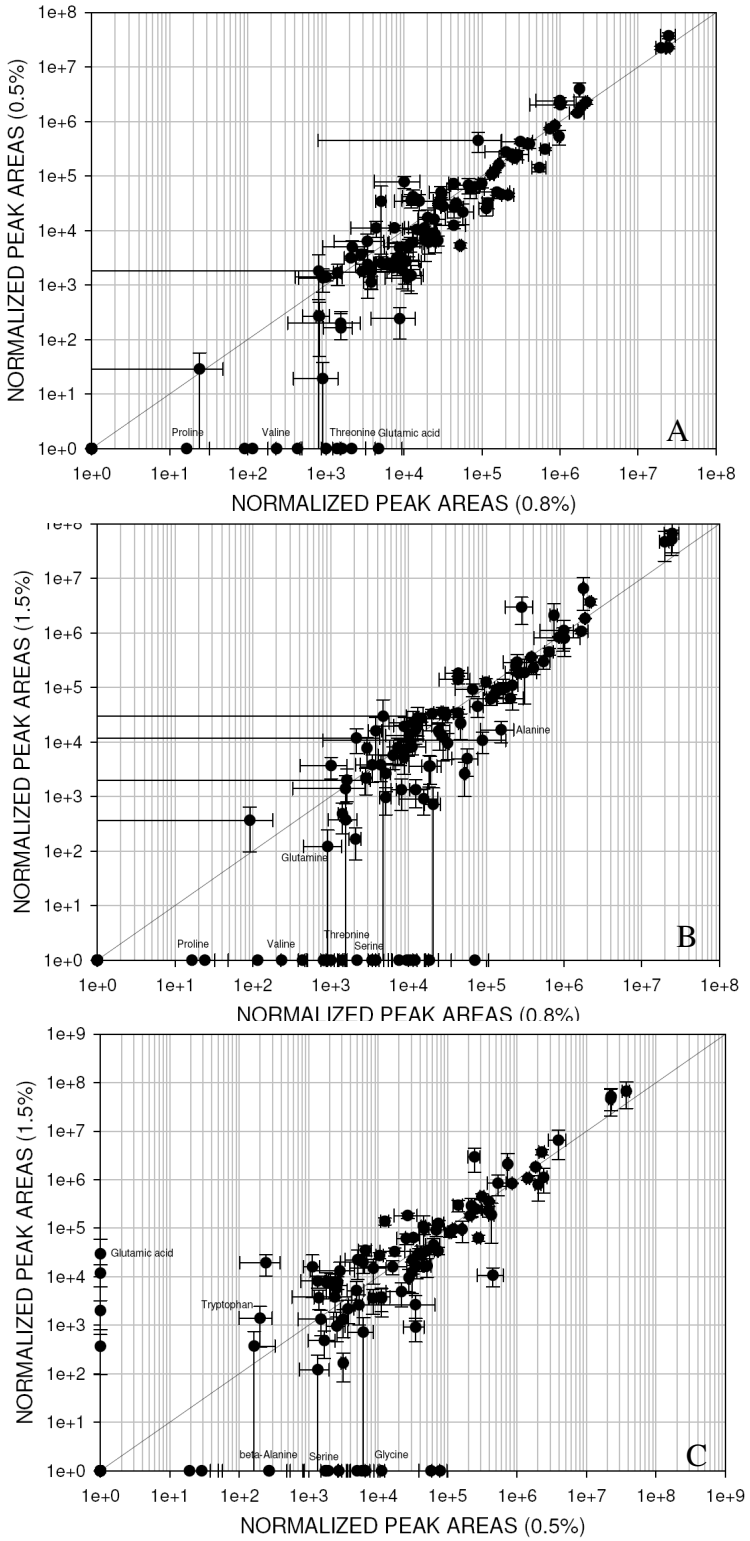

Figure 40. Comparison of the results after quenching of *E. coli* with an ethanol solution containing different concentrations of sodium chloride. **A** 0.5%-solution compared to the 0.8%-solution, **B** 1.5%-solution compared to the 0.8%-solution and **C** 1.5%-solution compared to the 0.5%-solution.

Besides the test regarding the quenching solution itself, also the influence of additional washing steps during quenching was examined. Most important for such an additional step is the low temperature which has to be hold. Otherwise the metabolism could change again. Thus, tests were performed using the quenching solution (40% ethanol and 0.8% (w/v) sodium chloride) as washing solution, too. Different experiments were done: without washing, one washing operation and two washing operations. The results are shown in figure 41. The plots clearly indicated a reduction of the relative concentrations of metabolites after each washing step. Still, some metabolites were only found in the washed samples (see figure 41A and B). These substances mostly were so called "unknowns" (structurally uncharacterized substances) and therefore a reason for the change could not be discovered.

Figure 41A displays the result after quenching and one washing operation compared to a performance without washing. It was clearly shown that only after one of these additional steps the majority of the identified substances could be found in decreased levels. Overall 57% of the relative metabolite concentrations were reduced.

After two times of washing the before noticed trend could be confirmed. In figure 41B, the two step washing is plotted against quenching without washing. Even more reductions were revealed and a lot of the substances were no more detectable in the washed sample (on the abscissa). Altogether, 60% of the metabolites were identified in decreased concentrations.

To reveal this effect of washing more clearly, in figure 41C the results of two times washed and one times washed samples is related. The majority of all identified metabolites showed a reduction after a second additional washing step. Nearly all metabolites are shifted.

Probably the shear stress caused this tremendous effect after washing. The reason is likely the resuspension of the pellet in the washing solution after centrifugation. During each washing step the metabolite levels were reduced, affecting over 70% of the compounds. Most affected are sugars, sugar phosphates but also intermediates of the tricarboxylic acid cycle.

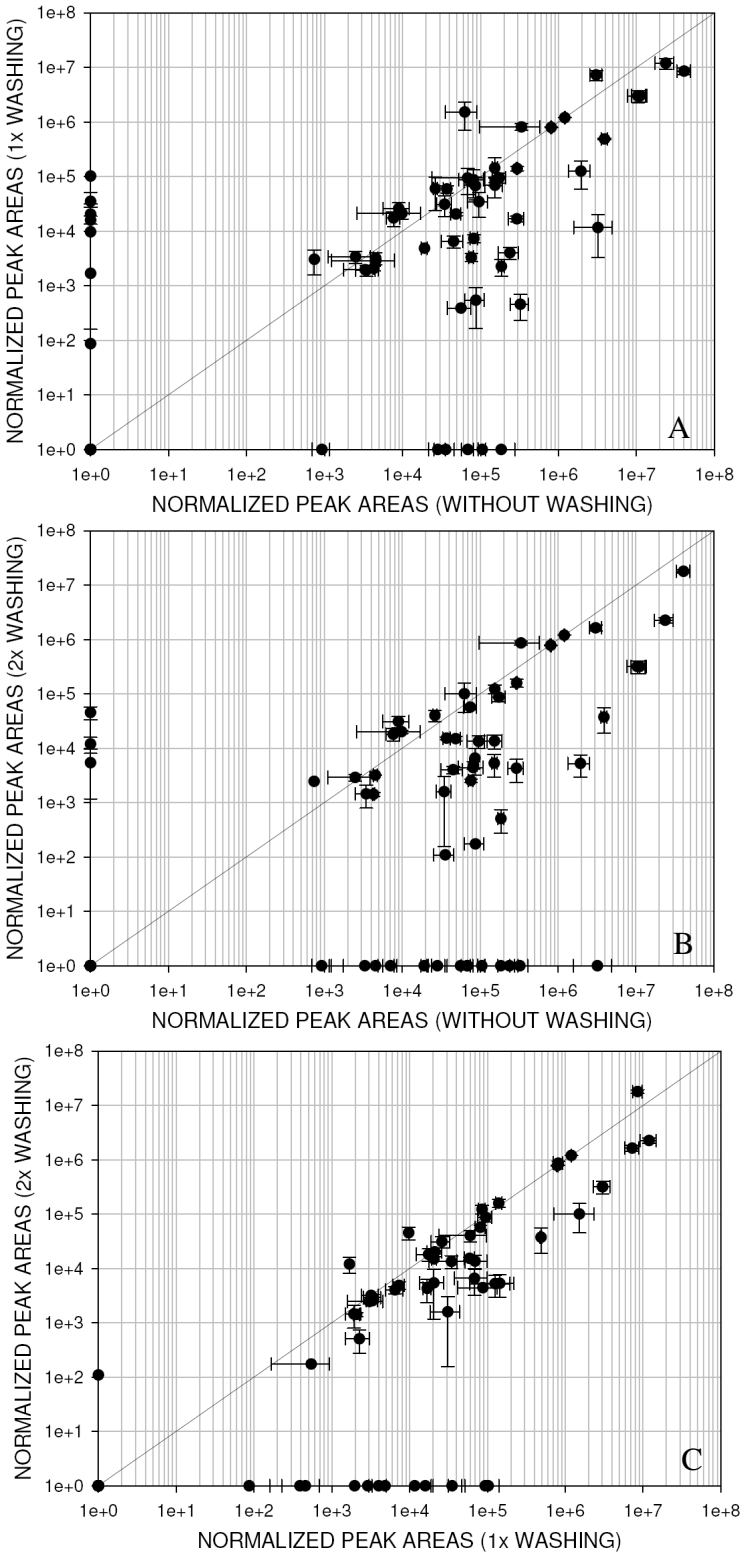

Figure 41. Comparison of the ethanol quenching performance with and without washing steps. **A** one washing operation is compared to quenching without washing, **B** two step washing is compared to quenching without washing and **C** quenching with one and two washing steps is compared to each other.

Because of this huge effect of washing of *E. coli* cells, the washing was not performed routinely in our ethanol quenching method. Since the aim was to evaluate a protocol suitable for quenching of different organisms, the washing was not applied on the two other microorganisms, too. Nevertheless, in the literature such a negative effect of a methanol method containing a washing step on *C. glutamicum* had been already described (Wittmann et al., 2004).

3.3.2 Difficulties in the cold glycerol saline quenching performance

The cold glycerol saline quenching method was recently described in the literature (Villas-Bôas et al., 2007). A detailed workflow of the method is shown in chapter 2.9.2. The quenching solution used consisted of 60% glycerol and 0.54% (w/v) sodium chloride. Due to the high viscosity of this solution the centrifugation speed and time had to be very high. The speed was over 4.5times higher than the performance in our unquenched protocol and the time was increased by a factor of nearly 7.

During this quenching method the pellet had to be resuspended in a 50% glycerol and 0.675% (w/v) sodium chloride washing solution. This solution again was very viscous. Consequently, the resuspension took quite long and another big problem occurred. Although the washing solution had been precooled to -20°C the whole mixture of cells and this solution could not be held at this low temperature.

A similar temperature problem occurred with the centrifuge itself. The machine was precooled to -9°C. But during quite long centrifugation steps at a very high speed the centrifuge could not hold this low temperature and warmed, reaching temperatures higher than 0°C.

Nevertheless, the protocol was applied and after cell lysis the polar phase was extracted and dried. But due to the high amount of glycerol in the solutions a quite high amount of this compound sticked to the sample. With this moiety a derivatization with MSTFA was not possible. Glycerol is very hygroscopic and this silylation step has to be performed in the absence of water. Villas-Bôas et al. already described this findings (Villas-Bôas et al., 2007), but in their opinion this amount of glycerol, which they quantified with less than 150 µl, was not distracting. They applied another derivatization compound (methyl

chloroformate) which is also working in the presence of water. In this study the moiety of glycerol on the samples could not be neglected because it was distracting. Furthermore, due to comparison purpose a change of the derivatization performance was not possible. Additionally, applying methyl chloroformate would reduce the number of different detectable substances. A silylation with MSTFA can be used for a broad range of substances (e.g. sugars and sugar derivatives, amino acids, organic acids, fatty acids, amines) whereas others are mostly suitable for a smaller number of compounds. Chloroformate can be used for the derivatization of e.g. amino acids, keto acids, fatty acids and aliphatic amines (Villas-Bôas et al., 2005).

In order to overcome this difficulty an additional washing step with ice cold sodium chloride solution (0.9% w/v) was tested. A reduction of the glycerol moiety was achieved. But because of the high viscosity of this compound it could not be completely removed. The amount sticking to the sample was still too high for further investigation.

Finally, because of the here mentioned problems this method had to be discarded. The produced results after measuring the samples with GC/MS were not analyzable.

3.3.3 Quenching of Escherichia coli

For quenching experiments with *E. coli* cells were cultivated as described in chapter 2.7.1. In order to compare the different applied protocols correctly, samples were always taken together and at least in triplicates for each method. As direct comparison our unquenched standard method (UQ) was also exerted.

In figure 42 the results of the ethanol quenching (EQ) are plotted in a scatterplot against the unquenched method. Displayed are the normalized peak areas which correspond to the relative intensities of the identified metabolites. A relatively high number of substances could only be detected in the ethanol quenched samples. This metabolites which can be seen on the ordinate were mostly sugars and phosphorylated compounds. The majority of substances was distributed cloud-like around the 45-degree line. In contrast, among others some of the amino acids were only detected in the unquenched samples and can be seen in figure 42 on the abscissa. Altogether, quite a high number of obvious differences can be found when analyzing the scatterplot. This might indicate that in the unquenched samples

the metabolism was not stopped but ongoing during sample preparation, whereas in the ethanol quenched samples a stopped metabolism was achieved.

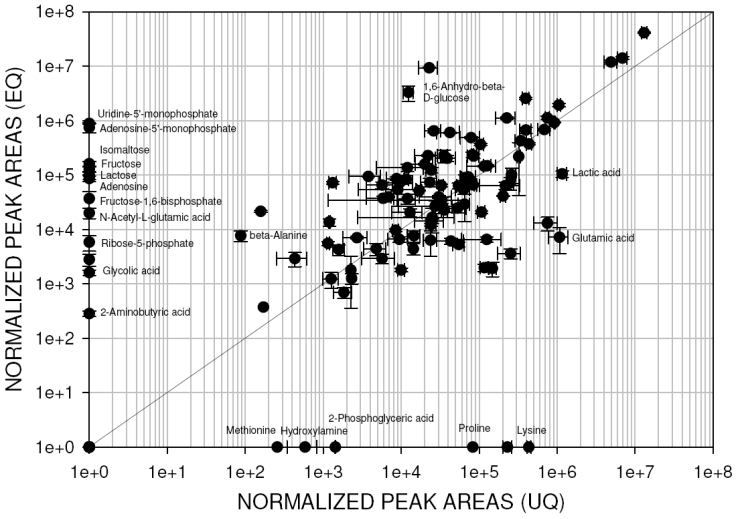

Figure 42. Scatterplot of ethanol quenched (EQ) and unquenched samples (UQ) of *E. coli*.

In order to confirm the hypothesis that the changes between the samples quenched with ethanol and the unquenched ones were due to the ongoing metabolism in the not quenched samples, an additional experiment was performed. Again *E. coli* was cultivated and harvested. Sample triplicates were handled according to the unquenched method or the ethanol quenching. But additionally, one triplicate was harvested together with the unquenched samples but was kept on ice for 30 min before further applying this method. Another group was harvested and quenched but was hold at -5°C for 30 min before further sample preparation according to the quenching protocol was done. The result of this test is shown in figure 43. Obviously the metabolism was not quenched when applying the standard performance (see figure 43A). The scatterplot revealed quite a lot differences when keeping the samples on ice for 30 min. The average calculated correlation coefficient using the logarithmic values of the relative concentration vectors was calculated with 0.83 ± 0.02 which confirmed the high number of changes.

Glucose and mannose were identified in higher relative concentrations in the samples directly prepared. This approved the hypothesis. Because they are isomers, these two compounds are hard to distinguish and hence are mostly identified together. If they were in higher values in the first prepared samples but reduced in the samples after 30 min standing

time, the carbon source glucose might have been consumed in the ongoing metabolism. Methionine had only been found in the unquenched samples in figure 42. But in figure 43A it even seems to be further synthesized during the 30 min standing time. A similar observation could be made for glutamic acid, being reduced in the ethanol quenched samples (figure 42), but even more increased in the unquenched samples after 30 min (figure 43A). Furthermore, some metabolites could only be detected in the unquenched samples kept on ice for 30 min.

In contrast, there are only few differences between samples quenched with ethanol and those stored for 30 min before further applying the quenching protocol (figure 43B). 2-aminobutyric acid was only detectable in the quenched samples without additional standing time but in quite low concentration. Two amino acids were slightly decreased after 30 min. Nicotinic acid was identified in increased value after additional standing time. Overall, the correlation coefficient was significant higher (0.94 ± 0.04) compared to the result of the unquenched performance.

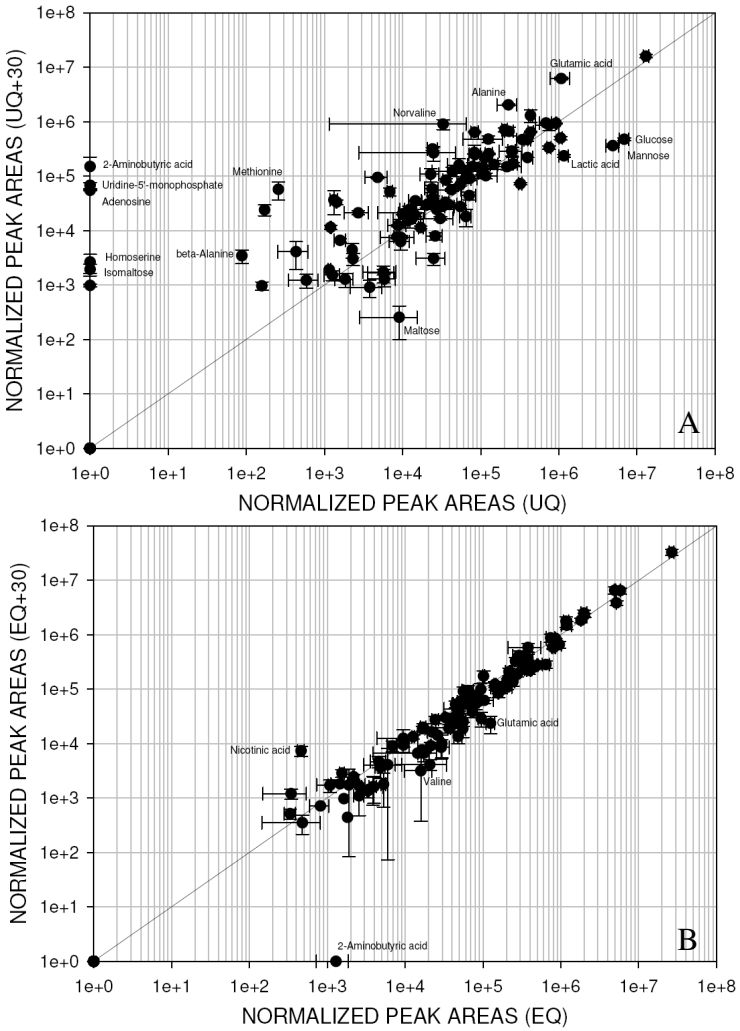

Figure 43. Scatterplots of unquenched (UQ) and ethanol quenched (EQ) samples. **A** unquenched samples compared to unquenched ones additionally held on ice for 30 min and **B** ethanol quenched samples compared to those stored for 30 min at -5°C.

This analysis could approve the hypothesis to receive good quenched samples when applying the ethanol quenching. On the other hand, when applying our standard protocol the metabolism was not stopped. The cooling step seems to be the most critical one. Cooling from 37°C to a lower temperature just by placing the cells on ice seemed not sufficient and additionally rather uncontrolled, whereas the fast cooling in a -30°C-cold isopropanol bath worked very well.

The comparison of the results from the methanol quenching and the unquenched method is shown in figure 44. A high number of differences could be found. A lot of amino acids

could only be detected in unquenched samples and can be seen on the abscissa, whereas some sugars and phosphorylated compounds could only be identified in methanol quenched samples. The majority of metabolites was spread around the 45-degree line revealing quite a lot reduced substances when applying the methanol quenching performance.

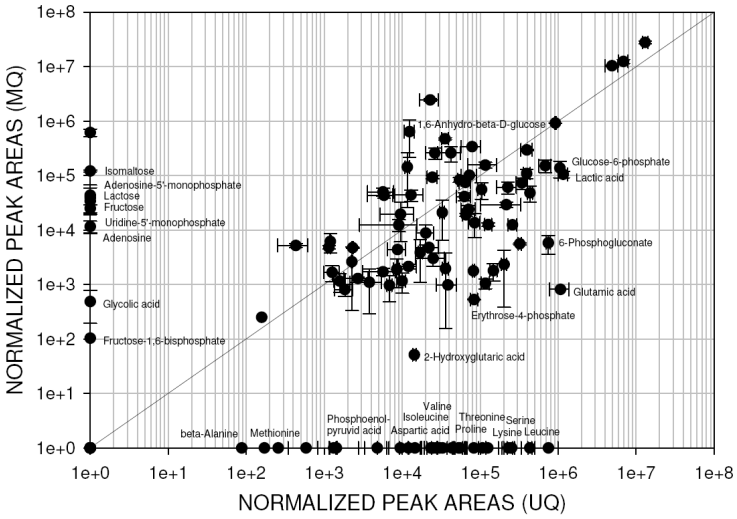

Figure 44. Scatterplot of methanol quenched (MQ) and unquenched samples (UQ) of *E. coli*.

For a direct comparison of both quenching methods their results are shown in direct relation in figure 45. Only one substance identified as “unknown” was found to be present in the methanol quenched but not in the ethanol quenched samples (on the ordinate). Substances that are described as “unknown” in our library are structurally not identified compounds which can be found repeatedly in the samples. They are not labeled in the scatterplots. The majority of detected compounds was found in higher concentrations in samples quenched with ethanol. A lot of phosphorylated compounds clearly showed this trend. Phosphorylated intermediary metabolites have very low time constants and thus are consumed in an ongoing metabolism.

Some amino acids could only be detected in ethanol quenched samples and can be found on the abscissa in figure 45. This comparison clearly demonstrated an improved result for samples after ethanol quenching.

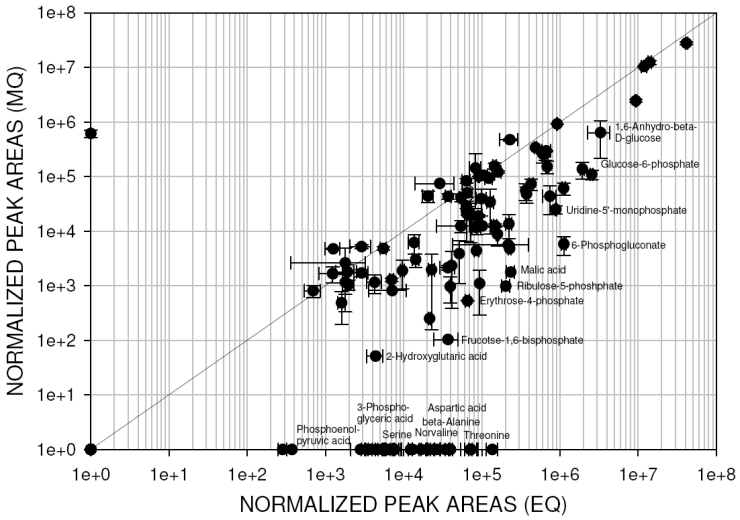

Figure 45. Scatterplot of methanol quenched (MQ) and ethanol quenched (EQ) samples of *E. coli*.

A direct overview about relative concentration ratios of some identified metabolites for all three methods is shown in table 21. Some of the best reproducible substances are outlined. As already seen in figure 44 and 45 a lot of substances were identified in lower concentrations in the methanol quenched samples. Especially the amino acids and several phosphorylated compounds showed this decrease in the direct comparison of methanol quenching to ethanol quenching. Uridine-5'-monophosphate and adenosine-5'-monophosphate were not detected in unquenched samples but were found after applying both quenching methods. In samples quenched with ethanol both substances were found in highest concentration. In summary, more than 80% of all identified metabolites showed lower concentrations after methanol quenching.

The results of figure 43 for the relation of ethanol quenched and unquenched samples were confirmed by the results in table 21. While phosphorylated compounds were most abundant in ethanol quenched samples, some amino acids revealed lower concentrations. Additionally, pyruvic acid was even 2fold increased in ethanol quenched samples. Moreover, pyruvic acid is a metabolite of the central metabolism which is involved in the important pathways and thus is consumed quite fast. All the given facts confirm the good results and make the use of an ethanol quenching method preferable.

Lactic acid was detected in over 10fold higher relative concentrations in the unquenched samples. However, succinic acid was only identified in moieties in quenched samples but

in quantifiable amounts in the unquenched samples. This compound was 6fold (EQ) or even 8fold (MQ) increased when applying our standard method without quenching (table 21). Possibly these two substances were accumulated due to continuous changes in the metabolism of the unquenched samples. In figure 43A was shown that the metabolism was not stopped during the standard performance, whereas a stopped organism was found after quenching with ethanol (figure 43B). An additional indication for this might be the increased values for malic acid and fumaric acid, intermediates of the tricarboxylic acid cycle, in ethanol quenched samples compared to the unquenched ones.

Table 21. Comparison of the relative concentrations of some identified amino acids, phosphorylated compounds and other metabolites in *E. coli* applying the different procedures.

Metabolite	Ratio EQ to UQ	Ratio MQ to UQ	Ratio MQ to EQ
amino acids			
Tyrosine	0.014 ± 12.2%	0.008 ± 16.3%	0.595 ± 16.9%
Threonine	0.105 ± 33.0%	not detected in MQ	not detected in MQ
Glutamic acid	0.075 ± 13.9%	0.001 ± 13.8%	0.114 ± 24.9%
Valine	0.536 ± 65.5%	0.014 ± 18.5%	0.035 ± 23.8%
Glycine	0.547 ± 8.2%	0.048 ± 54.7%	0.088 ± 48.7%
Alanine	3.336 ± 21.9%	0.197 ± 27.5%	0.063 ± 19.7%
Phenylalanine	5.556 ± 13.5%	0.141 ± 25.3%	0.024 ± 25.1%
Aspartic acid	35.437 ± 60.0%	not detected in MQ	not detected in MQ
phosphorylated compounds			
Glycerol-3-phosphate	0.989 ± 10.4%	0.216 ± 22.4%	0.218 ± 20.4%
Xylulose-5-phosphate	1.316 ± 10.0%	0.202 ± 22.3%	0.154 ± 19.9%
Erythrose-4-phosphate	1.114 ± 7.6%	0.022 ± 7.9%	0.017 ± 2.8%
6-Phosphogluconate	1.317 ± 9.9%	0.009 ± 50.4%	0.007 ± 50.0%
3-Phosphoglyceric acid	1.238 ± 17.0%	not detected in MQ	not detected in MQ
Glucose-6-phosphate	1.930 ± 5.9%	0.462 ± 29.1%	0.231 ± 27.8%
Ribulose-5-phosphate	3.415 ± 24.8%	0.109 ± 28.7%	0.063 ± 29.2%
Uridine-5'-monophosphate	not detected in UQ	not detected in UQ	0.025 ± 15.1%

Metabolite	Ratio EQ to UQ	Ratio MQ to UQ	Ratio MQ to EQ
Fructose-1,6-biphosphate	not detected in UQ	not detected in UQ	0.001 ± 33.5%
Adenosine-5'-monophosphate	not detected in UQ	not detected in UQ	0.055 ± 38.1%
others			
Lactic acid	0.086 ± 20.1%	0.079 ± 21.2%	0.916 ± 24.5%
α-Ketoglutaric acid	0.105 ± 19.4%	not detected in MQ	not detected in MQ
Succinic acid	0.161 ± 7.1%	0.017 ± 50.6%	0.121 ± 51.4%
Citric acid	0.601 ± 12.5%	0.053 ± 7.2%	0.097 ± 20.0%
Fumaric acid	2.369 ± 10.5%	0.170 ± 27.1%	0.073 ± 24.9%
Pyruvic acid	2.156 ± 11.2%	0.678 ± 11.6%	0.338 ± 9.6%
Malic acid	2.762 ± 6.4%	0.015 ± 18.5%	0.005 ± 21.1%

Another important result of the method comparison was the difference in the achieved standard errors. The ethanol method had the lowest error of 16% corresponding to the best reproducibility. The unquenched method revealed a slightly higher error of 17% whereas the methanol method had a standard error of 32% which is double the error rate of ethanol quenching, assuming a high variance in the samples. Furthermore, the number of identified metabolites was the highest in samples quenched with ethanol and the lowest when quenched with methanol. Altogether, 124 different metabolites were found when applying our internal library. The distribution and the number of identified metabolites are shown in a venn diagram in figure 46. 36% more metabolites could be detected in samples quenched with ethanol than after methanol quenching.

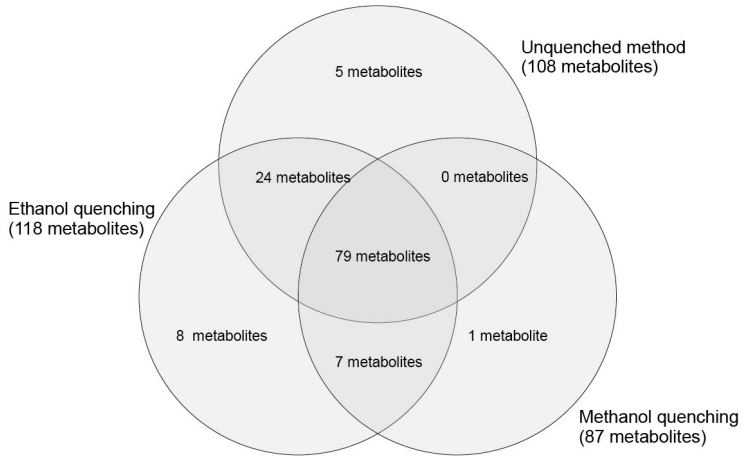

Figure 46. Division of 124 identified metabolites from three applied methods for *E. coli*.

First analysis of the supernatants was also done. A big problem during such analysis with GC/MS had been the high glucose concentration in the medium. Because cells were harvested in the middle of the exponential growth phase to show a stable phenotype, a quite high amount of the sugar was still present in the medium. To circumvent an overloading of the GC-column as well as the MS-detector, samples had to be analyzed in small amounts. But due to the high dilution of possibly leaked metabolites, concentrations of these substances might be below detection limit. Nevertheless, some analyses were done. In samples quenched with methanol, pyruvic acid was found in 1.5fold enhanced concentration in the supernatant when compared to unquenched ones.

Because of the results shown in figure 42 and table 21 the supernatant of ethanol quenched samples was analyzed in order to seek amino acids. Some had been only found in the extracts of unquenched samples. However, no high amounts of amino acids derived from cell leakage could be identified. Only aspartate was found in a high concentration. But this substance can be secreted from *E. coli* and furthermore, it was even found in high concentration in the corresponding quenched extracts. Additionally, 10fold higher amounts were determined in the supernatant of unquenched samples. Thus, a clear indication for cell leakage could not be found.

3.3.4 Quenching of Corynebacterium glutamicum

For quenching experiments with *C. glutamicum* cells were cultivated as described in chapter 2.7.1. To compare the different applied protocols correctly, samples were always taken together and at least in triplicates for each method (ethanol quenching, methanol quenching and standard method without quenching).

In figure 47 the results of the ethanol quenching are plotted in a scatterplot against the unquenched method. Displayed are the normalized peak areas which correspond to the relative intensities of the identified metabolites. Some metabolites could only be detected in samples quenched with ethanol and were found in the scatterplot on the ordinate. Furthermore, a lot of substances, for example some sugars and organic acids, were identified in higher relative concentrations in the quenched samples. The majority of compounds is located around the 45-degree line showing only small differences. Still some metabolites, like threonine and gamma-glutamylleucine, were higher concentrated in the unquenched samples. Altogether, the scatterplot indicated a better result after quenching because of the high number of increased substances.

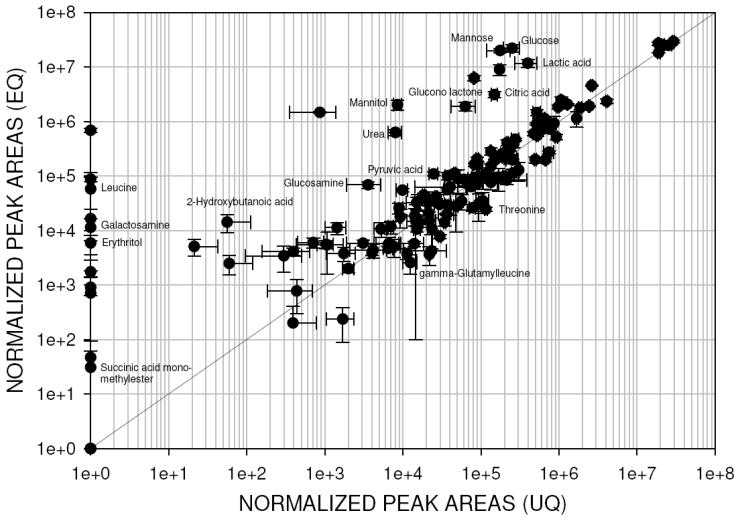

Figure 47. Scatterplot of ethanol quenched (EQ) and unquenched (UQ) samples of *C. glutamicum*.

In order to find out whether the metabolism really was completely stopped after quenching with ethanol and if any changes appeared during the standard, unquenched performance, an

experiment with additional standing times over 30 min was prepared. The results for both methods are displayed in figure 48. Hardly any changes were visible when comparing the standard method with routinely preparation with those additionally hold on ice for 30 min and similarly handled afterwards (see figure 48A). Just two sugars were detectable in samples without standing time but not in 30 min-samples. The calculated correlation coefficient of the logarithmic values of the concentration vectors revealed very good values of 0.94 ± 0.03, confirming only few changes - a fact that could already be seen in the scatterplot.

The result for the comparison of the ethanol quenching in figure 48B showed a similar picture as for the unquenched method. Some substances could only be detected in samples directly prepared (on the abscissa) and some only in samples stored over 30 min and handled afterwards by applying the same method (on the ordinate). But the majority of samples did not show any changes. Some amino acids were slightly varying. The correlation coefficient revealed a very good value of 0.94 ± 0.01, confirming only few changes and a nearly completely stopped metabolism.

Overall the results for the unquenched and ethanol quenched method were almost identical. Most of the enzymes seemed to be already stopped when reducing the temperature from 30°C for cultivation to 4°C in the unquenched method. Nevertheless, for temperature decrease the material was kept on ice which made it hard to control the process running inside. Consequently, it can not clearly be said that all enzymes were stopped, whereas in the quenching performance this cooling step was done controlled and due to the higher drop of temperature surely all enzymes were affected.

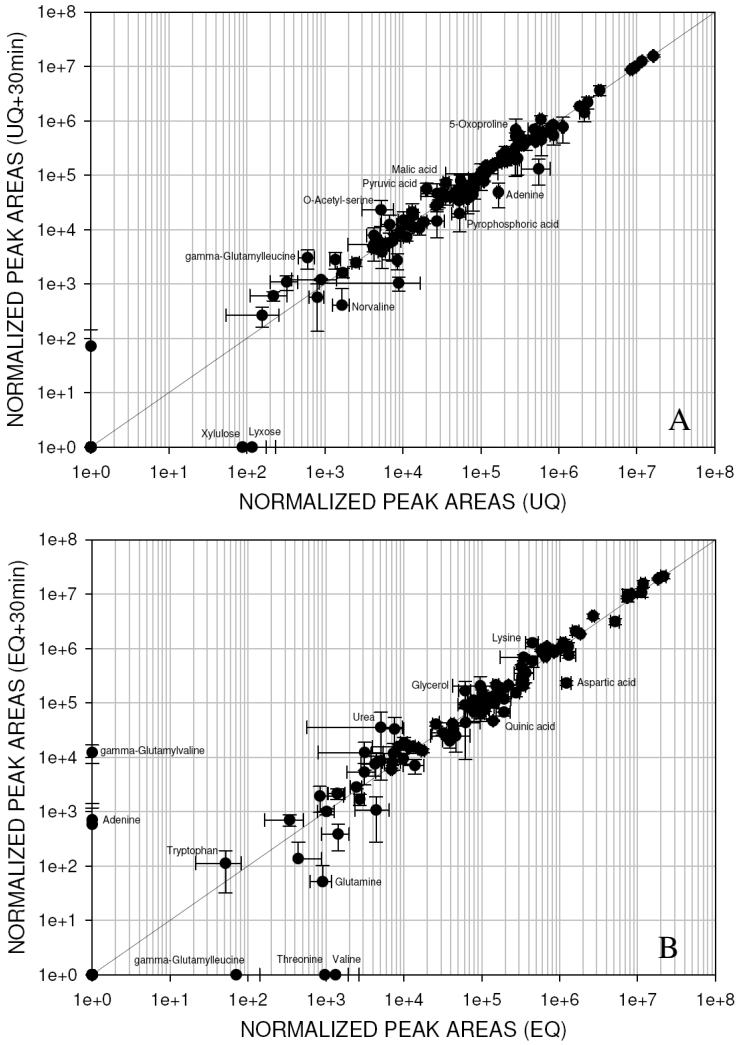

Figure 48. Scatterplots of unquenched (UQ) and ethanol quenched (EQ) samples. **A** unquenched samples compared to unquenched ones that were additionally held on ice for 30 min and **B** ethanol quenched samples compared to those stored for 30 min at -8°C.

The comparison of samples quenched with methanol and unquenched ones showed a completely different picture. In figure 49 the scatterplot is displayed. Nearly all metabolites were distributed cloud-like. Only some were located on the 45-degree line. The metabolites galactosamine, erythritol, succinic acid monomethylester and leucine could only be identified in methanol quenched samples, whereas 2,6-diaminopimelic acid, nicotinamide, glutamine and adenine were only detected in the unquenched ones. Furthermore, a lot of amino acids were found in higher concentrations in unquenched samples. This observation had already been described in the literature for the methanol method (Wittmann et al., 2004). But, for example, some sugars and other metabolites were detected in increased

levels in the methanol quenched samples. Altogether both methods led to completely different results.

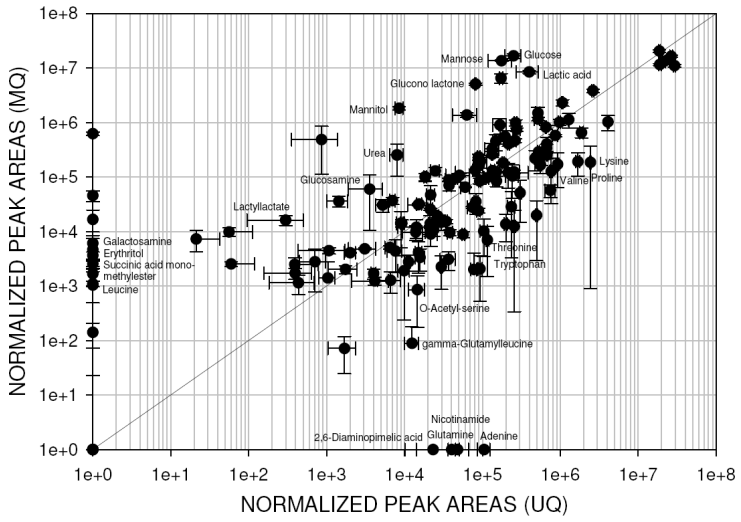

Figure 49. Scatterplot of methanol quenched (MQ) and unquenched (UQ) samples of *C. glutamicum*.

In order to allow a better evaluation of the results coming from the comparison of the methanol method and the unquenched method, a comparison of both quenching methods was done. The scatterplot is shown in figure 50. The metabolites were distributed like a cloud around the 45-degree line with a trend in direction of the ethanol method. Especially some amino acids were detected in increased amounts in samples quenched with ethanol. Furthermore, 2,6-diaminopimelic acid, nicotinamide, adenine and glutamine were not identifiable in methanol quenched samples but in ethanol quenched ones. These four compounds on the abscissa had already been detected as missing when compared to the unquenched method (see figure 49).

Other metabolites, for example, lactylactate and succinic acid monomethylester, were detected in higher concentrations in the methanol quenched samples. Just to remind, the latter one even had been missing and the first had occurred in a lower value in unquenched samples (see figure 49).

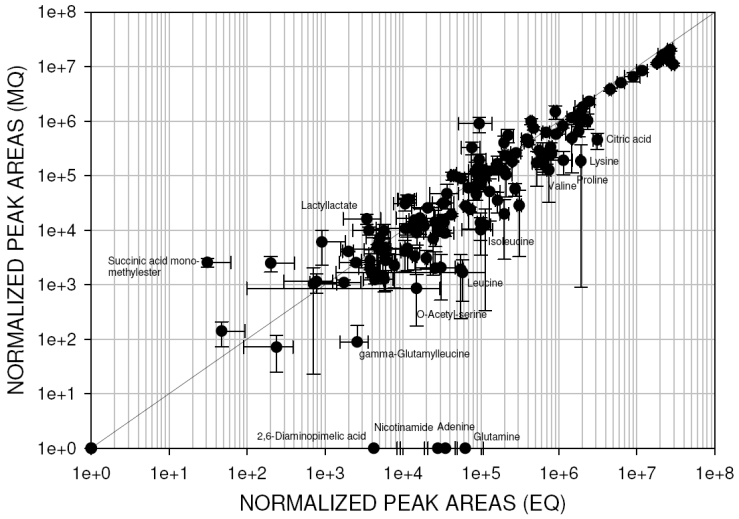

Figure 50. Scatterplot of methanol quenched (MQ) and ethanol quenched (EQ) samples of *C. glutamicum*.

A direct overview regarding the relative concentration ratios of some identified metabolites for all three methods is given in table 22. Some of the best reproducible substances are outlined. As already presented in figure 49 the methanol quenching compared to the unquenched method showed a loss in the relative concentrations of more than 50% of the identified metabolites. The comparison of the applied methods revealed the best result for the ethanol quenched samples. Around 64% of all identified metabolites were found in higher concentrations in these samples compared to unquenched ones. Additionally, when related to the methanol quenched samples, even more than 70% of the compounds had larger values in samples quenched with ethanol.

Table 22. Comparison of the relative concentrations of some identified amino acids, phosphorylated compounds and other metabolites in *C. glutamicum* applying the different procedures.

Metabolite	Ratio EQ to UQ	Ratio MQ to UQ	Ratio MQ to EQ
amino acids			
Aspartic acid	0.469 ± 8.1%	0.183 ± 25.8%	0.376 ± 27.4%
Glycine	0.630 ± 33.0%	0.101 ± 19.8%	0.159 ± 33.0%
Glutamic acid	0.728 ± 6.3%	0.260 ± 8.4%	0.344 ± 13.9%
Alanine	1.264 ± 15.3%	0.659 ± 4.9%	0.536 ± 20.4%

Metabolite	Ratio EQ to UQ	Ratio MQ to UQ	Ratio MQ to EQ
Tyrosine	1.269 ± 14.7%	0.613 ± 15.0%	0.443 ± 22.9%
Phenylalanine	2.072 ± 6.0%	0.736 ± 33.2%	0.375 ± 25.9%
phosphorylated compounds			
Glycerol-3-phosphate	0.282 ± 4.9%	0.093 ± 24.3%	1.320 ± 24.5%
Fructose-1,6-biphosphate	0.583 ± 9.0%	0.224 ± 20.0%	0.416 ± 31.5%
Phosphoenolpyruvic acid	0.934 ± 9.8%	0.685 ± 11.2%	0.733 ± 13.3%
Glucosamine-6-phosphate	0.943 ± 21.1%	0.642 ± 17.6%	0.738 ± 22.9%
2-Phosphoglyceric acid	0.965 ± 4.5%	0.334 ± 6.7%	0.344 ± 6.8%
3-Phosphoglyceric acid	1.152 ± 3.6%	0.454 ± 11.1%	0.394 ± 11-0%
Glucose-6-phosphate	1.233 ± 9.5%	1.453 ± 13.2%	1.152 ± 9.4%
Mannose-6-phosphate	1.470 ± 12.4%	2.708 ± 12.2%	1.897 ± 13.9%
Uridine-5'-monophosphate	1.514 ± 3.0%	0.984 ± 5.9%	0.638 ± 6.0%
Adenosine-5'-monophosphate	1.595 ± 7.2%	0.834 ± 9.1%	0.517 ± 9.4%
others			
Trehalose	0.916 ± 2.9%	0.658 ± 3.2%	0.723 ± 2.2%
Fumaric acid	1.092 ± 14.4%	1.743 ± 24.7%	1.553 ± 28.4%
N-acetyl-L-glutamic acid	1.455 ± 2.1%	0.909 ± 5.7%	0.631 ± 5.2%
Malic acid	1.554 ± 11.1%	1.587 ± 5.8%	1.030 ± 11.8%
α-Ketoglutaric acid	2.607 ± 11.3%	3.335 ± 7.8%	1.251 ± 14.1%
Succinic acid	2.744 ± 13.0%	2.159 ± 19.4%	0.787 ± 19.3%
Pyruvic acid	5.988 ± 8.2%	9.646 ± 10.1%	1.521 ± 11.1%
Citric acid	21.904 ± 7.9%	2.806 ± 26.5%	0.129 ± 26.8%
Lactic acid	29.550 ± 24.7%	22.900 ± 24.9%	0.775 ± 14.3%

The average relative standard error of all tested methods was estimated to evaluate the reproducibility. The error of the unquenched method, which had been established for *C. glutamicum* (Strelkov et al., 2004, Börner et al., 2007), revealed the lowest value of 14%. Nevertheless, the standard error of the ethanol quenching was only 18% whereas the methanol quenching showed an error of 23%. This outcome indicated the best results for ethanol quenching and the standard method. Due to the identified increased amounts of metabolites in samples quenched with ethanol, this method obtained the best results.

Overall, 160 different metabolites were identified applying our internal library for analysis of divers methods. Figure 51 shows the venn diagram of the distribution of the compounds

according to the methods. Again, the best result was achieved for ethanol quenching leading to the highest number of 151 detected metabolites. Over 80% of all metabolites were found in all three methods.

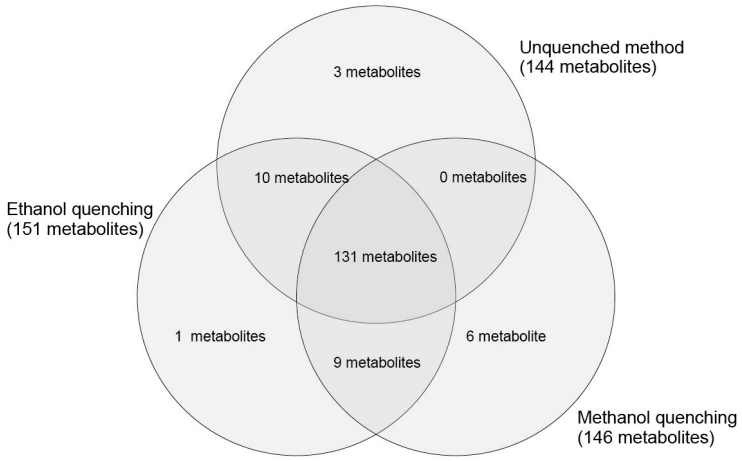

Figure 51. Distribution of the identified metabolites to the corresponding methods for *C. glutamicum*.

To find an indication why some metabolites were reduced in a defined method, first experiments to analyze the supernatants were performed. One problem, already mentioned in chapter 3.3.3 for *E. coli*, was the high amount of glucose in the medium. Possibly glucose was even sticking to the pellets and therefore was found in increased levels (glucose and mannose) in both quenching methods (see figure 47 and 49). Due to two washing steps in the unquenched standard performance, such moieties on the cells might be removed. Nevertheless, additional washing steps caused shear stress, as could be shown in chapter 3.3.3 for *E. coli*, and thus were omitted in the quenching performances. In the literature the methanol quenching of *C. glutamicum* was described applying an additional washing step. Dramatic losses in the levels of amino acids and phosphorylated compounds were the result (Wittmann et al., 2004).

However, in these experiments it was not possible to find such a high amount of metabolites in the supernatant of methanol quenched samples. The lower values of 50% of the metabolites (compared to unquenched samples) could thus not be ascribed to leakage during quenching. Even if some metabolite concentrations might be below the detection limit, a lot of substances (see table 22) were reduced to such values that detection still

should have been possible. Nevertheless, some metabolites of the tricarboxylic acid cycle, like fumaric acid, malic acid and succinic acid were found in the supernatant of methanol quenched samples. Also lactic acid, pyruvic acid as well as the amino acids alanine and glycine were detected. However, a direct correlation between the compounds in the supernatant and a possible decrease of their levels in the extracts could not be found. Some substances might simply be secreted from the cells, others might have been in higher concentrations because of cell lysis of several cells during growth. This might be especially the reason for metabolites of the central metabolism. They are not likely to be secreted. Furthermore, because of their occurrence in the supernatant a clear separation of cells and medium during harvesting should be always done to be able to quantify metabolite amounts correctly. Newer methods using the whole broth (Canelas et al., 2008) could lead to overestimations of the internal metabolite amounts (Bolten et al., 2007).
Glycine was detected in increased amounts in cell extracts of unquenched samples (see table 22). Though, it was also found in four times higher amounts in the supernatant of the corresponding samples than in ethanol quenched ones. Possibly this amino acid had been built in high concentrations and was excreted during growth of the bacterium.

3.3.5 Quenching of Saccharomyces cerevisiae

For quenching experiments *S. cerevisiae* cells were cultivated as described in chapter 2.7.1. A comparison of the different applied protocols was done. Therefore samples were always taken together and at least in triplicates for each method (ethanol quenching, methanol quenching and standard method without quenching).
In figure 52 the results of the ethanol quenching are shown in a scatterplot compared to the unquenched method. Displayed are the normalized peak areas which correspond to the relative intensities of the identified metabolites. The majority of detected metabolites had the same values in both methods. Only few substances, for example fructose, were only identified in ethanol quenched samples. Some compounds were found in increased levels in quenched samples. Uracil, 3-phosphoglyceric acid and phosphoenolpyruvic acid, had higher concentrations in unquenched samples. Overall, ethanol quenching worked very satisfying for yeast cells leading to even higher values and hardly any reduced ones.

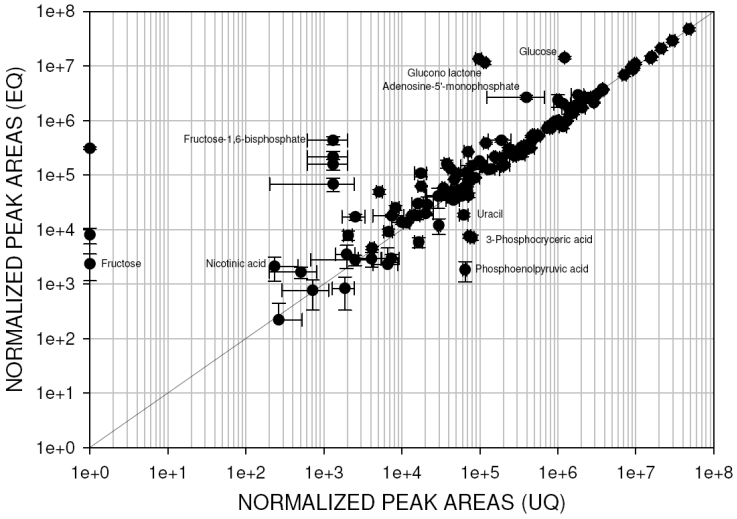

Figure 52. Scatterplot of ethanol quenched (EQ) and unquenched (UQ) samples of S. *cerevisiae*.

Additional experiments were performed to analyze whether the metabolism was stopped after harvesting the samples for ethanol quenching and standard method without quenching. Therefore, representative samples were hold on ice for 30 min before applying the unquenched method, respectively at -8°C for 30 min before handling them according to the ethanol quenching protocol. The result for both methods is shown in figure 53. The comparison of directly treated unquenched samples and those stored before further processing revealed an ongoing metabolism (figure 53A). Some metabolites had been detectable in the directly prepared samples but were not identified in the samples with the additional standing time (on the abscissa). Furthermore, histidine was only found in stored samples (on the ordinate). Most of the metabolites were located around the 45-degree line but the tendency showed higher concentrations of some substances in the directly handled samples. Possibly, these substances, for example some phosphorylated compounds, were further converted during standing time and thus detected in lower values in the other samples. This would hint to a not completely stopped metabolism when applying our standard, unquenched method. Nevertheless, the calculated correlation coefficient using the logarithmic relative concentration vectors was 0.95 ± 0.01, indicating only few changes and confirming the before described findings.

Ethanol quenched samples and those stored for 30 min before further processing were compared and are shown in figure 53B. Nearly all metabolites were located around the 45-

degree line. Some phosphorylated compounds were found in slightly higher concentrations in directly prepared samples. 2-aminobutyric acid was detected in stored samples only and was found on the ordinate. The calculated correlation coefficient revealed a very good value of 0.96 ± 0.01, confirming the determination of a stopped metabolism when applying ethanol quenching.

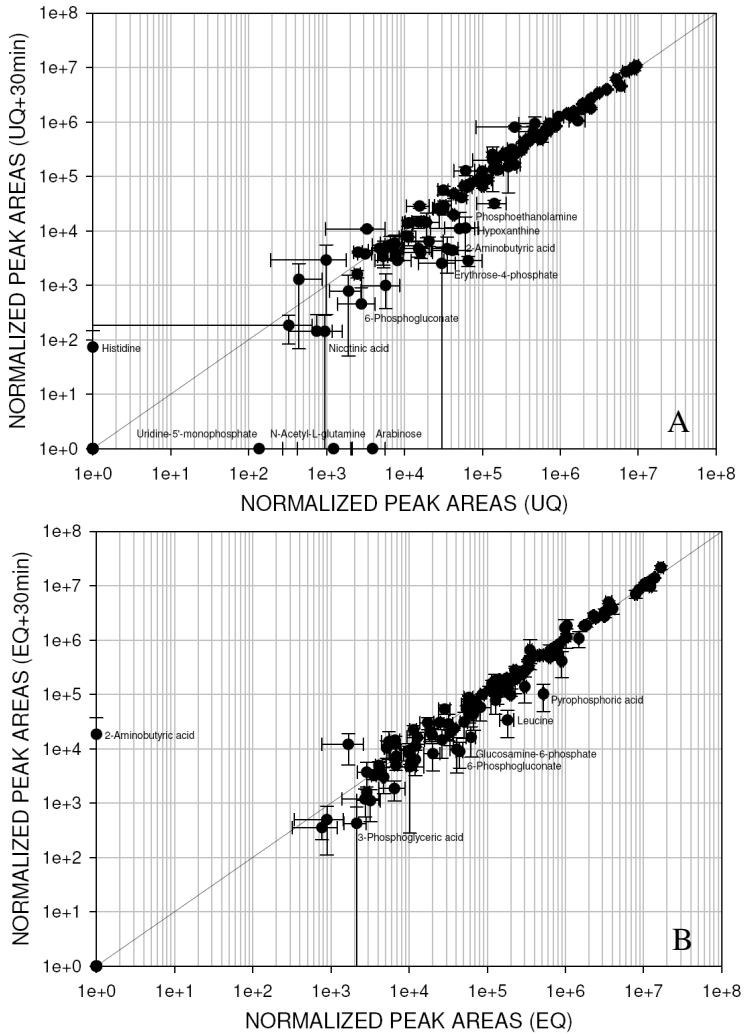

Figure 53. Scatterplots of unquenched (UQ) and ethanol quenched (EQ) samples. **A** unquenched samples compared to unquenched ones additionally held on ice for 30 min and **B** ethanol quenched samples compared to those stored for 30 min at -8°C.

The comparison of the methanol quenching and the unquenched method revealed a similar picture as the relation of ethanol quenching and unquenched protocol (see figure 52) had done. The scatterplot is shown in figure 54. Most of the metabolites were spread around the

45-degree line. Some compounds like 3-phosphoglyceric acid and phosphoenolpyruvic acid were slightly increased in samples of the unquenched method. A lot of phosphorylated compounds were identified in higher values in methanol quenched samples. Fructose and hydroxylamine were only found in the quenched samples. The methanol method seemed to work very efficient and produced satisfying results for this organism. Only few substances were reduced whereas a lot of metabolites could be identified in increased levels.

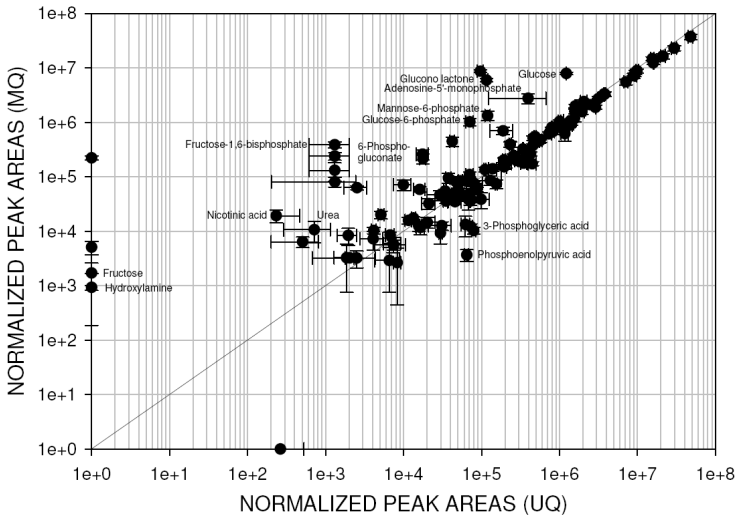

Figure 54. Scatterplot of methanol quenched (MQ) and unquenched (UQ) samples of S. *cerevisiae*.

In order to estimate which of the both tested quenching methods worked best, they were directly compared (figure 55). Most of the metabolites showed the same concentration in both methods. Hydroxylamine was only identified in methanol quenched samples. Some substances, for example some phosphorylated compounds, were slightly increased in samples quenched with methanol. Other compounds like cysteine and pyruvic acid were slightly higher concentrated after ethanol quenching. The scatterplot confirmed a similar result after quenching for both methods which was only slightly differing for a few metabolites.

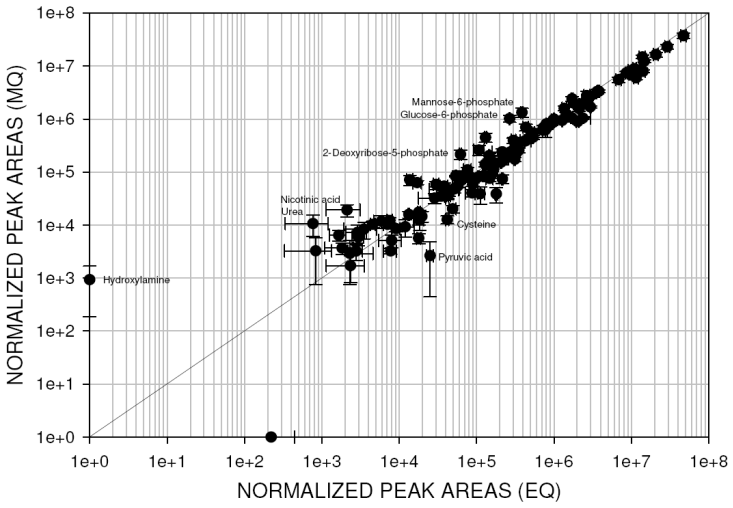

Figure 55. Scatterplot of methanol quenched (MQ) and ethanol quenched (EQ) samples of S. *cerevisiae*.

A direct overview regarding the relative concentration ratios of some representative compounds of the identified metabolites for all three methods is shown in table 23. In contrast to the other tested organisms, the results for all performances did not so much differ for yeast. About 64% of all identified metabolites showed increased concentrations in samples quenched with ethanol when compared to the unquenched ones. In samples quenched with methanol still 58% of the detected metabolites revealed higher values than in unquenched samples. The direct comparison of both quenching methods gave an increased level for 60% of the metabolites in ethanol quenched samples. This again indicated a very similar performance of both quenching methods, but also a slightly better result for samples quenched with the performance that was improved in this study.

Table 23. Comparison of the relative concentrations of some identified amino acids, phosphorylated compounds and other metabolites in *S. cerevisiae* applying the different procedures.

Metabolite	Ratio EQ to UQ	Ratio MQ to UQ	Ratio MQ to EQ
amino acids			
Leucine	0.715 ± 6.3%	0.612 ± 7.9%	0.832 ± 14.3%
Proline	0.767 ± 3.0%	0.661 ± 5.9%	0.874 ± 6.9%
Valine	0.874 ± 2.0%	0.825 ± 5.1%	0.946 ± 5.3%
Phenylalanine	0.878 ± 6.5%	0.94 ± 8.3%	1.070 ± 5.4%

Metabolite	Ratio EQ to UQ	Ratio MQ to UQ	Ratio MQ to EQ
Tyrosine	0.999 ± 4.5%	0.952 ± 4.9%	0.950 ± 3.5%
Alanine	1.035 ± 4.4%	0.916 ± 6.3%	0.889 ± 5.0%
Threonine	1.083 ± 1.9%	1.016 ± 4.7%	0.936 ± 4.3%
Lysine	1.132 ± 8.7%	1.060 ± 9.6%	0.925 ± 4.9%
Glutamic acid	1.148 ± 5.8%	1.089 ± 6.2%	0.930 ± 3.8%
Glutamine	1.238 ± 14.9%	0.846 ± 19.9%	0.683 ± 15.8%
Aspartic acid	1.455 ± 15.2%	1.147 ± 9.7%	0.817 ± 3.3%
Serine	1.517 ± 6.7%	1.483 ± 18.6%	0.960 ± 10.9%
Tryptophan	1.585 ± 25.3%	1.511 ± 25.7%	0.937 ± 4.0%
phosphorylated compounds			
3-Phosphoglyceric acid	0.078 ± 1.3%	0.111 ± 1.6%	1.414 ± 30.5%
Erythrose-4-phosphate	0.905 ± 5.2%	0.956 ± 7.0%	1.068 ± 10.4%
Glycerol-3-phosphate	0.922 ± 3.2%	1.116 ± 14.5%	1.261 ± 19.4%
Xylulose-5-phosphate	0.984 ± 5.0%	1.380 ± 15.9%	1.445 ± 19.7%
Ribulose-5-phosphate	1.010 ± 4.9%	1.508 ± 15.8%	1.562 ± 18.3%
others			
Succinic acid	0.619 ± 2.5%	0.585 ± 4.4%	0.966 ± 6.3%
Fumaric acid	0.758 ± 3.0%	1.023 ± 7.1%	1.351 ± 8.1%
Malic acid	0.847 ± 1.4%	0.626 ± 3.3%	0.740 ± 3.7%
Lactic acid	1.026 ± 4.4%	0.862 ± 6.4%	0.847 ± 5.4%
Citric acid	1.399 ± 7.8%	1.322 ± 14.6%	0.922 ± 8.1%
Pyruvic acid	2.047 ± 32.4%	0.695 ± 28.5%	0.458 ± 11.4%

Applying our internal standard library, altogether 152 metabolites were identified for *S. cerevisiae* when testing the different quenching methods. The distribution is shown in a venn diagram in figure 56. Only slightly differing numbers of metabolites were detected in the different samples. Nearly 97% of all found metabolites were detectable in all three methods. For the ethanol quenching performance the lowest average standard error of 10% was obtained. The methanol method led to an error of 17%, whereas the unquenched performance reached a standard error of 16%.

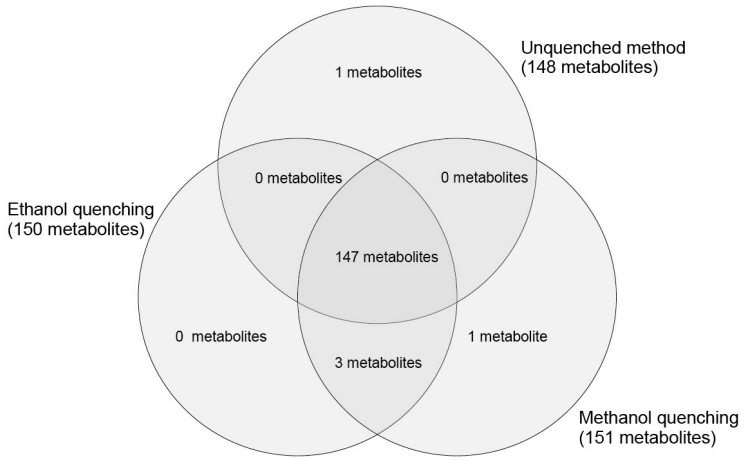

Figure 56. Distribution of the identified metabolites to the corresponding methods for *S. cerevisiae*.

Some experiments to analyze the supernatants were performed. Again, the difficulty was the high amount of glucose in the medium. Increased levels of identified glucose in both quenching methods (see figure 52 and 54) already indicated this issue. Only metabolites from the central metabolism, for example pyruvic acid, lactic acid and oxalic acid, were in the supernatants. But these compounds additionally showed increased concentrations in the corresponding cell extracts. Therefore, they were likely derived from cell lysis during growth rather than from cell leakage during quenching. Increased levels of amino acids or phosphorylated compounds could not be detected. In fact, higher values of the latter ones found in the extracts of the quenched samples (see figure 52 and 54) indicated a proper quenching of the metabolism, whereas these compounds were further converted and thus reduced in the unquenched ones.

4 Summary

For a comprehensive metabolome analysis of microorganisms, a high-throughput method for metabolome analysis using gas chromatography coupled to mass spectrometry had been developed. As model organism the fast growing bacterium *Corynebacterium glutamicum* was used. The established method combined multiparallel growth in micro titer plates and a semi-automated pre-analytical sample preparation. Despite the significantly decreased culture volume, metabolome analysis was successfully performed. Due to the semi-automation a time efficiency for the pre-analytical steps by a factor of 15 could be achieved in the high-throughput method compared to the standard method. Additionally, the standard error of the analysis was reduced as well. It decreased from 25% in the standard performance to 13%. Furthermore, with the shortened GC/MS run and an adapted library it was possible to measure around 72 single samples per day and machine - which was four times more than with standard runs - and still identify a high number of metabolites. The high reproducibility of this established method was proven with a very high correlation coefficient of independent wild type samples of 0.99 ± 0.01.

The development of such a reliable high-throughput method was the prerequisite for the screening of a large transposon mutant collection for the identification of mutants with an altered metabolome. For the identification of suitable screening criteria a pilot project with around 320 randomly selected and representative transposon mutants was performed. In first instance mutant samples were compared to the wild type raised under the same conditions together with the mutant on the same plate. This led to the identification of first differences. Nevertheless, it was not possible to distinguish between changes directly caused by the genetic perturbation and those resulting from biological and environmental variance. Thus, a reference list was generated combining all the information from wild type samples of different cultivations and operators. The list represented the native wild type state. Comparison of the single wild type samples and this reference list revealed significant differences due to biological and environmental changes but also from performance variations (especially the GC/MS machine). Moreover, directly comparing this reference list against the mutants changes due to the genetic modification were found and interesting phenotypes identified. With the calculated threshold for each metabolite significant changes in compound levels were revealed. The investigation of the ten to

twenty most abundant substances of a sample and the method of hierarchical clustering gave further indications of possibly affected pathways. Further information was obtained after identification of the insertion site of the transposon. A correlation of the disrupted gene and the derived phenotype could be performed.

In parallel to the development and the evaluation of the high-throughput screening of transposon mutants from *Corynebacterium glutamicum* research was done on the field of quenching of microorganism. To stop the metabolome in the moment of harvesting is especially important, if, for example, different growth conditions have to be investigated. The differences might be very small and any changes could be overwhelmed by an unquenched metabolism. Thus, a quenching performance that was established in our group which used a cold ethanol solution was optimized and evaluated using three different microorganisms: *Corynebacterium glutamicum, Escherichia coli* and *Saccharomyces cerevisiae*. For comparison, our standard method was used as unquenched control method, and also two published quenching methods were applied whereof only one revealed useful results. With the new developed method improved results could be achieved for all organisms. The number of identified metabolites as well as the detected relative concentrations were mostly the highest combined with a low standard error. Furthermore, the completely stopped metabolism could be confirmed when applying ethanol quenching. The correlation coefficients of samples stored for 30 minutes under quenched conditions and those directly handled after quenching reached high values of 0.94...0.96 depending on the organism. The most striking results in this test were revealed for *E. coli*. As Gram-negative organism it is at high risk for cell leakage. Nevertheless, applying our quenching performance, no leakage was found.

5 Outlook

The developed high-throughput metabolome analysis and the established screening criteria can be used for an investigation of the whole transposon mutant bank of *Corynebacterium glutamicum.* It can also be applied on other microorganisms. The prerequisite is a growth of the organism to high optical densities and a well established standard library for identification of the metabolites.

The information from such a screening combined with those of the identified disrupted gene will provide a deeper understanding of the gene function. Furthermore, novel gene functions might be obtained. Therefore, this protocol can be applied to close existing gaps in pathways and can in the end create a complete overview about all enzymes present in the organism.

Using all the information about the different phenotypes, accumulations in desired pathways can easily be found. The relation to the disrupted gene can lead to new conclusions and interesting observations in regulations.

The developed ethanol quenching protocol can be used for the investigation of different growth conditions of microorganisms. Especially interesting might be the differentiation of the growth phases. Variations after cultivation on different carbon and nitrogen sources can also be investigated.

A refinement of the quenching method could possibly be the variation of the ratio of culture and quenching solution. The high amount of sugar detected in quenched extracts might be from medium moieties and could possibly be removed this way.

6 References

Abe, S., Takayama, K.-I. and Kinoshita, S., *Taxonomical Studies on Glutamic Acid-Producing Bacteria.* J Gen Appl Microbiol, 1967. **13**: p. 279-301.

Abbott, A., *A post-genomic challenge: learning to read patterns of protein synthesis.* Nature, 1999. **402**: p. 715-720.

Adams, M.A., et al., *Simultaneous determination by capillary gas chromatography of organic acids, sugars, and sugar alcohols in plant tissue extracts as their trimethylsilyl derivatives.* Anal Biochem, 1999. **266**(1): p. 77-84.

Bathe, B., Kalinowski, J. and Pühler, A., *A physical and genetic map of the Corynebacterium glutamicum ATCC 13032 chromosome.* Mol Gen Genet, 1996. **252**: p. 255-265.

Bolten, C.J., et al., *Sampling for Metabolome Analyis of Microorganisms.* Anal Chem, 2007. **79**: p. 3843-3849.

Börner, J., Buchinger, S. and Schomburg, D., *A high-throughput method for microbial metabolome analysis using gas-chromatography/mass spectrometry.* Anal Biochem, 2007. **367**: p. 143-151.

Buchholz, A., R. Takors, and C. Wandrey, *Quantification of Intracellular Metabolites in Escherichia coli K12 Using Liquid Chromatographic-Electrospray Ionization Tandem Mass Spectrometric Techniques.* Anal Biochem, 2001. **295**: p. 129-137.

Buchholz, A., et al., *Metabolomics: quantification of intracellular metabolite dynamics.* Biomol Eng, 2002. **19**: p. 5-15.

Buziol, S., et al., *New Bioreactor-Coupled Rapid Stopped-Flow Sampling Technique for Measurements of Metabolite Dynamics on a Subsecond Time Scale.* Biotechnol Bioeng, 2002. **80**(6): p. 632-636.

Canelas, A.B., et al., *Leakage-free rapid quenching technique for yeast metabolomics.* Metabolomics, 2008 (DOI 10.1007/s11306-008-0116-4).

Castellani, A. and Chalmers, A.J., *Manual of Tropical Medicine*. 3rd ed. 1919, New York: Williams Wood and Co.

Castrillo, J.I., et al., *An optimized protocol for metabolome analysis in yeast using direct infusion electrospray mass spectrometry.* Phytochemistry, 2003. **62**: p. 929-937.

Celis, J.E., et al., *Gene expression profiling: monitoring transcription and translation products using DNA microarrays and proteomics.* FEBS Lett, 2000. **480**(1): p. 2-16.

Claes, W.A., Pühler, A. and Kalinowski, J., *Identification of Two prpDBC Gene Clusters in Corynebacterium glutamicum and Their Involvement in Propionate Degradation via the 2-Methylcitrate Cycle.* J Bacteriol, 2002. **184**(10): p. 2728-2739.

Covert, M.W., et al., *Integration high-throughput and computational data elucidates bacterial networks.* Nature, 2004. **429**: p. 92-96.

De Keersmaecker, S.C.J., et al., *Integration of omics data: how well does it work for bacteria?* Mol Microbiol, 2006. **62**(5): p. 1239-1250.

de Koning, W. and van Dam, K., *A Method for the Determination of Changes of Clycolytic Metabolites in Yeast on a Subsecond Time Scale Using Extraction at Neutral pH.* Anal Biochem, 1992. **204**: p. 118-123.

Derynck, R., et al., *Expression of human fibroblast interferon gene in Escherichia coli.* Nature, 1980. **287**: p. 193-197.

Dickinson, J.R. and Schweizer, M., *The metabolism and molecular physiology of Saccharomyces cerevisiae*. 1999, London: Taylor & Francis.

Duetz, W.A., et al., *Methods for Intense Aeration, Growth, Storage, and Replication of Bacterial Strains in Microtiter Plates.* Appl Environ Microbiol, 2000. **66**(6): p. 2641-2646.

Duetz, W.A. and Witholt,B., *Oxygen transfer by orbital shaking of square vessels and deepwell microtiter plates of various dimensions.* Biochem Eng J, 2004. **17**: p. 181-185.

Dunn, W.B., Bailey, N.J.C. and Johnson, H.E., *Measuring the metabolome: current analytical technologies.* Analyst, 2005. **130**: p. 606-625.

Dunn, W.B., *Current trends and future requirements for the mass spectrometric investigation of microbial, mammalian and plant metabolomes.* Phys Biol, 2008. **5**.

Edwards, J.L., et al., *Negative mode sheathless capillary electrophoresis electrospray ionization-mass spectrometry for metabolite analysis of prokaryotes.* J Chromatogr A, 2006. **1106**: p. 80-88.

Eggeling, L., Pfefferle, W. and Sahm, H., *Amino acids*, in *Basic Biotechnology*, C. Ratledge and B. Kristiansen, Editors. 2001, Cambridge University Press: Cambridge. p. 281-303.

Feldhaus, P., *Entwicklung eines Hochdurchsatzverfahrens zur Identifizierung von Transposon-Insertionsstellen für Knock-out-Mutanten von Corynebacterium glutamicum*, in *Institut für Biochemie*. 2005, Universität zu Köln: Köln. p. 82.

Feng, X., et al., *Mass spectrometry in systems biology: An overview.* Mass Spectrom Rev, 2008: p. DOI: 10.1002/mas.20182.

Fiehn, O., et al., *Metabolite profiling for plant functional genomics.* Nat Biotechnol, 2000. **18**: p. 1157-1161.

Fiehn, O., et al., *Identification of Uncommon Plant Metabolites Based on Calculation of Elemental Compositions Using Gas Chromatography and Quadrupole Mass Spectrometry.* Anal Chem, 2000a. **72**: p. 3573-3580.

Fiehn, O., *Metabolomics - the link between genotypes and phenotypes.* Plant Mol Biol, 2002. **48**: p. 155-171.

Fox, A., *Carbohydrate profiling of bacteria by gas chromatography-mass spectrometry and their trace detection in complex matrices by gas chromatography-tandem mass spectrometry.* J Chromatogr A, 1999. **843**: p. 287-300.

Garcia, D.E., et al., *Separation and mass spectrometry in microbial metabolomics.* Curr Opin Microbiol 2008. **11**: p. 233-239.

Glazer, A. and Nikaido, H., *Microbial Biotechnology: Fundamentals of Applied Microbiology.* Vol. second. 2007: Cambridge University Press.

Goeddel, D.V., et al., *Expression in Escherichia coli of chemically synthesized genes for human insulin.* Proc Nati Acad Sci USA, 1979. **76**(1): p. 106-110.

Goffeau, A., et al., *Life with 6000 genes.* Science, 1996. **274**: p. 546-567.

Gonzalez, B., Francois, J., and Renaud, M., *A rapid and reliable method for metabolite extraction in yeast using boiling buffered ethanol.* Yeast, 1997. **13**: p. 1347-1356.

Grindley, N.D.F. and Reed, R.R., *Transpositional Recombination in Prokaryotes.* Ann Rev Biochem, 1985. **54**.

Grob, K. and Konrad, G., *Split and splitless injection in capillary gas chromatography.* 1993, Heidelberg: Hüthig. p. 571.

Gross, J.H., *Mass Spectrometry - a textbook*. 2004, Berlin Heidelberg: Springer.

Halket, J.M., et al., *Chemical derivatization and mass spectral libraries in metabolic profiling by GC/MS and LC/MS/MS.* J Exp Bot, 2005. **56**(410): p. 219-243.

Hamer, L., et al., *Recent advances in large-scale transposon mutagenesis.* Curr Opin Chem Biol, 2001. **5**: p. 67-73.

Hanahan, D., *'Studies on transformation of Escherichia coli with plasmids.* J Mol Biol, 1983. **166**: p. 577-580.

Hans, M.A., Heinzle, E., and Wittmann, C., *Quantification of intracellular amino acids in batch cultures of Saccharomyces cerevisiae.* Appl Microbiol Biotechnol, 2001. **56**: p. 776-779.

Hayes, F., *Transposon-Based Strategies for Microbial Functional Genomics and Proteomics.* Annu Rev Genet, 2003. **37**: p. 3-29.

Herebian, D., et al., *In vivo labeling with stable isotopes as a tool for the identification of unidentified peaks in the metabolome analysis of Corynebacterium glutamicum by GC/MS.* Biol Chem, 2007. **388**: p. 865-871.

Hübschmann, H., *Handbuch der GC/MS: Grundlagen und Anwendung*. 2001, Weinheim: VCH.

Ikeda, M. and Nakagawa, S., *The Corynebacterium glutamicum genome: features and impacts on biotechnological processes.* Appl Microbiol Biotechnol, 2003. **62**: p. 99-109.

Ikeda, M., *Amino acid production processes.* Adv Biochem Eng Biotechnol, 2003a. **79**: p. 1-35.

Ishii, N., et al., *Metabolome analysis and metabolic simultaion.* Metabolomics, 2005. **1**(1): p. 29-37.

Jäger, C., *Vergleich absoluter Metabolitkonzentrationen von Corynebacterium glutamicum, Escherichia coli und Pseudomonas putida*, in *Institut für Biochemie*. 2007, Universität zu Köln: Köln. p. 133.

Jensen, N.B.S., Jokumsen, K. V., and Villadsen, J., *Determination of the phosphorylated sugars of the Embden-Meyerhoff-Parnas pathway in Lactococcus lactis using fast sampling technique and solid phase extraction.* Biotechnol Bioeng, 1999. **63**(3): p. 356-362.

Jeol Instructions *JMS-T100GC The AccuTOF GC Introduction,* 2005

Kalinowski, J., et al., *The complete Corynebacterium glutamicum ATCC 13032 genome sequence and its impact on the production of $_L$-aspartate-derived amino acids and vitamins.* J Biotechnol , 2003. **104**(1-3): p. 5-25.

Kell, D.B., *Metabolomics and systems biology: making sence of the soup.* Curr Opin Microbiol, 2004. **7**(3): p. 296-307.

Kell, D.B., *Metabolomics, modelling and machine learning in systems biology - towards an understanding of the languages of cells.* FEBS J, 2006. **273**: p. 873-894.

Kinoshita, S., *A Short History of the Birth of the Amino Acid Industry in Japan*, in *Handbook of Corynebacterium glutamicum*, L. Eggeling and M. Bott, Editors. 2005, Taylor & Francis Group. p. 3-5.

Kitano, H., *Systems Biology: A brief overview.* Science, 2002. **295**: p. 1662-1664.

Kovàts, E., Adv Chromatogr, 1956. **1**: p. 229-247.

Kumar, S., Wittmann, C. and Heinzle, E., *Minibioreactors.* Biotechnol Lett, 2004. **26**: p. 1-10.

Larsson, G. and Törnkvist, M., *Rapid sampling, cell inactivation and evaluation of low extracellular glucose concentrations during fed-batch cultivation.* J Biotechnol, 1996. **49**: p. 69-82.

Liebl, W., *Corynebacterium Taxonomy*, in *Handbook of Corynebacterium glutamicum*, L. Eggeling and M. Bott, Editors. 2005, Taylor & Francis Group. p. 9-34.

Liu, E.T., *Systems Biology, Integrative Biology, Commentary Predictive Biology.* Cell, 2005. **121**: p. 505-506.

Loret, M.O., Pedersen, L., and Francois, J., *Revised procedures for yeast metabolites extraction: application to a glucose pulse to carbon-limited yeast cultures, which reveals a transient activation of the purine salvage pathway.* Yeast, 2007. **24**: p. 47-60.

Maharjan, R.P. and Ferenci, T., *Global metabolite analysis: the influence of extraction methodology on metabolome profiles of Escherichia coli.* Anal Biochem, 2003. **313**: p. 145-154.

Mahillon, J. and Chandler, M., *Insertion Sequences.* Microbiol Mol Biol Rev, 1998. **62**(3): p. 725-774.

Mashego, M.R., et al., *Critical Evaluation of Sampling Techniques for Residual Glucose Determination in Carbon-Limited Chemostat Culture of Saccharomyces cerevisiae.* Biotechnol Bioeng, 2003. **83**(4): p. 395-399.

Mashego, M.R., et al., *Microbial metabolomics: past, present and future methodologies.* Biotechnol Lett, 2007. **29**: p. 1-16.

Moritz, B., et al., *Kinetic properties of the glucose-6-phosphate and 6-phosphogluconate dehydrogenases from Corynebacterium glutamicum and their application for predicting pentose phosphate pathway flux in vivo.* Eur J Biochem, 2000. **267**: p. 3442-3452.

Mormann, S., et al., *Random mutagenesis in Corynebacterium glutamicum ATCC 13032 using an IS6100-based transposon vector identified the last unknown gene in the histidine biosynthesis pathway.* BMC Genomics, 2006. **7**(205).

Neidhardt, F.C. and Umbarger, H.E., *Chemical Composition of Escherichia coli*, in *Escherichia coli and Salmonella typhimurium - Cellular and Molecular Biology*, F.C. Neidhardt, Editor. 1996, ASM Press.

NCBI, www.ncbi.nlm.nih.gov

O'Farrell, P.H., *High Resolution Two-Dimensional Electrophoresis of Proteins.* J Biol Chem, 1975. **250**(10): p. 4007-4021.

Peterson, C.L. and Herskowitz, I., *Characterization of the yeast SWI1, SWI2 and SWI3 gene, which encode a global activator of transcription.* Cell, 1992. **68**: p. 573-583.

Plassmeier, J., et al., *Investigation of central carbon metabolism and the 2methylcitrate cycle in Corynebacterium glutamicum by metabolic profiling using gas chromatography-mass spectrometry.* J Biotechnol, 2007. **130**: p. 354-363.

Raamsdonk, L.M., et al., *A functional genomics strategy that uses metabolome data to reveal the phenotype of silent mutations.* Nat Biotechnol, 2001. **19**: p. 45-50.

Rahman, S.A., et al., *Metabolic pathway analysis web service (Pathway Hunter Tool CUBIC).* Bioinformatics, 2005. **21**(7): p. 1189-1193.

Reimer, L., *Charakterisierung von Corynebacterium glutamicum Transposonmutanten und Entwicklung einer Quenchmethode für Mikroorganismen*, in *Bioinformatik & Biochemie*. 2008, Technische Universität Braunschweig: Braunschweig. p. 129.

Roessner, U., et al., *Simultaneous analysis of metabolites in potato tuber by gas chromatography-mass spectrometry.* Plant J, 2000. **23**(1): p. 131-142.

Roessner, U., et al., *Metabolic Profiling Allows Comprehensive Phenotyping of Genetically or Environmentally Modified Plant Systems.* Plant Cell, 2001. **13**: p. 11-29.

Ross-Macdonald, P., et al., *Large-scale analysis of the yeast genome by transposon tagging and gene disruption.* Nature, 1999. **402**: p. 413-418.

Schäfer, A., et al., *High-Frequency Conjugal Plasmid Transfer from Gram-Negative Escherichia coli to Various Gram-Positive Coryneform Bacteria.* J Bacteriol, 1990. **172**(3): p. 1663-1666.

Schäfer, U., et al., *Automated Sampling Device for Monitoring Intracellular Metabolite Dynamics.* Anal Biochem, 1999. **270**: p. 88-96.

Schäfer, A., et al., *Small mobilizable multi-purpose cloning vectors derived from the Escherichia coli plasmids pK18 and pK19: selection of definded deletions in the chromosome of Corynebacterium glutamicum.* Gene, 1994. **145**: p. 69-73.

Schauer, N., et al., *GC-MS libraries for the rapid identification of metabolites in complex biological samples.* FEBS Lett 2005. **579**: p. 1332-1337.

Schena, M., et al., *Quantitative Monitoring of Gene Expression Patterns with a Complementary DNA Microarray.* Science, 1995. **270**: p. 467-470.

Schomburg, I., Chang,A. and Schomburg, D., *BRENDA, enzyme data and metabolic information.* Nucleic Acids Res, 2002. **30**: p. 47-49.

Soga, T., et al., *Simultaneous determination of anionic intermediates for Bacillus subtilis metabolic pathways by capillary electrophoresis electrospray ionization mass spectrometry.* Anal Chem, 2002. **74**: p. 2233-2239.

Soga, T., et al., *Quantitative metabolome analysis using capillary electrophoresis mass spectrometry.* J Proteome Res., 2003. **2**(5): p. 488-494.

Somerville, C. and Somerville, S., *Plant Functional Genomics.* Science, 1999. **285**: p. 380-383.

Stein, S.E., *An Integration Method for Spectrum Extraction and Compound Identification from GC/MS Data*. 1999, Mass Spectrometry Data Center, Physical and Chemical Properties Division, National Institute of Standards and Technology: Gaithersburg, MD. p. 1-30.

Strelkov, S., von Elstermann, M. and Schomburg, D., *Comprehensive analysis of metabolites in Corynebacterium glutamicum by gas chromatography/mass spectrometry.* Biol Chem, 2004. **385**: p. 853-861.

Suzuki, N., et al., *High-throughput transposon mutagenesis of Corynebacterium glutamicum and Construction of a single-gene disruptant mutant library.* Appl Environ Microbiol, 2006. **72**(5): p. 3750-3755.

Sweetlove, L.J., Last, R.L. and Fernie, A.R., *Predictive Metabolic Engineering: A Goal for Systems Biology.* Plant Physiol, 2003. **132**: p. 420-425.

Tamkun, J.W., et al., *brahma: a regulator of Drosophila homeotic genes structurally transcriptional activator SNF2/SWI2.* Cell, 1992. **68**: p. 561-572.

Tauch, A., et al., *The Corynebacterium xerosis Composite Transposon Tn5432 Consists of Two Identical Insertion Sequences, Designated IS1249, Flanking the Erythromycin Resistance Gene ermCX.* Plasmid, 1995. **34**: p. 119-131.

Tauch, A., et al., *The 27.8-kb R-plasmid pTET3 from Corynebacterium glutamicum encodes the aminoglycoside adenyltransferase gene cassette aadA9 and the regulated tetracycline efflux system Tet 33 flanked by active copies of the widespread insertion sequence IS6100.* Plasmid, 2002. **48**(2): p. 117-129.

Tauch, A., et al., *Strategy to sequence the genome of Corynebacterium glutamicum ATCC 13032: use of a cosmid and a bacterial artificial chromosome library.* J Biotechnol, 2002a. **95**: p. 25-38.

vanDeemter, J.J., Zuiderweg, F.J. and Klinkenberg, A., *Longitudinal diffusion and resistance to mass transfer as causes of nonideality in chromatography.* Chem Eng Science, 1956. **5**: p. 271-289.

Vertès, A.A., Inui, M. and Yukawa, H., *Manipulating Corynebacteria, from Individual Genes to Chromosomes.* Appl Environ Microbiol, 2005. **71**(12): p. 7633-7642.

Villas-Bôas, S.G., et al., *Simultaneous analysis of amino and nonamino organic acids as methyl chloroformate derivatives using gas chromatography-mass spectrometry.* Anal Biochem, 2003. **322**: p. 134-138.

Villas-Bôas, S.G., et al., *Mass Spectrometry in Metabolome Analysis.* Mass Spectrom Rev 2005. **24**: p. 613-646.

Villas-Bôas, S.G., et al., *Global metabolite analysis of yeast: evaluation of sample preparation methods.* Yeast, 2005a. **22**: p. 1155-1169.

Villas-Bôas, S.G. and Bruheim, P., *Cold glycerol-saline: The promising quenching solution for accurate intracellular metabolite analysis of microbial cells.* Anal Biochem, 2007. **370**: p. 87-97.

Wendisch, V.F., et al., *Emerging Corynebacterium glutamicum systems biology.* J Biotechnol, 2006. **124**: p. 74-92.

Weckwerth, W., *Metabolomics in Systems Biology.* Annu Rev Plant Biol, 2003. **54**.

Weckwerth, W., *Integration of metabolomics and proteomics in molecular plant physiology - coping with the complexity by data-dimensionality reduction.* Physiol Plant, 2008. **132**: p. 176-189.

Weuster-Botz, D., *Sampling Tube Device for Monitoring Intracellular Metabolite Dynamics.* Anal Biochem. 1997. **246**: p. 225-233.

Winder, C.L., et al., *Global Metabolic Profiling of Escherichia coli Cultures: an Evaluation of Methods for Quenching and Extraction of Intracellular Metabolites.* Anal Chem, 2008. **80**(8): p. 2939-2948.

Wittmann, C., et al., *Impact of the cold shock phenomenon on quantification of intracellular metabolites in bacteria.* Anal Biochem, 2004. **327**: p. 135-139.

Wittmann, C., Kim, H.M. and Heinzle, E., *Metabolic Network Analysis of Lysine Producing Corynebacterium glutamicum at a Miniaturized Scale.* Biotechnol Bioeng, 2004a. **87**(1).

Zimmermann, H.F., et al., *Rapid Evaluation of Oxygen and Water Permeation through Microplate Sealing Tapes.* Biotechnol Prog, 2003. **19**: p. 1061-1063.

http://www3.niaid.nih.gov/NR/rdonlyres/49477C30-0513-47BE-88FC-17974CB1F952/0/e_coli.jpg

http://www.magma.ca/~scimat/Yeast-2m.jpg

7 Appendix

Table A. Library 3.4.0, comparison of the retention times for a 60 min run and a 18 min run

Derivative	RI in 60 min run	RI in 18 min run	Abs. differenz
!1-Cyclohexenol_1TMS	1051.0	1057.8	6.8
!2-Hydroxypyridine_TMS	1032.4	1041.1	8.7
!Carbonic_acid_ 1MeOX_2TMS	1144.3	1138.9	5.4
!Cyclohexanol_TMS	1003.1	1011.4	8.3
!Decane	1000.0	1000.0	-
!Decanol_TMS	1388.4	1388.7	0.3
!Dicyclohexyl	1313.1	1314.6	1.5
!Docosane	2200.0	2200.0	-
!Docosanol_1TMS	2565.8	2568.2	2.4
!Dodecane	1200.0	1200.0	-
!Dodecanol_1TMS	1573.6	1558.2	15.4
!Dotriacontane	3200.0	3200.0	-
!Nonadecane	1900.0	1900.0	-
!Nonanol_1TMS	1293.9	1295.7	1.8
!Octacosane	2800.0	2800.0	-
!Pentadecane	1500.0	1500.0	-
!Pentadecanol_TMS	1867.3	1871.7	4.4
!Phosphate_3TMS	1278.2	1263.5	14.7
!Phosphate_mono-methylester_2TMS	1177.5	1180.6	3.1
!Ribitol_5TMS	1727.1	1708.5	18.6
#!Octamethyltrisiloxane	1072.4	977.9	94.5
#1,2,3-Benzenetriol_3TMS	1600.1	1591.6	8.5
#2,4,5,6-Tetrahydroxypyrimidine	1752.3	1754.8	2.5
#2-Deoxyarabinose_3TMS	1488.8	1487.5	1.3
#3-Hydroxy-decanoic_acid_2TMS	1659.8	1660.7	0.9

Derivative	RI in 60 min run	RI in 18 min run	Abs. differenz
#5-Chlorouracil_2TMS	1457.0	1456.2	0.8
#Alloxanic_acid_4TMS	1677.2	1689.7	12.5
#Aminomalonic_acid_3TMS	1466.2	1468.7	2.5
#Dodecanoic_acid_1TMS	1660.5	1647.9	12.6
#N-Carboxyhydroxyl-amine_2TMS	1188.6	1191.3	2.7
#Octadecanoic_acid_1TMS	2236.6	2236.5	0.1
#Pantothenic_acid_(deriv)_3TMS	1982.5	1967.4	15.1
#trans-9-Hexadecenoic_acid_1TMS	2021.1	2028.4	7.3
1,3-Diphosphoglyceric_acid	2674.0	2674.1	0.1
1,6-Anhydro-beta-D-glucose_3TMS	1705.1	1691.8	13.3
1-Monooleoyl-glycerol_2TMS	2757.9	2734.0	23.9
1-Monopalmitoyl-glycerol_2TMS	2600.6	2574.9	25.7
1-Monostearoyl- glycerol_2TMS	2780.5	2773.1	7.4
2,6-Diaminopimelic_ acid_4TMS	1990.8	1962.3	28.5
2-Aminobenzoic_ acid_1TMS	1483.9	1482.7	1.2
2-Aminobenzoic_ acid_2TMS	1617.9	1618.1	0.2
2-Aminobutyric_ acid_1_2TMS	1174.2	1166.3	7.9
2-Aminobutyric_ acid_2_2TMS	1430.8	1430.4	0.4
2-Deoxy-D-glucose_1_1MeOX_4TMS	1794.6	1797.8	3.2
2-Deoxy-D-glucose_2_1MeOX_4TMS	1797.8	1801.0	3.2
2-Deoxyribose_1	1582.9	1582.4	0.5

Derivative	RI in 60 min run	RI in 18 min run	Abs. differenz
2-Deoxyribose_2	1586.5	1586.1	0.4
2-Hydroxybutanoic_ acid_2TMS	1130.4	1130.7	0.3
2-Hydroxyglutaric_ acid_3TMS	1574.7	1556.1	18.6
2-Ketoglutaric_ acid_1MeOX_2TMS	1581.2	1558.2	23.0
2-Monooleoyl-glycerol_2TMS	2725.0	2739.8	14.8
2-Phosphoglyceric_ acid_4TMS	1793.2	1756.4	36.8
3,4-Dihydroxy-benzoic_acid	1821.5	1825.2	3.7
3-Amino-2-piperidone_2TMS	1459.0	1458.2	0.8
3-Dehydroshikimate_ 3TMS_1MeOX	1800.6	1803.9	3.3
3-Hydroxybutyric_ acid_2TMS	1163.2	1161.1	2.1
3-Indoleacetonitrile_ (TRP)_1TMS	1868.0	1872.5	4.5
3-OH-2-tetradecyl- octanoate_2TMS	3478.5	3441.0	37.5
3-Phosphoglyceraldehyde_1	1719.1	1721.0	1.9
3-Phosphoglyceraldehyde_2	1734.3	1736.5	2.2
3-Phosphoglyceric_ acid_4TMS	1811.0	1785.7	25.3
4-Aminobenzoic_ acid_1TMS	1651.7	1652.5	0.7
4-Aminobenzoic_ acid_2TMS	1833.7	1837.6	3.9
4-OH-phenyl- pyruvate_1MeOX_2TMS	1904.0	1910.2	6.2
5-Aminolevulinate_ 1_1MeOX_3TMS	1766.1	1768.8	2.7
5-Aminolevulinate_ 2_1MeOX_3TMS	1788.7	1791.8	3.1

Derivative	RI in 60 min run	RI in 18 min run	Abs. differenz
5'-Methylthio-adenosine_2TMS	2731.2	2736.9	5.7
5'-Methylthio-adenosine_3TMS	2782.6	2777.4	5.2
5-Oxoproline_1TMS	1499.6	1494.9	4.7
5-Oxoproline_2TMS	1518.1	1510.2	7.9
9-Octadecenal_(Z)	1999.8	2006.9	7.1
Adenine_2TMS	1869.1	1860.8	8.3
Adenosine_3TMS	2594.7	2592.3	2.4
Adenosine_4TMS	2639.7	2621.2	18.5
Adenosine-mono-phosphate_1_4TMS	3047.9	3081.3	33.4
Adenosine-mono-phosphate_2_5TMS	3061.8	3023.0	38.8
Adipic_acid_2TMS	1506.3	1504.5	1.8
Alanine_2TMS	1106.8	1104.3	2.5
Alanine_3TMS	1362.9	1357.1	5.8
Arabinose_1_1MeOX_ 4TMS	1669.6	1670.4	0.8
Arabinose_2_1MeOX_ 4TMS	1671.7	1661.4	10.3
Asparagine_3TMS	1681.0	1682.2	1.2
Asparagine_4TMS	1634.1	1634.5	0.4
Asparagine_xTMS	1588.3	1587.9	0.4
Aspartic_acid_2TMS	1431.9	1416.1	15.8
Aspartic_acid_3TMS	1520.9	1499.8	21.1
Aspartic_acid_4TMS	1602.4	1602.3	0.1
Benzoic_acid_1TMS	1249.7	1248.7	1.0
beta-Alanine_1TMS	1008.7	1016.8	8.1
beta-Alanine_2TMS	1191.2	1185.3	5.9
beta-Alanine_3TMS	1431.3	1421.1	10.2
Cadaverine_2TMS	1444.2	1443.6	0.6
Cadaverine_4TMS	1833.1	1837.0	3.9
Chorismic_acid_(assumed)_ TMS	1887.9	1892.7 4.8	

Derivative	RI in 60 min run	RI in 18 min run	Abs. differenz
cis-Aconitat_3TMS	1756.7	1759.2	2.5
Citric_acid_4TMS	1825.5	1798.2	27.3
Creatinine_3TMS	1552.9	1551.9	1.0
Cycloleucine_2TMS	1191.5	1194.1	2.6
Cycloleucine_3TMS	1373.7	1512.3	138.6
Cystathionine_4TMS	2206.2	2216.2	10.0
Cysteine_1_xMeOX_xTMS	1316.0	1317.4	1.4
Cysteine_2_xMeOX_xTMS	1606.5	1606.5	0.0
Cysteine_3_xMeOX_xTMS	1881.9	1886.6	4.7
Cysteine_3TMS	1563.0	1562.2	0.8
Cysteine_4TMS	1421.7	1421.5	0.2
Cytosin_2TMS	1523.1	1524.2	1.1
Diethylenglycol_2TMS	1248.0	1242.3	5.7
Dihydroorotic_acid_3TMS	1770.9	1773.7	2.8
Dihydroxyacetone_2TMS	1227.3	1230.1	2.8
Eicosanol_TMS	2365.8	2372.4	6.6
Erythritol_4TMS	1509.2	1873.3	364.1
Erythrose-4-phos_ 1_1MeOX_4TMS	1903.2	1905.7	2.5
Erythrose-4-phos_ 2_1MeOX_4TMS	1918.7	1908.2	10.5
Fructose_1_1MeOX_5TMS	1869.2	1858.0	11.2
Fructose_2_1MeOX_5TMS	1878.8	1867.6	11.2
Fructose_3-TMS_5TMS	1804.3	1800.3	4.0
Fructose_4-TMS_5TMS	1816.6	1848.3	31.7
Fructose-1,6-bisP_ 1_1MeOX_7TMS	2677.9	2682.0	4.1
Fructose-1,6-bisP_ 2_1MeOX_7TMS	2724.3	2705.0	19.3
Fructose-1,6-bis-phosphate_7TMS	2677.9	2644.4	33.5
Fructose-6-phosphate_ 1MeOX_5TMS	2310.3	2294.3	16.0

Derivative	RI in 60 min run	RI in 18 min run	Abs. differenz
Fucose_1_1MeOX_4TMS	1731.5	1733.6	2.1
Fucose_2_1MeOX_4TMS	1743.1	1745.4	2.3
Fumaric_acid_2TMS	1362.4	1343.9	18.5
Galactosamine_5TMS	1938.5	1945.0	6.5
Galactosamine_6TMS	1875.1	1879.7	4.6
Galactosamine_ MeOX_6TMS	1954.1	1960.8	6.7
Galactosamine_ MeOX_7TMS	1930.5	1937.0	6.5
Galacturonic_acid_1_ 1MeOX_5TMS	1938.4	1944.9	6.5
Galacturonic_acid_2_ 1MeOX_5TMS	1956.0	1962.7	6.7
gamma-Glutamyl-leucine_2TMS	2183.9	2178.4	5.5
gamma-Glutamyl-leucine_3TMS	2220.5	2210.4	10.1
gamma-Glutamyl-leucine_4TMS	2112.3	2120.5	8.2
gamma-Glutamyl-valine_2TMS	2135.2	2126.9	8.3
gamma-Glutamyl-valine_3TMS	2174.7	2165.5	9.2
gamma-Glutamyl-valine_4TMS	2076.2	2052.3	23.9
Glucono_lactone_4TMS	1886.2	1875.0	11.2
Glucono_lactone_xTMS	1892.6	1881.3	11.3
Glucono-1,4-lactone_ 1MeOX_3TMS	1894.2	1899.1	4.9
Glucosamine_1	1913.5	1919.8	6.3
Glucosamine_2	1937.8	1944.3	6.5
Glucosamine_3	1950.1	1956.7	6.6
Glucosamine-6-phos_ 1_1MeOX_6TMS	2359.7	2355.1	4.6

Derivative	RI in 60 min run	RI in 18 min run	Abs. differenz
Glucosamine-6-phos_ 2_1MeOX_6TMS	2366.7	2352.2	14.5
Glucose_1_1MeOX_5TMS	1891.8	1869.1	22.7
Glucose_1-TMS_5TMS	1889.4	1878.2	11.2
Glucose_2_1MeOX_5TMS	1910.0	1885.8	24.2
Glucose_2-TMS_5TMS	1981.6	1959.7	21.9
Glucose-6-phosphate1 _1MeOX_6TMS	2323.4	2300.1	23.3
Glucose-6-phosphate2 _1MeOX_6TMS	2340.2	2323.2	17.0
Glucose-6-phosphate3 _6TMS	2396.4	2404.2	7.8
Glutamic_acid_2TMS	1532.7	1518.6	14.1
Glutamic_acid_3TMS	1628.5	1610.4	18.1
Glutamic_acid_methyl-ester_2TMS	1510.2	1508.5	1.7
Glutamine_3TMS	1778.4	1762.7	15.7
Glutamine_4TMS	1738.4	1721.0	17.4
Glutaric_acid_2TMS	1413.7	1406.5	7.2
Glyceraldehyde_1	1207.0	1210.2	3.2
Glyceraldehyde_2	1224.5	1227.4	2.9
Glyceric_acid_3TMS	1343.4	1321.0	22.4
Glycerol_3TMS	1282.1	1261.9	20.2
Glycerol-2-phosphate_4TMS	1732.4	1727.2	5.2
Glycerol-3-phosphate_4TMS	1767.8	1741.8	26.0
Glycerone_phosphate1_ 1MeOX_3TMS	1753.9	1756.4	2.5
Glycerone_phosphate2_ 1MeOX_3TMS	1764.8	1767.5	2.7
Glycine_2TMS	1126.6	1123.4	3.2
Glycine_3TMS	1313.8	1302.9	10.9
Glycolic_acid_2TMS	1083.0	1076.9	6.1
Guanidine_4TMS	1233.5	1236.3	2.8
Guanine_3TMS	2135.0	2143.4	8.4

Derivative	RI in 60 min run	RI in 18 min run	Abs. differenz
Heneicosanol_1TMS	2468.6	2473.0	4.4
Heptadecanol_TMS	2062.9	2070.6	7.7
Hexadec-9-enal	1958.0	1964.7	6.7
Hexadecanal	1876.4	1881.0	4.6
Hexadecanoic_acid_1TMS	2047.1	2036.9	10.2
Hexadecanol_1TMS	1964.0	2407.1	443.1
Hexanoic_acid_1MeOX	1296.4	1298.2	1.8
Histidine_3TMS	1915.6	1921.9	6.3
Homocysteine_3TMS	1669.3	1668.8	0.5
Homoserine_2TMS	1368.7	1352.1	16.6
Homoserine_3TMS	1453.0	1435.8	17.2
Hydroxylamine_3TMS	1114.8	1116.2	1.4
Hypoxanthine_2TMS	1811.5	1862.9	51.4
Indolepyruvic_acid_1_ 1MeOX_2TMS	2135.9	2144.2	8.4
Indolepyruvic_acid_2_ 1MeOX_2TMS	2200.6	2210.7	10.1
Inosine_4TMS	2582.4	2584.4	2.0
Inositol_6TMS	2086.3	2094.2	7.9
Isocitric_acid_4TMS	1831.0	1834.8	3.8
Isoleucine_2TMS	1296.3	1288.1	8.2
Isoleucine_xTMS	1176.0	1175.8	0.2
Isomaltose_1_1MeOX_ 8TMS	2870.5	2878.2	7.7
Isomaltose_2_1MeOX_ 8TMS	2900.7	2848.2	52.5
Lactic_acid_2TMS 1	062.9	1061.4	1.5
Lactose_1_1MeOX_8TMS	2692.8	2684.9	7.9
Lactose_2_1MeOX_8TMS	2706.9	2693.5	13.4
Lactyllactat_2TMS	1396.1	1391.6	4.5
Leucine_2TMS	1274.1	1265.2	8.9
Lysine_3TMS	1849.9	1844.1	5.8
Lysine_4TMS	1918.1	1898.3	19.8
Lyxose_1_1MeOX_4TMS	1654.7	1655.5	0.8
Lyxose_2_1MeOX_4TMS	1668.7	1658.4	10.3

Derivative	RI in 60 min run	RI in 18 min run	Abs. differenz
Maleic_acid_2TMS	1312.4	1313.9	1.5
Malic_acid_3TMS	1488.3	1468.7	19.6
Malic_acid-1-methylester_2TMS	1396.1	1396.3	0.2
Malic_acid-4-methylester_2TMS	1375.5	1376.0	0.5
Malonic_acid_2TMS	1202.5	1205.9	3.4
Maltose_1_1MeOX_8TMS	2736.3	2710.9	25.4
Maltose_2_1MeOX_8TMS	2760.2	2713.8	46.4
Maltotriose_1_1MeOX_11TMS		3541.2	0.4
Maltotriose_2_1MeOX_11TMS	3570.3	3570.2	0.1
Mannitol_6TMS	1925.5	1944.3	18.8
Mannose_1_1MeOX_5TMS	1883.1	1869.1	14.0
Mannose_2_1MeOX_5TMS	1894.6	1890.0	4.6
Mannose-6-phosphate1_1MeOX_6TMS	2324.5	2300.1	24.4
Mannose-6-phosphate2_1MeOX_6TMS	2333.6	2346.4	12.8
Methionine_2TMS	1520.2	1517.6	2.6
Methionine_xTMS	1413.7	1412.9	0.8
Myristic_acid_amide	1974.2	1981.1	6.9
Myristic_acid_amide_1TMS	2043.5	2051.0	7.5
N-Acetylalanine_1TMS	1268.5	1270.7	2.2
N-Acetylglucosamine1_1MeOX_4TMS	2069.0	2065.2	3.8
N-Acetylglucos-amine2_1MeOX_4TMS	2077.0	2084.8	7.8
N-Acetyl-L-glutamic _acid_2TMS	1788.4	1771.0	17.4

Derivative	RI in 60 min run	RI in 18 min run	Abs. differenz
N-Acetyl-L-glutamic_acid_ 3TMS	1766.1	1755.7	10.4
N-Acetyl-L-glutamine_ 2TMS	1931.7	1916.0	15.7
N-Acetyl-L-glutamine _3TMS	1910.1	1916.4	6.3
N-Acetyl-L-glutamine _4TMS	1862.4	1866.8	4.4
N-Acetylmannos-amine1 _1MeOX_4TMS	2074.8	2082.7	7.8
N-Acetylmannos-amine2 _1MeOX_4TMS	2087.4	2095.4	7.9
N-Acetylneuraminic_acid_1	2628.7	2629.7	1.0
N-Acetylneuraminic_acid_2	2666.1	2666.3	0.2
N-Ac-glucosamine-6-P _1MeOX_5TMS	1990.6	1997.6	7.0
n-Butylamine_2TMS	1106.5	1111.7	5.2
Nicotinamide_1TMS	1482.3	1480.1	2.2
Nicotinamide_xTMS	1472.1	1471.1	1.0
Nicotinic_acid_1TMS	1300.3	1302.9	2.6
Norleucine_2TMS	1329.0	1284.8	44.2
Norleucine_3TMS	1548.5	1547.5	1.0
Norvaline_1TMS	1116.7	1121.6	4.9
Norvaline_2TMS	1244.0	1201.1	42.9
Norvaline_3TMS	1478.5	1477.4	1.1
O-Acetyl-serine_2TMS	1402.1	1385.0	17.1
Octadecanal	2025.1	2032.5	7.4
Octadecanol_TMS	2161.5	2163.9	2.4
Octanol_TMS	1186.8	1189.6	2.8
Oleic_acid_amide	2370.1	2376.6	6.5
Ornithine_1_4TMS	1817.5	1816.5	1.0
Ornithine_2_4TMS	1761.0	1763.6	2.6
Ornithine_3_5TMS	2039.5	2047.0	7.5
Ornithine_4_3TMS 8	1621.	1622.0	0.2
Orotic_acid_3TMS	1751.4	1753.8	2.4
Oxalic_acid_2TMS	1139.3	1137.7	1.6

Derivative	RI in 60 min run	RI in 18 min run	Abs. differenz
Oxaloacetic_acid_1MeOX _2TMS	1475.7	1474.6	1.1
Palmitic_acid_amide	2177.0	2185.8	8.8
Palmitic_acid_amide_1TMS	2240.1	2249.4	9.3
Phenylalanine_1TMS	1545.8	1545.7	0.1
Phenylalanine_2TMS	1629.4	1625.0	4.4
Phenylpyruvic_acid_1	1522.6	1521.1	1.5
Phenylpyruvic_acid_2	1591.0	1590.7	0.3
Phosphoenolpyruvic_acid _3TMS	1599.2	1583.3	15.9
Phosphoethanolamine _4TMS	1787.0	1790.1	3.1
Prephenic_acid_3TMS_ 1MeOX	2083.4	2091.3	7.9
Proline_1TMS	1172.7	1175.8	3.1
Proline_2TMS	1302.3	1296.3	6.0
Pyridoxine_3TMS	1888.3	1893.1	4.8
Pyrophosphoric_acid_4TMS	1669.4	1645.9	23.5
Pyrrole-2-carboxylic _acid_2TMS	1356.6	1357.4	0.8
Pyruvic_acid_1MeOX_ 1TMS	1055.7	1070.9	15.2
Pyruvic_acid_2TMS	1091.9	1625.0	533.1
Quebrachitol_5TMS	1859.1	1863.4	4.3
Quinic_acid_5TMS	1855.7	1835.7	20.0
Rhamnose_1	1723.7	1725.7	2.0
Rhamnose_2	1729.4	1731.5	2.1
Ribose_1MeOX_4TMS	1685.7	1675.4	10.3
Ribose-5-phosphate_1MeOX_5TMS	2112.0	2297.2	185.2
Ribulose-5-phos_1_ 1MeOX_5TMS	2101.7	2109.0	7.3
Ribulose-5-phos_2_ 1MeOX_5TMS	2118.6	1746.0	372.6
Ribulose-5-phos_5TMS	2116.0	2317.5	201.5

Derivative	RI in 60 min run	RI in 18 min run	Abs. differenz
Sarcosine_2TMS	1140.0	1106.7	33.3
Sarcosine_xTMS	1387.0	1379.9	7.1
Serine_2TMS	1258.2	1248.7	9.5
Serine_3TMS	1368.7	1350.5	18.2
Serine_4TMS	1570.9	1570.2	0.7
Shikimic_acid_4TMS	1815.3	1818.8	3.5
Sorbitol_6TMS	1932.1	1938.6	6.5
Spermidine_4TMS	2187.4	2196.3	8.9
Spermine_5TMS	2747.9	2746.4	1.5
Succinic_acid_2TMS	1325.4	1309.5	15.9
Succinic_acid_methylester_1TMS	1179.3	1173.4	5.9
Succinyllactate_2TMS	1649.9	1650.6	0.7
Sucrose_8TMS	2643.6	2648.5	4.9
Tartaric_acid_4TMS	1648.0	1648.7	0.7
Tetradecanol_1TMS	1773.8	1758.5	15.3
Threonine_2TMS	1297.4	1289.8	7.6
Threonine_3TMS	1392.6	1375.1	17.5
Thymidine-mono-phosphate_3TMS	2824.9	2882.6	57.7
Thymine_2TMS	1408.4	1396.4	12.0
Trehalose_8TMS	2741.2	2736.9	4.3
Trehalose_phosphate_9TMS	3192.8	3201.6	8.8
Tricarballylic_acid_3TMS	1740.3	1742.6	2.3
Tridecanol_TMS	1677.2	1678.4	1.2
Triethanolamin_3TMS	1637.1	1637.6	0.5
Tryptophane_1_1TMS	2157.9	2166.5	8.6
Tryptophane_2_2TMS	2181.8	2190.6	8.8
Tryptophane_3_(1xRing)_2TMS	2189.8	2210.4	20.6
Tryptophane_4_3TMS	2203.1	2216.2	13.1
Tyrosine_2TMS	1882.5	1877.5	5.0
Tyrosine_3TMS	1939.8	1921.1	18.7

Derivative	RI in 60 min run	RI in 18 min run	Abs. differenz
Unknown#bth_pae_002	1655.5	1656.3	0.8
Unknown#bth_pae_003	2056.2	2063.8	7.6
Unknown#bth_pae_004	1156.5	1160.2	3.7
Unknown#bth_pae_005	2183.1	2191.9	8.8
Unknown#bth_pae_007	1017.3	1025.1	7.8
Unknown#bth_pae_008	1031.8	1184.1	152.3
Unknown#bth_pae_009	1067.1	1063.8	3.3
Unknown#bth_pae_010	1131.8	1136.2	4.4
Unknown#bth_pae_011	1158.5	1162.1	3.6
Unknown#bth_pae_012	1161.8	1158.7	3.1
Unknown#bth_pae_013	1169.8	1157.9	11.9
Unknown#bth_pae_014	1178.4	1181.4	3.0
Unknown#bth_pae_015	1194.7	1190.3	4.4
Unknown#bth_pae_016	1241.6	1235.0	6.6
Unknown#bth_pae_017	1246.4	1232.3	14.1
Unknown#bth_pae_018	1268.2	1270.4	2.2
Unknown#bth_pae_019	1282.2	1284.2	2.0
Unknown#bth_pae_020	1329.3	1330.5	1.2
Unknown#bth_pae_021	1333.9	1330.8	3.1
Unknown#bth_pae_022	1371.4	1396.4	25.0
Unknown#bth_pae_023	1375.4	1365.3	10.1
Unknown#bth_pae_024	1385.3	1375.1	10.2
Unknown#bth_pae_025	1411.4	1411.3	0.1
Unknown#bth_pae_026	1412.7	1398.1	14.6
Unknown#bth_pae_027	1414.0	1413.9	0.1
Unknown#bth_pae_028	1422.0	1421.8	0.2
Unknown#bth_pae_029	1424.5	1424.2	0.3
Unknown#bth_pae_030	1454.4	1453.6	0.8
Unknown#bth_pae_031	1472.5	1471.5	1.0
Unknown#bth_pae_032	1505.1	1493.3	11.8
Unknown#bth_pae_033	1515.8	1499.8	16.0
Unknown#bth_pae_034	1524.1	1522.6	1.5
Unknown#bth_pae_035	1530.4	1529.0	1.4

Derivative	RI in 60 min run	RI in 18 min run	Abs. differenz
Unknown#bth_pae_036	1549.1	1548.1	1.0
Unknown#bth_pae_037	1554.3	1553.4	0.9
Unknown#bth_pae_038	1567.3	1562.4	4.9
Unknown#bth_pae_039	1586.9	1748.1	161.2
Unknown#bth_pae_040	1593.5	1593.7	0.2
Unknown#bth_pae_041	1596.1	1595.9	0.2
Unknown#bth_pae_042	1630.4	1630.8	0.4
Unknown#bth_pae_043	1641.9	1642.5	0.6
Unknown#bth_pae_044	1643.0	1581.2	61.8
Unknown#bth_pae_045	1647.7	1648.4	0.7
Unknown#bth_pae_046	1649.4	1650.1	0.7
Unknown#bth_pae_047	1667.9	1668.9	1.0
Unknown#bth_pae_048	1681.6	1682.8	1.2
Unknown#bth_pae_049	1702.4	1704.0	1.6
Unknown#bth_pae_050	1703.1	1704.7	1.6
Unknown#bth_pae_051	1707.3	1709.0	1.7
Unknown#bth_pae_052	1735.4	1737.6	2.2
Unknown#bth_pae_053	1736.3	1725.7	10.6
Unknown#bth_pae_054	1740.7	1743.0	2.3
Unknown#bth_pae_055	1754.4	1756.9	2.5
Unknown#bth_pae_056	1768.1	1752.3	15.8
Unknown#bth_pae_057	1777.8	1762.7	15.1
Unknown#bth_pae_058	1991.9	1998.9	7.0
Unknown#sst_cgl_002	1116.2	1121.1	4.9
Unknown#sst_cgl_003	1150.5	1154.4	3.9
Unknown#sst_cgl_004	1193.1	1195.7	2.6
Unknown#sst_cgl_006	1231.2	1785.7	554.5
Unknown#sst_cgl_008	1248.7	1230.7	18.0
Unknown#sst_cgl_009	1250.2	1245.5	4.7
Unknown#sst_cgl_010a	1254.8	1248.2	6.6
Unknown#sst_cgl_011	1259.5	1249.6	9.9
Unknown#sst_cgl_012	1264.8	1197.7	67.1
Unknown#sst_cgl_014	1285.9	1287.8	1.9

Derivative	RI in 60 min run	RI in 18 min run	Abs. differenz
Unknown#sst_cgl_015	1291.6	1284.8	6.8
Unknown#sst_cgl_020	1401.8	1401.9	0.1
Unknown#sst_cgl_022	1410.5	1388.2	22.3
Unknown#sst_cgl_023	1411.8	1411.7	0.1
Unknown#sst_cgl_024	1438.6	1431.3	7.3
Unknown#sst_cgl_026	1460.2	1459.4	0.8
Unknown#sst_cgl_027	1470.1	1457.2	12.9
Unknown#sst_cgl_028	1478.9	1477.8	1.1
Unknown#sst_cgl_029	1482.3	1481.1	1.2
Unknown#sst_cgl_030	1493.1	1476.9	16.2
Unknown#sst_cgl_033	1551.1	1533.2	17.9
Unknown#sst_cgl_035	1587.3	1574.9	12.4
Unknown#sst_cgl_036	1590.9	1595.1	4.2
Unknown#sst_cgl_037	1601.4	1601.3	0.1
Unknown#sst_cgl_038	1605.0	1591.6	13.4
Unknown#sst_cgl_039	1621.0	1621.2	0.2
Unknown#sst_cgl_040	1636.9	1637.4	0.5
Unknown#sst_cgl_041	1638.3	1638.8	0.5
Unknown#sst_cgl_042	1649.9	1650.6	0.7
Unknown#sst_cgl_043	1654.8	1655.6	0.8
Unknown#sst_cgl_044	1657.2	1658.0	0.8
Unknown#sst_cgl_045	1660.9	1661.8	0.9
Unknown#sst_cgl_046	1661.5	1662.4	0.9
Unknown#sst_cgl_048	1676.9	1678.1	1.2
Unknown#sst_cgl_049	1696.3	1697.9	1.6
Unknown#sst_cgl_050	1705.4	1707.1	1.7
Unknown#sst_cgl_052	1715.4	1704.9	10.5
Unknown#sst_cgl_053	1708.7	1706.4	2.3
Unknown#sst_cgl_054	1730.0	1732.1	2.1
Unknown#sst_cgl_055	1733.4	1725.1	8.3
Unknown#sst_cgl_056	1735.3	1737.5	2.2
Unknown#sst_cgl_058	1746.5	1748.9	2.4
Unknown#sst_cgl_060	1758.1	1760.7	2.6

Derivative	RI in 60 min run	RI in 18 min run	Abs. differenz
Unknown#sst_cgl_062	1772.1	1771.9	0.2
Unknown#sst_cgl_064	1786.2	1789.2	3.0
Unknown#sst_cgl_065	1798.4	1801.7	3.3
Unknown#sst_cgl_068	1811.6	1815.1	3.5
Unknown#sst_cgl_072	1830.0	1833.8	3.8
Unknown#sst_cgl_073	1833.8	1837.7	3.9
Unknown#sst_cgl_074	1834.1	1838.0	3.9
Unknown#sst_cgl_075	1840.9	1825.3	15.6
Unknown#sst_cgl_076	1843.5	1827.4	16.1
Unknown#sst_cgl_077	1845.5	1849.6	4.1
Unknown#sst_cgl_078	1847.3	1842.0	5.3
Unknown#sst_cgl_081	1894.9	1944.3	49.4
Unknown#sst_cgl_082	1902.3	1908.5	6.2
Unknown#sst_cgl_083	1938.6	1945.1	6.5
Unknown#sst_cgl_084	1957.3	1936.5	20.8
Unknown#sst_cgl_085	1969.6	1976.4	6.8
Unknown#sst_cgl_087	1989.4	1996.4	7.0
Unknown#sst_cgl_087a	1989.4	1996.4	7.0
Unknown#sst_cgl_088	1995.0	2004.5	9.5
Unknown#sst_cgl_089	2008.5	1990.6	17.9
Unknown#sst_cgl_090	2019.3	2000.9	18.4
Unknown#sst_cgl_091	2028.0	2028.0	0.0
Unknown#sst_cgl_092	2052.4	2060.0	7.6
Unknown#sst_cgl_093	2061.7	2069.4	7.7
Unknown#sst_cgl_094	2097.4	2080.6	16.8
Unknown#sst_cgl_095	2101.5	2647.3	545.8
Unknown#sst_cgl_096	2129.7	2132.1	2.4
Unknown#sst_cgl_098	2152.8	2161.4	8.6
Unknown#sst_cgl_100	2190.4	2199.3	8.9
Unknown#sst_cgl_101	2195.7	2175.8	19.9
Unknown#sst_cgl_102	2207.0	2217.0	10.0
Unknown#sst_cgl_104	2223.7	2224.9	1.2
Unknown#sst_cgl_105	2238.6	2230.7	7.9

Derivative	RI in 60 min run	RI in 18 min run	Abs. differenz
Unknown#sst_cgl_106	2244.1	2246.8	2.7
Unknown#sst_cgl_107	2249.1	2233.6	15.5
Unknown#sst_cgl_108	2252.9	2261.9	9.0
Unknown#sst_cgl_109	2257.8	2245.1	12.7
Unknown#sst_cgl_110	2275.7	2288.5	12.8
Unknown#sst_cgl_111	2282.3	2274.1	8.2
Unknown#sst_cgl_112	2283.6	2292.0	8.4
Unknown#sst_cgl_113	2292.4	2304.0	11.6
Unknown#sst_cgl_114	2295.6	3137.0	841.4
Unknown#sst_cgl_115	2331.8	2339.1	7.3
Unknown#sst_cgl_116	2331.8	2320.3	11.5
Unknown#sst_cgl_117	2365.8	2366.6	0.8
Unknown#sst_cgl_120	2615.1	2606.6	8.5
Unknown#sst_cgl_121	2635.0	2601.0	34.0
Unknown#sst_cgl_122	2666.0	2644.4	21.6
Unknown#sst_cgl_123	2673.7	2673.8	0.1
Unknown#sst_cgl_124	2681.9	2681.8	0.1
Unknown#sst_cgl_125	2696.7	2696.3	0.4
Unknown#sst_cgl_126	2858.9	2848.2	10.7
Unknown#sst_cgl_128	2878.8	2842.9	35.9
Unknown#sst_cgl_129	3413.2	3377.1	36.1
Unknown#sst_cgl_130	3464.4	3466.0	1.6
Unknown#sst_cgl_131	3493.1	3494.2	1.1
Unknown#sst_cgl_132	3515.6	3556.9	41.3
Unknown#sst_cgl_133	3522.7	3523.3	0.6
Unknown#sst_cgl_A03	1689.5	1690.9	1.4
Unknown#sst_cgl_A04	1723.6	1712.6	11.0
Unknown#sst_cgl_A08	2358.8	2352.2	6.6
Unknown#sst_cgl_A09	2381.3	2367.3	14.0
Unknown#sst_cgl_A10	2731.9	2716.5	15.4
Unknown#sst_cgl_A11	1746.7	1733.5	13.2
Unknown#sst_cgl_A12	1876.8	1869.9	6.9
Unknown#sst_cgl_A13	1797.9	1801.2	3.3

Derivative	RI in 60 min run	RI in 18 min run	Abs. differenz
Unknown#sst_cgl_A14	1797.1	1800.3	3.2
Unknown#sst_cgl_A15	2051.8	2042.0	9.8
Unknown#sst_cgl_A16	2260.0	2253.8	6.2
Unknown#sst_cgl_A17	2276.4	2256.7	19.7
Unknown#sst_cgl_A18	2294.0	2288.5	5.5
Unknown#sst_cgl_D03	1088.9	1094.6	5.7
Unknown#sst_cgl_D04	1129.0	1133.5	4.5
Unknown#sst_cgl_D05	1143.4	1147.5	4.1
Unknown#sst_cgl_D07	1149.1	1153.0	3.9
Unknown#sst_cgl_D08	1149.9	1153.8	3.9
Unknown#sst_cgl_D09	1155.4	1156.7	1.3
Unknown#sst_cgl_D11	1116.6	1115.3	1.3
Uracil_2TMS	1346.9	1335.7	11.2
Urea_2TMS	1261.9	1243.8	18.1
Uridine_3TMS	2459.1	2453.4	5.7
Uridine-5'-mono-phosphate_5TMS	2872.1	2903.8	31.7
Valine_1TMS	1093.7	1093.6	0.1
Valine_2TMS	1214.5	1202.8	11.7
Xanthine_3TMS	2027.0	2034.4	7.4
Xylose_1_1MeOX_4TMS	1653.4	1654.2	0.8
Xylose_2_1MeOX_4TMS	1664.3	1665.3	1.0
Xylulose_1MeOX_4TMS	1685.1	1668.7	16.4
Xylulose_4TMS	1697.6	1687.2	10.4
Xylulose-5-phos_1_1MeOX_5TMS	2099.9	2288.5	188.6
Xylulose-5-phos_2_1MeOX_5TMS	2117.3	1743.9	373.4

Table B. Reference list derived from more than 150 wild type samples.

Metabolite	Relative intensity	Standard error	Relative error	Occurrence [%]
!2-Hydroxypyridine	2435.85	210.31	0.09	70.5
!Carbonic acid	15149.27	1290.32	0.09	99.4
!Docosanol	288.88	253.60	0.88	1.3
!Dodecanol	2752.17	1634.70	0.59	29.5
!Phosphoric acid	1252671.21	65554.72	0.05	99.4
!Ribitol	274174.13	7972.93	0.03	100.0
#!Octamethyltrisiloxane	6602.83	857.32	0.13	19.2
#1,2,3-Benzenetriol	14435.80	14279.78	0.99	14.1
#Alloxanic acid	55.73	10.78	0.19	1.3
#Aminomalonic acid	755.74	45.98	0.06	55.1
#Boric acid	491.68	92.99	0.19	10.3
#Carbodiimide	7201.30	1739.34	0.24	12.8
#Dodecanoic acid	935.59	193.22	0.21	66.7
#Octadecanoic acid	40254.45	2489.45	0.06	99.4
#Pantothenic acid (deriv)	569.74	116.27	0.20	1.9
1,6-Anhydro-beta-D-glucose	4332.28	2570.24	0.59	91.7
1-Monooleoylglycerol	806.80	190.31	0.24	53.8
1-Monopalmitoylglycerol	474.15	55.54	0.12	71.8
1-Monostearoylglycerol	405.67	296.27	0.73	3.2
2,6-Diaminopimelic acid	8250.63	866.51	0.11	78.8
2-Aminobutyric acid	3636.05	149.83	0.04	80.1
2-Deoxyribose-5-phosphate	1385.91	400.53	0.29	35.3
2-Hydroxybutanoic acid	286.75	29.71	0.10	67.9
2-Hydroxyglutaric acid	14112.38	967.71	0.07	96.2
2-Monooleoylglycerol	322.04	74.57	0.23	1.3
2-Phosphoglyceric acid	9604.27	1072.40	0.11	50.6
3,4-Dihydroxy-benzoic acid	37.79	17.02	0.45	1.3
3-Hydroxy-2-tetradecyl-octanoic acid	14228.57	873.70	0.06	64.7

Metabolite	Relative intensity	Standard error	Relative error	Occurrence [%]
3-Hydroxybutyric acid	15455.33	6583.49	0.43	59.0
3-Phosphoglyceric acid	48014.11	2403.83	0.05	98.1
5-Deoxy-5-Methylthioadenosine	3094.07	186.66	0.06	77.6
5-Oxoproline	72190.42	4351.51	0.06	100.0
6-Phosphogluconate	16023.55	4489.46	0.28	78.2
Adenine	19593.11	1349.46	0.07	88.5
Adenosine	5834.98	386.53	0.07	91.7
Adenosine-5'-monophosphate	159524.63	10027.94	0.06	89.1
Alanine	199516.43	12361.10	0.06	100.0
alpha-Ketoglutaric acid	25658.96	1981.61	0.08	98.7
Arabinose	29.82	9.96	0.33	4.5
Aspartic acid	234366.03	21545.59	0.09	98.7
Benzoic acid	42557.81	8353.91	0.20	98.1
beta-Alanine	30070.10	1741.39	0.06	99.4
Citric acid	61369.68	4457.95	0.07	97.4
Cycloleucine	422776.53	22234.30	0.05	67.9
Cytosin	455.13	19.88	0.04	55.8
Diethyleneglycol	693.89	65.86	0.09	54.5
Dihydroxyacetone	755.03	136.80	0.18	3.2
Erythritol	77401.46	19971.35	0.26	34.6
Erythrose-4-phosphate	17643.90	4215.33	0.24	26.3
Fructose	6279.84	1148.30	0.18	34.0
Fructose-1,6-bisphosphate	87215.71	10986.46	0.13	73.7
Fructose-6-phosphate	371.42	112.12	0.30	33.3
Fumaric acid	59113.95	2972.63	0.05	98.7
gamma-Glutamylleucine	5876.95	453.08	0.08	87.2
gamma-Glutamylvaline	96431.11	13144.57	0.14	90.4
Glucono lactone	5798.52	656.51	0.11	10.3
Glucosamine-6-phosphate	9458.00	2283.89	0.24	78.8

Metabolite	Relative intensity	Standard error	Relative error	Occurrence [%]
Glucose	19859.54	1965.41	0.10	99.4
Glucose-6-phosphate	53411.33	10301.17	0.19	84.6
Glutamic acid	2441393.78	153198.06	0.06	99.4
Glutamine	125686.69	10569.10	0.08	91.7
Glyceraldehyde	64421.87	9471.10	0.15	3.8
Glyceric acid	3396.18	249.10	0.07	95.5
Glycerol	11218.20	600.07	0.05	99.4
Glycerol-2-phosphate	267.57	66.32	0.25	5.8
Glycerol-3-phosphate	110402.89	6423.03	0.06	98.7
Glycerone phosphate	8980.64	688.90	0.08	1.9
Glycine	14909.37	1894.88	0.13	98.1
Glycolic acid	4028.23	1415.27	0.35	85.3
Hexadecanoic acid	36940.36	2323.03	0.06	96.8
Hexadecanol	1635.10	265.28	0.16	76.9
Homocysteine	98.30	6.48	0.07	41.7
Homoserine	2263.01	136.15	0.06	94.9
Hydroxylamine	864.52	117.04	0.14	95.5
Hypoxanthine	7325.67	415.27	0.06	14.7
Isoleucine	5814.27	378.63	0.07	95.5
Isomaltose	23305.64	4886.10	0.21	72.4
Lactic acid	190774.66	11493.32	0.06	99.4
Lactose	8663.13	618.48	0.07	76.9
Lactyllactate	66.97	4.55	0.07	48.1
Leucine	5290.23	385.42	0.07	84.6
Lysine	390974.75	20153.38	0.05	98.1
Malic acid	59626.98	3517.51	0.06	98.7
Malonic acid	3677.79	637.38	0.17	87.8
Maltose	978513.02	50457.25	0.05	99.4
Mannitol	70215.31	1874.65	0.03	75.0
Mannose	19602.76	2116.21	0.11	89.7
Mannose-6-phosphate	22770.72	5544.96	0.24	78.8

Metabolite	Relative intensity	Standard error	Relative error	Occurrence [%]
Methionine	7689.80	1419.71	0.18	69.2
N-Acetylglucosamine	975.45	457.03	0.47	1.9
N-Acetyl-L-glutamic acid	26229.31	1411.65	0.05	98.1
N-Acetyl-L-glutamine	7139.73	538.01	0.08	88.5
Nicotinamide	5754.91	417.48	0.07	94.9
Nicotinic acid	677.81	144.41	0.21	66.0
Norleucine	6051.60	705.64	0.12	5.8
Norvaline	52247.33	7961.22	0.15	16.0
O-Acetyl-serine	2699.09	304.77	0.11	71.2
Octadecanol	356.55	193.47	0.54	55.1
Ornithine	1222.36	235.26	0.19	60.9
Oxalic acid	1550.10	344.73	0.22	12.2
Phenylalanine	4720.46	246.96	0.05	98.1
Phosphoenolpyruvic acid	8388.03	509.77	0.06	98.1
Proline	111191.89	7851.08	0.07	96.2
Pyrophosphoric acid	157201.55	10830.68	0.07	96.2
Pyruvic acid	3241.00	167.39	0.05	98.1
Quebrachitol	1868.04	843.88	0.45	7.7
Quinic acid	16179.20	1056.99	0.07	98.1
Ribose-5-phosphate	265.48	83.05	0.31	31.4
Ribulose-5-phosphate	14161.04	3199.53	0.23	75.6
Sarcosine	20171.68	4982.86	0.25	18.6
Serine	175540.49	11555.24	0.07	99.4
Succinic acid	117805.67	6287.84	0.05	99.4
Succinic acid monomethylester	515.43	24.53	0.05	78.2
Sucrose	879.04	163.68	0.19	57.7
Tetradecanol	969.97	443.09	0.46	65.4
Threonine	11566.91	863.05	0.07	98.7
Thymine	1165.04	80.25	0.07	71.2
Trehalose	832327.93	36735.82	0.04	98.7

Metabolite	Relative intensity	Standard error	Relative error	Occurrence [%]
Tridecanol	113.64	16.20	0.14	1.9
Tryptophan	45358.59	3105.14	0.07	93.6
Tyrosine	17709.60	1205.45	0.07	98.1
Unknown#bth_pae_001	2380.16	498.81	0.21	19.2
Unknown#bth_pae_008	24090.42	6061.03	0.25	21.8
Unknown#bth_pae_009	18351.06	2616.53	0.14	33.3
Unknown#bth_pae_012	14936.55	1214.10	0.08	3.8
Unknown#bth_pae_013	1756.56	89.96	0.05	99.4
Unknown#bth_pae_015	1386.50	80.52	0.06	3.2
Unknown#bth_pae_017	36399.32	2016.21	0.06	92.3
Unknown#bth_pae_021	293.71	59.83	0.20	89.7
Unknown#bth_pae_022	177.23	23.56	0.13	22.4
Unknown#bth_pae_023	2415.91	315.92	0.13	94.2
Unknown#bth_pae_024	114.49	13.73	0.12	55.1
Unknown#bth_pae_026	2520.29	1373.57	0.55	6.4
Unknown#bth_pae_030	107.59	61.75	0.57	1.3
Unknown#bth_pae_032	11750.84	1781.92	0.15	10.3
Unknown#bth_pae_033	2003.92	250.81	0.13	78.8
Unknown#bth_pae_034	570.00	31.66	0.06	3.8
Unknown#bth_pae_038	753.25	270.83	0.36	63.5
Unknown#bth_pae_039	19192.66	1736.34	0.09	37.8
Unknown#bth_pae_040	2231.14	363.30	0.16	78.2
Unknown#bth_pae_044	10286.59	759.67	0.07	3.8
Unknown#bth_pae_056	15955.15	758.14	0.05	89.7
Unknown#bth_pae_057	2457.57	154.99	0.06	82.7
Unknown#sst_cgl_006	85958.63	10144.47	0.12	36.5
Unknown#sst_cgl_008	105362.39	5503.49	0.05	98.7
Unknown#sst_cgl_009	1453.09	109.83	0.08	93.6
Unknown#sst_cgl_010a	6336.09	5303.17	0.84	1.9
Unknown#sst_cgl_010b	1164.65	222.69	0.19	60.3
Unknown#sst_cgl_011	612.76	150.90	0.25	55.8

Metabolite	Relative intensity	Standard error	Relative error	Occurrence [%]
Unknown#sst_cgl_012	591.88	23.64	0.04	53.8
Unknown#sst_cgl_015	803.12	157.10	0.20	30.1
Unknown#sst_cgl_022	974.78	570.14	0.58	8.3
Unknown#sst_cgl_024	298.92	150.37	0.50	1.9
Unknown#sst_cgl_027	2256.45	210.79	0.09	92.3
Unknown#sst_cgl_030	10061.76	630.65	0.06	90.4
Unknown#sst_cgl_033	1563.26	288.09	0.18	28.2
Unknown#sst_cgl_035	2966.32	204.30	0.07	73.7
Unknown#sst_cgl_036	79.84	12.34	0.15	22.4
Unknown#sst_cgl_038	32207.71	5454.31	0.17	94.9
Unknown#sst_cgl_046	545.61	237.30	0.43	2.6
Unknown#sst_cgl_049	59.70	5.47	0.09	30.8
Unknown#sst_cgl_052	422.73	26.28	0.06	1.9
Unknown#sst_cgl_053	13250.95	4579.26	0.35	63.5
Unknown#sst_cgl_055	11508.30	616.68	0.05	98.7
Unknown#sst_cgl_062	26320.28	1197.01	0.05	59.0
Unknown#sst_cgl_075	219.07	10.02	0.05	56.4
Unknown#sst_cgl_076	1775.49	521.93	0.29	7.1
Unknown#sst_cgl_078	551.70	110.69	0.20	10.3
Unknown#sst_cgl_081	19802.29	1738.43	0.09	85.3
Unknown#sst_cgl_084	22601.98	1462.62	0.06	91.0
Unknown#sst_cgl_088	1539.97	143.06	0.09	48.1
Unknown#sst_cgl_089	7304.82	526.78	0.07	90.4
Unknown#sst_cgl_090	7600.26	393.38	0.05	97.4
Unknown#sst_cgl_091	1302.06	153.01	0.12	79.5
Unknown#sst_cgl_094	2069.73	658.80	0.32	3.8
Unknown#sst_cgl_095	845.63	239.62	0.28	7.1
Unknown#sst_cgl_096	169.81	31.12	0.18	15.4
Unknown#sst_cgl_101	37009.21	3586.77	0.10	91.7
Unknown#sst_cgl_103	344.21	14.28	0.04	47.4
Unknown#sst_cgl_104	48407.90	3418.05	0.07	81.4

Metabolite	Relative intensity	Standard error	Relative error	Occurrence [%]
Unknown#sst_cgl_105	464.54	94.76	0.20	8.3
Unknown#sst_cgl_106	2667.15	152.35	0.06	76.3
Unknown#sst_cgl_107	3284.83	943.11	0.29	16.0
Unknown#sst_cgl_109	2896.07	329.61	0.11	79.5
Unknown#sst_cgl_110	1316.76	200.58	0.15	34.6
Unknown#sst_cgl_111	123347.19	9859.37	0.08	73.7
Unknown#sst_cgl_113	14756.09	3362.95	0.23	76.9
Unknown#sst_cgl_116	98479.45	10930.54	0.11	51.3
Unknown#sst_cgl_117	957.84	90.79	0.09	1.9
Unknown#sst_cgl_119	5611.39	843.48	0.15	25.6
Unknown#sst_cgl_120	12476.03	2592.69	0.21	78.2
Unknown#sst_cgl_121	41810.95	2797.02	0.07	80.8
Unknown#sst_cgl_122	10093.63	552.75	0.05	71.2
Unknown#sst_cgl_126	36072.62	4868.42	0.13	76.9
Unknown#sst_cgl_128	34896.52	3292.44	0.09	75.0
Unknown#sst_cgl_129	4282.36	351.25	0.08	75.0
Unknown#sst_cgl_132	4977.88	262.49	0.05	3.2
Unknown#sst_cgl_134	3094.29	837.04	0.27	8.3
Unknown#sst_cgl_A04	173608.06	10740.51	0.06	96.8
Unknown#sst_cgl_A08	8702.87	2223.62	0.26	76.3
Unknown#sst_cgl_A09	13404.75	653.49	0.05	64.1
Unknown#sst_cgl_A10	5719.48	717.15	0.13	51.9
Unknown#sst_cgl_A11	283.82	18.37	0.06	91.7
Unknown#sst_cgl_A12	100.69	15.25	0.15	36.5
Unknown#sst_cgl_A15	185.45	34.34	0.19	41.7
Unknown#sst_cgl_A16	897.01	89.29	0.10	76.3
Unknown#sst_cgl_A17	928.59	50.12	0.05	68.6
Unknown#sst_cgl_A18	54.19	12.34	0.23	3.2
Unknown#sst_cgl_D09	618.07	159.28	0.26	23.7
Uracil	2443.61	209.28	0.09	91.0
Urea	2216.69	497.65	0.22	89.1

Metabolite	Relative intensity	Standard error	Relative error	Occurrence [%]
Uridine	30813.36	2104.58	0.07	98.7
Uridine-5'-monophosphate	59262.43	4098.11	0.07	76.3
Valine	64258.67	3481.45	0.05	99.4
Xylulose	684.51	98.22	0.14	53.2
Xylulose-5-phosphate	27678.53	6569.23	0.24	35.9

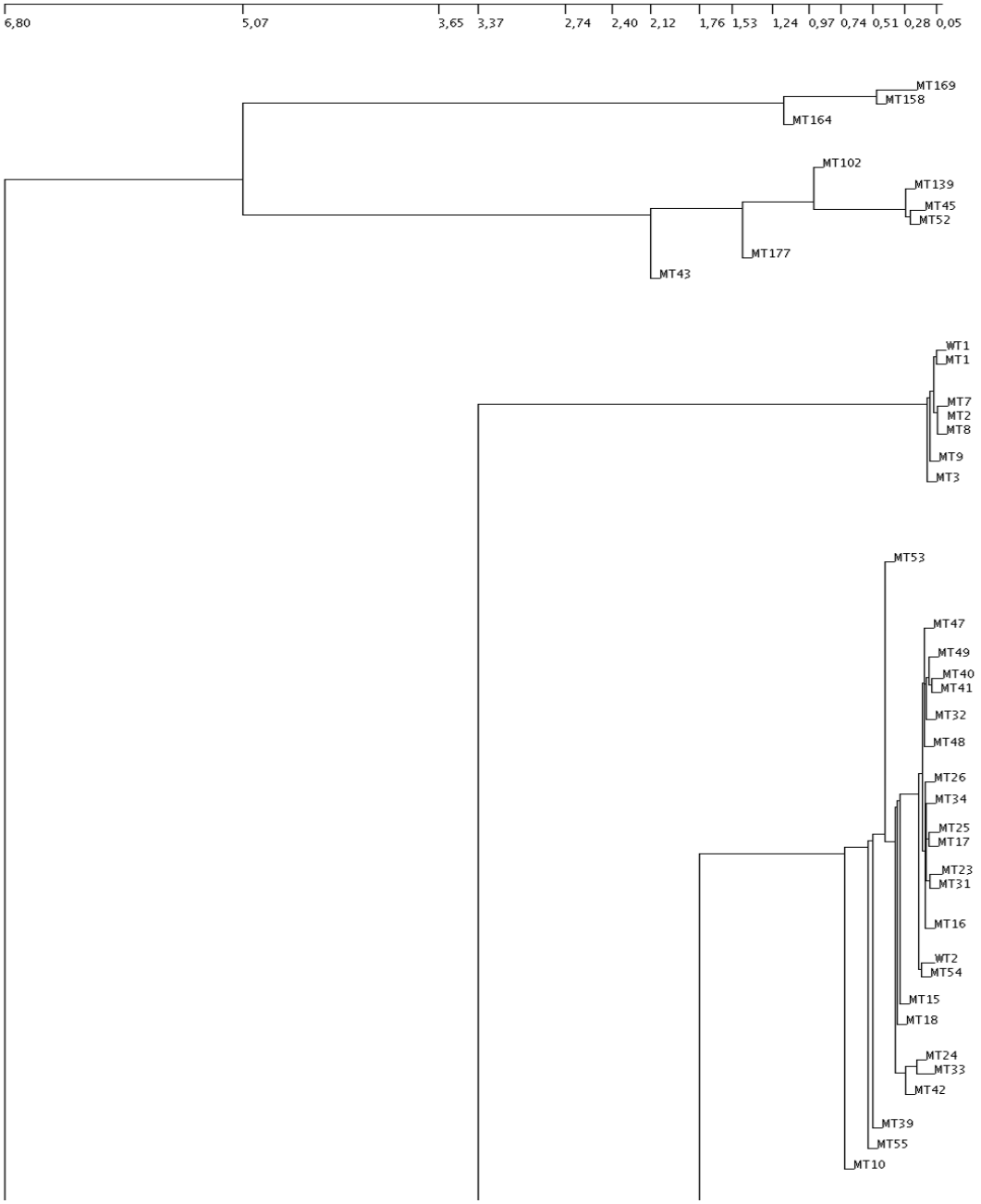
6,80
5,07
3,65
3,37
2,74
2,40
2,12
1,76
1,53
1,24
0,97
0,74
0,51
0,28
0,05
MT169
MT158
MT164
MT102
MT139
MT45
MT52
MT177
MT43
WT1
MT1
MT7
MT2
MT8
MT9
MT3
MT53
MT47
MT49
MT40
MT41
MT32
MT48
MT26
MT34
MT25
MT17
MT23
MT31
MT16
WT2
MT54
MT15
MT18
MT24
MT33
MT42
MT39
MT55
MT10

...

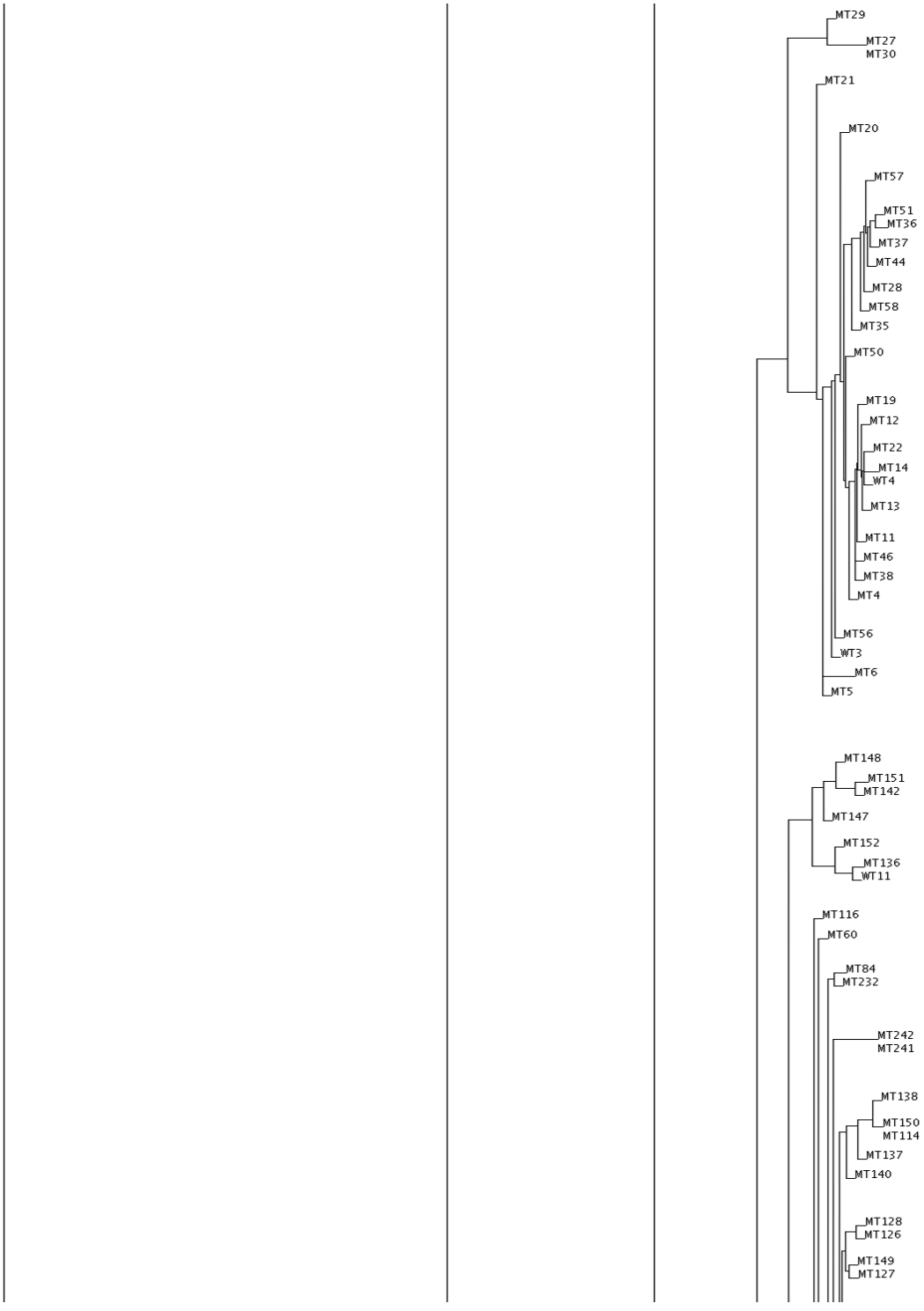
MT29
MT27
MT30
MT21
MT20
MT57
MT51
MT36
MT37
MT44
MT28
MT58
MT35
MT50
MT19
MT12
MT22
MT14
WT4
MT13
MT11
MT46
MT38
MT4
MT56
WT3
MT6
MT5
MT148
MT151
MT142
MT147
MT152
MT136
WT11
MT116
MT60
MT84
MT232
MT242
MT241
MT138
MT150
MT114
MT137
MT140
MT128
MT126
MT149
MT127

...

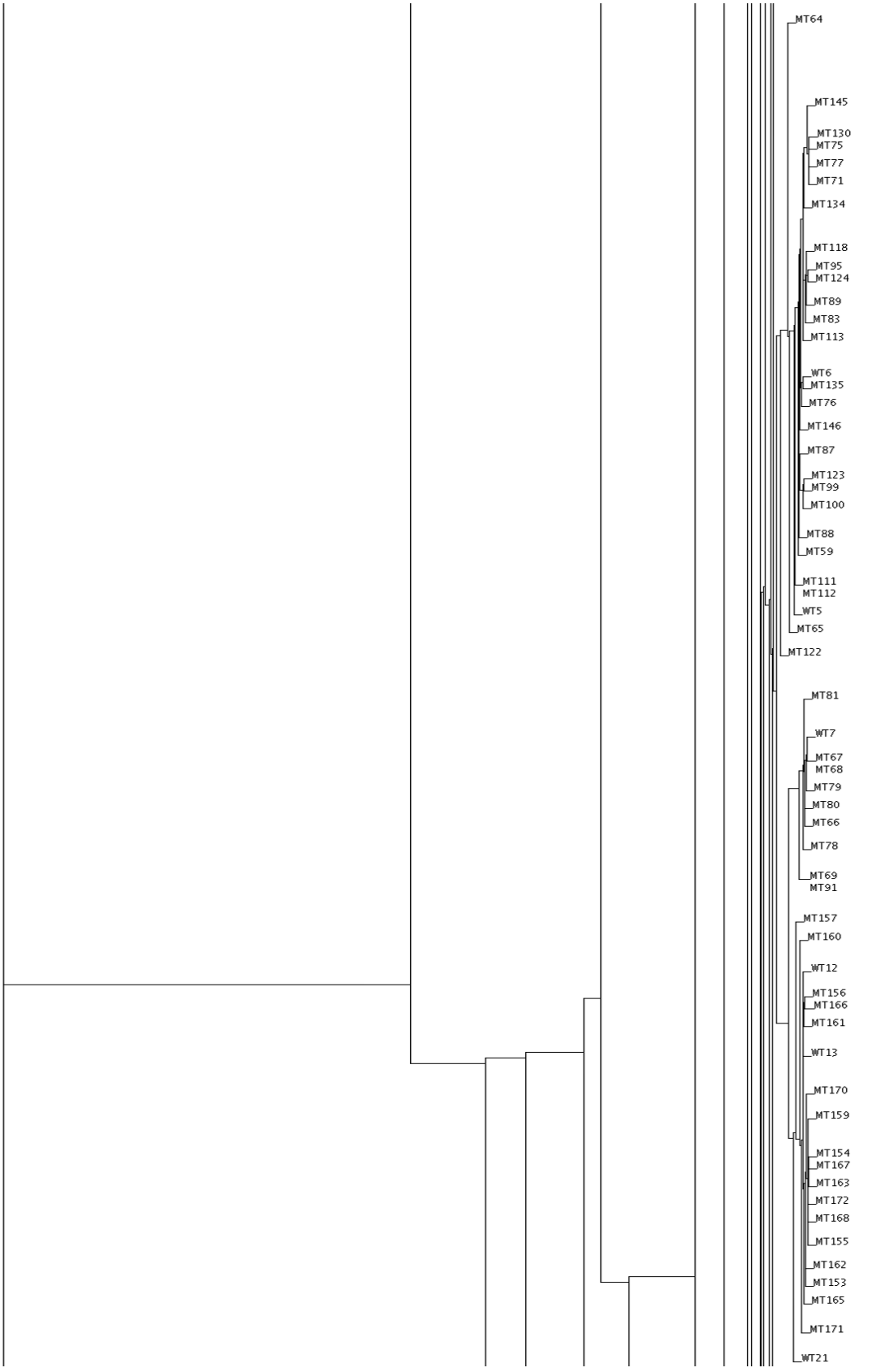
MT64
MT145
MT130
MT75
MT77
MT71
MT134
MT118
MT95
MT124
MT89
MT83
MT113
WT6
MT135
MT76
MT146
MT87
MT123
MT99
MT100
MT88
MT59
MT111
MT112
WT5
MT65
MT122
MT81
WT7
MT67
MT68
MT79
MT80
MT66
MT78
MT69
MT91
MT157
MT160
WT12
MT156
MT166
MT161
WT13
MT170
MT159
MT154
MT167
MT163
MT172
MT168
MT155
MT162
MT153
MT165
MT171
WT21

...

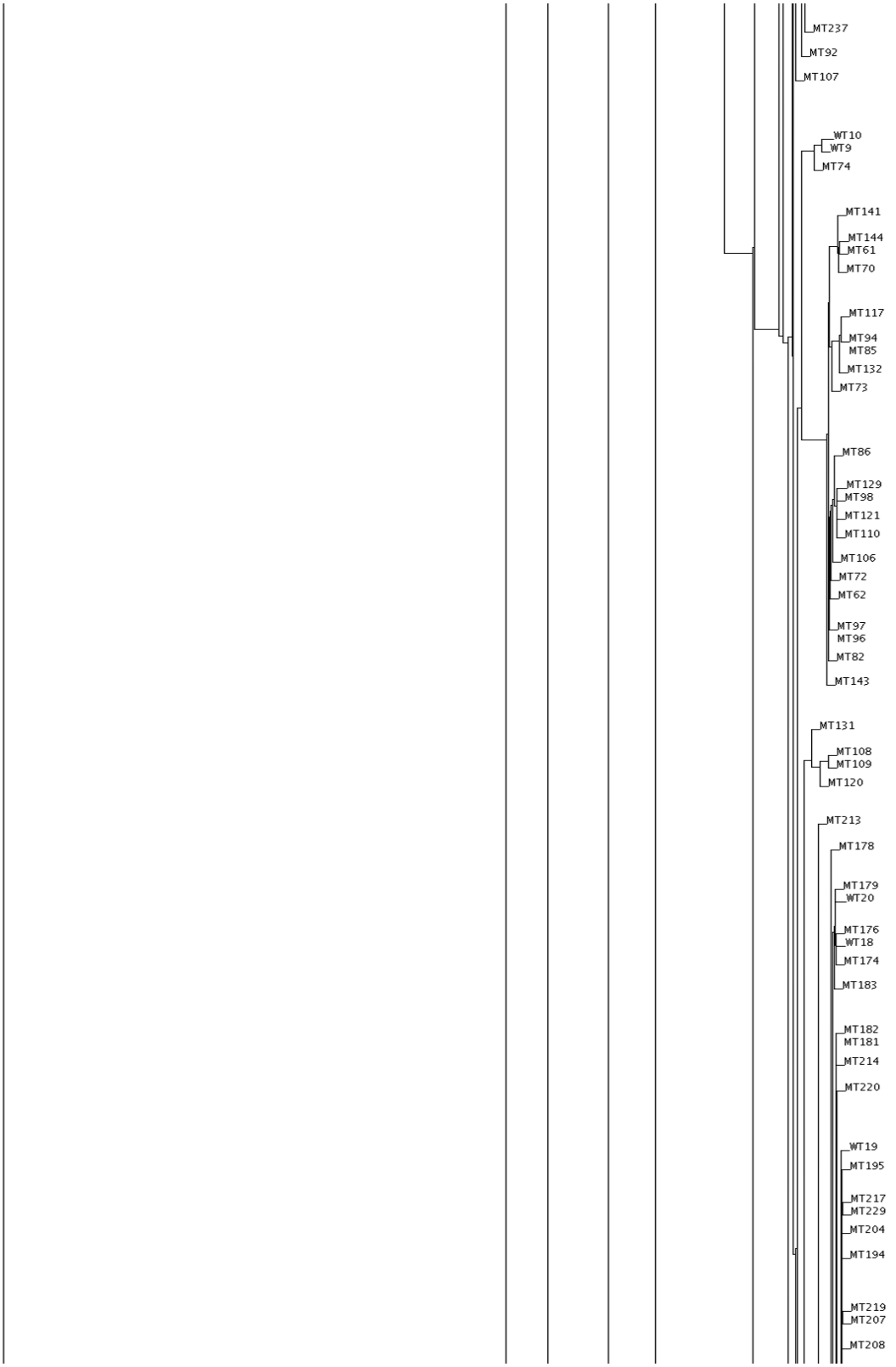
MT237
MT92
MT107
WT10
WT9
MT74
MT141
MT144
MT61
MT70
MT117
MT94
MT85
MT132
MT73
MT86
MT129
MT98
MT121
MT110
MT106
MT72
MT62
MT97
MT96
MT82
MT143
MT131
MT108
MT109
MT120
MT213
MT178
MT179
WT20
MT176
WT18
MT174
MT183
MT182
MT181
MT214
MT220
WT19
MT195
MT217
MT229
MT204
MT194
MT219
MT207
MT208

...

Figure A. Dendrogram of 255 samples (mutants and wild type). Splitted for a better overview.

Table C. List of the 10...20 most intensive metabolites (without “unknowns”) in 318 analyzed transposon mutants. Information about the occurrence as most intensive compound as well as their pathways and additional information are combined.

Metabolite	Most intensive compound [%]	Pathway	Other name	Additional information
Phosphoric acid	99.69	oxidative phosphorylation, peptidoglycane biosynthese	phosphate, orthophosphate	
Ribitol	95.31	internal standard		
Trehalose	93.13	starch and sucrose metabolism		differentiation trehalose and maltose difficult (isomers)
Glutamic acid	95.94	glutamate metabolism, urea cycle and metabolism of amino groups, argininge and proline metabolism, D-glutamine and D-glutamate metabolism, glutathione metabolism, nitrogen metabolism, aminoacyl-tRNA biosynthese, ABC-transporter for glutamate (secretion)		
Lysine	85.63	lysine biosynthese, aminoacyl-tRNA biosynthese	2,6-diamino-hexanoic acid	
Maltose	85.00	starch and sucrose metabolism		differentiation trehalose and maltose difficult (isomers)

Metabolite	Most intensive compound [%]	Pathway	Other name	Additional information
Alanine	82.81	alanine and aspartate metabolism, D-alanine metabolism, selenoaminoacid metabolism, aminoacyl-tRNA biosynthese		
Lactic acid	81.88	glycolysis, pyruvate metabolism		
Glycerol-3-phosphate	80.00	glycerophospholipid metabolism, glycerolipidmetabolism, ABC transporter evailable	glycerophosphoric acid	
Serine	63.13	glycin, serine and threonine metabolism, cysteine metabolism, aminoacyl-tRNA biosynthese		
Succinic acid	63.13	citrate cycle, oxidative phosphorylation, glyoxylate and dicarboxylate metabolism		
Aspartic acid	61.56	urea cycle and metabolism of amino groups, alanine and aspartate metabolism, glycine, serine and threonine metabolism, lysine biosynthese, beta-alanine metabolism,	2-aminosuccinic acid	

Metabolite	Most intensive compound [%]	Pathway	Other name	Additional information
		nitrogen metabolism, aminoacyl-tRNA biosynthese		
Adenosine-5'-monophosphate	55.31	purine metabolism	AMP	formation after usage of adenosine-5'-diphospate and -triphosphate
5-Oxoproline	53.75	glutathione metabolism	pyroglutamic acid, pyroglutamate	formation due to cyclization of glutamate and glutamine
Pyrophosphoric acid	49.06	oxidative Phosphorylierung		
gamma-Glutamylvaline	40.31	-		dipeptide
Fumaric acid	35.31	citrate cycle, oxidative phosphorylation, urea cycle and metabolism of amino groups	fumarate, trans-butenedioic acid	
Proline	31.56	arginine and proline metabolism, aminoacyl-tRNA biosynthesis	2-pyrrolidinecarboxylic acid	
Malic acid	31.25	citrate cycle		
Cycloleucine	30.94	valine, leucine, isoleucine biosynthese, aminoacyl-tRNA biosynthese	leucine	only leucine in KEGG

Metabolite	Most intensive compound [%]	Pathway	Other name	Additional information
Mannitol	26.25	fructose and mannose metabolism		
Glucose-6-phosphate	22.81	glycolysis,pentose phosphate pathway, aminoacyl-tRNA biosynthesis	alpha-D-glucose 6-phosphate	
Fructose-1,6-bisphosphate	25.31	glycolysis, pentose phosphate pathway, fructose and mannose metabolism	beta-D-fructose 1,6-bisphosphate	
Valine	20.31	valine, leucine and isoleucine biosynthese/degradation, aminoacyl-tRNA biosynthese	2-amino-3-methylbutyric acid	
Octadecanoic acid	19.38	Fatty acid biosynthese		no enzyme for this reaction in C. glutamicum in KEGG
Tryptophan	19.06	phenylalanine, tyrosine and tryptophan biosynthesis, aminoacyl-tRNA biosynthesis	(S)-alpha-amino-beta-(3-indolyl)-propionic acid	hardly any enzymes for the tryptophan metabolism in C. glutamicum in KEGG
Citric acid	18.75	tryptophan metabolism, phenylalanine, tyrosine and tryptophan biosynthesis, aminoacyl-tRNA biosynthesis		
Isomaltose	18.75	starch and sucrose metabolism		
Glutamine	18.44	D-glutamine and D-glutamate metabolism, purine metabolism,		

Metabolite	Most intensive compound [%]	Pathway	Other name	Additional information
		pyrimidine metabolism, glutamate metabolism, nitrogen metabolism		
6-Phosphogluconate	17.81	pentose phosphate pathway	6-phospho-D-gluconate	
Erythritol	17.81	-		in no pathway in KEGG
Mannose-6-phosphate	18.13	fructose and mannose metabolism		
Glucosamine-6-phosphate	10.94	glutamate metabolism, aminosugars metabolism	D-glucosamine phosphate	
Hexadecanoic acid	10.94	fatty acid biosynthese/metabolism		
3-Hydroxybutyric acid	8.75	synthesis and degradation of ketone bodies		enzyme not annotated, formation of acetoacetate from this compound
Uridine	8.75	pyrimidine metabolism		
Carbonic acid	7.50	nitrogen metabolism		
Erythrose-4-phosphate	7.19	pentose phosphate pathway		

Metabolite	Most intensive compound [%]	Pathway	Other name	Additional information
Glucose	5.94	glycolysis, starch and sucrose metabolism		differentiation glucose and mannose difficult (isomers)
Glycerol	6.25	glycerolipid metabolism	glycerin, 1,2,3-propanetriol	
Mannose	6.25	fructose and mannose metabolism		differentiation glucose and mannose difficult (isomers)
Uridine-5'-monophosphate	6.25	pyrimidine metabolism,peptidoglycan biosynthesis	UMP	formation after usage of uridine-5'-diphospate and -triphosphate
Glycolic acid	5.00	glyoxylate and dicarboxylate metabolism	glycolate	
Urea	4.38	arginine and proline metabolism, ABC-transporter available (for branched-chain amino acids), urea cycle and metabolism of amino groups	carbamide	enzyme for formation of urea directly from arginine not annotated in C. glutamicum, but due to instabilities arginine dissociates to ornithine and urea
Hydroxylamine	3.75	nitrogen metabolism		enzyme not annotated
Ribulose-5-phosphate	2.81	pentose phosphate pathway		hard to distinguish from xylulose-5-phosphate, both

Metabolite	Most intensive compound [%]	Pathway	Other name	Additional information
				compounds can directly be converted to each other
2-Hydroxypyridine	2.50	-		residues from derivatization compound
Dodecanol	2.19	-		not in KEGG
Xylulose-5-phosphate	2.19	pentose phosphate pathway		hard to distinguish from ribulose-5-phosphate, both compounds can directly be converted to each other
Malonic acid	1.88	beta-alanine metabolism --> fatty acid biosynthesis		enzyme not annotated for C. glutamicum
Benzoic acid	1.56	benzoate degredation via hydroxylation/via CoA ligation, side product in phenylalanine metabolism	benzoate	
beta-Alanine	1.56	alanine and aspartate metabolism, beta-alanine metabolism	3-aminopropionate	
Nicotinamide	1.56	nicotinate and nicotinamide metabolism	nicotinic acid amide, niacinamide, vitamine PP	

Metabolite	Most intensive compound [%]	Pathway	Other name	Additional information
Methionine	1.25	methionine metabolism, aminoacyl-tRNA biosynthesis	L-2-amino-4-methylthiobutyric acid	
2-Hydroxyglutaric acid	0.94	butanoate metabolism	2-hydroxyglutarate	enzyme not annotated for C. glutamicum
Glucono lactone	0.94	Pentose Phosphate Pathway	D-glucono-1,5-lactone	enzyme not annotated for C. glutamicum
Glyceraldehyde	0.94	fructose and mannose metabolism, glycolipid metabolism	D-glyceraldehyde	
Norvaline	0.94	-	L-2-aminopentanoic acid	no pathway in KEGG, relate to valine
2-Hydroxybutanoic acid	0.63	propanoate metabolism	2-hydroxybutyrate	
3-Phosphoglyceric acid	0.63	glycolysis	3-phosphoglycerate, glycerate 3-phosphate	
Xylulose	0.63	pentose and glucuronate interconversions		
3-Hydroxy-2-tetradecyl-octanoic acid	0.31	-		not pathway in KEGG

Metabolite	Most intensive compound [%]	Pathway	Other name	Additional information
Ornithine	0.31	urea cycle and metabolism of amino groups, arginine and proline metabolism		not possible to be differentiated from arginine, see arginine

Table D. List of analyzed transposon mutants and summary of the important characteristics.

Number	Mutant	OD	Standard deviation of the OD	r to wild type on same plate	Error [%]	Number of increased metabolites	Number of reduced metabolites	Number of varying metabolites	r to reference list	Affected enzyme (gene name)
MT1	A1_B2P6	6.58	0.64	0.818	-	11	48	59	0.503	
MT2	A2_B2P6	6.62	0.24	0.872	16.95	17	44	61	0.533	
MT3	A3_B2P6	6.70	0.37	0.878	23.93	23	46	69	0.527	
MT4	A4_B2P6	7.23	0.78	0.967	12.52	16	33	49	0.809	
MT5	A5_B2P6	6.13	0.11	0.986	12.28	9	29	38	0.776	
MT6	A6_B2P6	6.34	0.11	0.895	14.15	18	41	59	0.791	
MT7	B1_B2P6	6.31	0.59	0.848	14.68	16	44	60	0.507	
MT8	B2_B2P6	6.19	0.89	0.843	16.16	13	46	59	0.510	
MT9	B3_B2P6	5.27	0.66	0.819	13.86	17	41	58	0.475	
MT10	B4_B2P6	5.83	0.36	0.939	16.82	14	38	52	0.633	

Number	Mutant	OD	Standard deviation of the OD	r to wild type on same plate	Error [%]	Number of increased metabolites	Number of reduced metabolites	Number of varying metabolites	r to reference list	Affected enzyme (gene name)
MT11	B5_B2P6	6.43	0.74	0.975	13.71	10	29	39	0.850	
MT12	B6_B2P6	5.55	0.60	0.951	13.38	8	37	45	0.813	
MT13	B7_B2P6	4.98	0.17	0.965	16.86	22	24	46	0.831	
MT14	B8_B2P6	5.60	0.52	0.969	13.92	17	26	43	0.847	
MT15	C1_B2P6	6.19	1.03	0.948	16.45	10	43	53	0.627	
MT16	C2_B2P6	5.42	0.62	0.937	13.50	9	50	59	0.621	
MT17	C3_B2P6	5.28	0.51	0.944	16.11	11	42	53	0.617	
MT18	C4_B2P6	5.85	0.47	0.967	13.97	13	40	53	0.659	
MT19	C5_B2P6	5.77	0.81	0.964	13.51	12	35	47	0.797	
MT20	C6_B2P6	4.82	0.17	0.928	17.42	10	33	43	0.811	
MT21	C7_B2P6	4.09	0.35	0.926	-	10	32	42	0.837	
MT22	C8_B2P6	5.31	0.75	0.968	13.10	13	28	41	0.853	
MT23	D1_B2P6	6.38	0.31	0.938	13.72	9	47	56	0.618	
MT24	D2_B2P6	5.44	0.97	0.921	22.91	13	40	53	0.717	
MT25	D3_B2P6	4.85	0.52	0.926	14.03	16	41	57	0.644	
MT26	D4_B2P6	5.86	0.90	0.969	13.76	12	41	53	0.662	

Number	Mutant	OD	Standard deviation of the OD	r to wild type on same plate	Error [%]	Number of increased metabolites	Number of reduced metabolites	Number of varying metabolites	r to reference list	Affected enzyme (gene name)
MT27	D5_B2P6	5.66	0.70	0.977	13.18	8	36	44	0.818	
MT28	D6_B2P6	4.45	0.33	0.918	14.92	9	34	43	0.805	
MT29	D7_B2P6	4.17	0.53	0.918	12.03	8	29	37	0.791	
MT30	D8_B2P6	4.93	0.67	0.959	14.86	10	29	39	0.824	
MT31	E1_B2P6	5.73	0.66	0.942	15.22	8	48	56	0.606	
MT32	E2_B2P6	3.73	0.47	0.915	13.82	22	42	64	0.585	
MT33	E3_B2P6	4.29	1.12	0.875	30.38	22	32	54	0.810	
MT34	E4_B2P6	5.73	0.44	0.973	14.00	12	41	53	0.653	
MT35	E5_B2P6	5.67	0.91	0.97	16.82	12	32	44	0.826	
MT36	E6_B2P6	4.89	0.39	0.852	15.65	22	30	52	0.676	
MT37	E7_B2P6	4.36	0.19	0.909	18.42	20	30	50	0.783	
MT38	E8_B2P6	5.03	1.14	0.948	16.39	15	34	49	0.813	
MT39	F1_B2P6	6.13	1.05	0.971	15.90	10	44	54	0.639	
MT40	F2_B2P6	6.14	0.85	0.932	15.36	9	48	57	0.615	
MT41	F3_B2P6	5.38	1.07	0.98	18.89	12	41	53	0.686	
MT42	F4_B2P6	5.81	0.29	0.97	17.17	15	37	52	0.714	

Number	Mutant	OD	Standard deviation of the OD	r to wild type on same plate	Error [%]	Number of increased metabolites	Number of reduced metabolites	Number of varying metabolites	r to reference list	Affected enzyme (gene name)
MT43	F5_B2P6	0.97	0.05	0.465	41.81	3	65	68	0.389	
MT44	F6_B2P6	4.88	0.29	0.936	15.03	7	37	44	0.782	
MT45	F7_B2P6	0.86	0.00	0.312	23.42	2	66	68	0.246	
MT46	F8_B2P6	5.49	0.92	0.982	12.00	21	23	44	0.850	
MT47	G1_B2P6	6.75	0.71	0.967	16.39	11	43	54	0.645	
MT48	G2_B2P6	7.03	0.70	0.963	16.93	7	46	53	0.663	
MT49	G3_B2P6	6.31	0.36	0.993	12.44	11	48	59	0.671	
MT50	G5_B2P6	5.84	0.46	0.982	22.15	6	36	42	0.870	
MT51	G6_B2P6	4.84	0.25	0.888	19.02	5	45	50	0.711	
MT52	G7_B2P6	0.81	0.03	0.342	23.23	1	67	68	0.263	
MT53	H1_B2P6	7.99	0.60	0.895	23.47	13	42	55	0.562	
MT54	H2_B2P6	7.85	1.20	0.953	17.71	8	51	59	0.609	
MT55	H3_B2P6	7.83	0.17	0.94	19.96	10	49	59	0.723	
MT56	H5_B2P6	5.56	0.64	0.934	16.55	6	44	50	0.854	
MT57	H6_B2P6	4.67	1.14	0.976	20.46	5	54	59	0.827	
MT58	H7_B2P6	5.70	0.91	0.937	18.11	5	51	56	0.805	

Number	Mutant	OD	Standard deviation of the OD	r to wild type on same plate	Error [%]	Number of increased metabolites	Number of reduced metabolites	Number of varying metabolites	r to reference list	Affected enzyme (gene name)
MT59	A1_B2P7	5.85	0.68	0.937	14.07	31	34	65	0.726	
MT60	A10_B2P7	5.75	0.24	0.944	15.11	23	41	64	0.714	
MT61	A11_B2P7	5.71	0.43	0.919	14.40	28	53	81	0.673	
MT62	A12_B2P7	5.91	0.35	0.963	22.44	23	52	75	0.776	
MT63	A2_B2P7	1.68	0.03	0.652	24.13	30	59	89	0.461	para-aminobenzoat synthase (*cgl0997, pabAB*)
MT64	A3_B2P7	5.33	0.35	0.881	15.15	33	29	62	0.773	
MT65	A4_B2P7	5.80	0.39	0.863	20.80	38	36	74	0.718	
MT66	A5_B2P7	7.28	0.45	0.949	7.11	92	9	101	0.686	
MT67	A6_B2P7	6.75	0.64	0.987	13.31	100	8	108	0.654	
MT68	A7_B2P7	7.02	0.74	0.957	8.06	98	9	107	0.663	
MT69	A8_B2P7	6.75	0.85	0.955	11.26	98	8	106	0.670	
MT70	A9_B2P7	6.61	0.46	0.93	11.31	21	57	78	0.714	
MT71	B1_B2P7	5.88	0.35	0.925	11.80	27	31	58	0.752	
MT72	B10_B2P7	5.11	0.23	0.955	30.26	25	51	76	0.715	
MT73	B11_B2P7	5.31	0.32	0.917	10.38	23	55	78	0.700	

Number	Mutant	OD	Standard deviation of the OD	r to wild type on same plate	Error [%]	Number of increased metabolites	Number of reduced metabolites	Number of varying metabolites	r to reference list	Affected enzyme (gene name)
MT74	B12_B2P7	5.87	0.37	0.964	23.42	22	48	70	0.837	
MT75	B2_B2P7	5.24	0.51	0.936	12.35	36	26	62	0.744	
MT76	B3_B2P7	4.94	0.11	0.95	21.60	38	16	54	0.743	
MT77	B4_B2P7	5.19	0.26	0.933	12.48	36	26	62	0.713	
MT78	B5_B2P7	6.89	0.89	0.959	7.94	97	9	106	0.684	
MT79	B6_B2P7	5.94	0.71	0.953	8.68	99	8	107	0.692	
MT80	B7_B2P7	6.19	0.05	0.966	7.98	95	7	102	0.686	
MT81	B8_B2P7	6.47	0.72	0.964	10.47	92	9	101	0.684	
MT82	B9_B2P7	6.45	0.42	0.898	12.73	19	63	82	0.675	
MT83	C1_B2P7	5.40	0.28	0.955	25.02	36	17	53	0.706	
MT84	C10_B2P7	2.52	0.34	0.808	18.86	14	69	83	0.699	
MT85	C11_B2P7	5.25	0.30	0.921	12.42	21	52	73	0.737	
MT86	C12_B2P7	5.97	0.41	0.95	24.58	20	55	75	0.797	
MT87	C2_B2P7	4.90	0.38	0.942	7.79	26	14	40	0.746	
MT88	C3_B2P7	4.58	0.10	0.951	18.72	37	13	50	0.732	hypothetical membrane protein (*cg0879*)

Number	Mutant	OD	Standard deviation of the OD	r to wild type on same plate	Error [%]	Number of increased metabolites	Number of reduced metabolites	Number of varying metabolites	r to reference list	Affected enzyme (gene name)
MT89	C4_B2P7	5.23	0.11	0.946	16.37	36	18	54	0.724	
MT90	C5_B2P7	5.81	0.91	-	-	-	-	-	-	
MT91	C6_B2P7	3.63	0.37	0.907	9.65	46	22	68	0.726	pseudouridine synthase (*cgl2138, rluD*)
MT92	C7_B2P7	5.01	0.31	0.918	16.06	41	12	53	0.717	hypothetical protein (*cgl0592*)
MT93	C8_B2P7	5.48	0.62	-	-	-	-	-	-	
MT94	C9_B2P7	5.88	0.64	0.939	14.13	19	53	72	0.770	
MT95	D1_B2P7	5.78	0.65	0.967	21.92	30	22	52	0.735	
MT96	D10_B2P7	4.68	0.52	0.795	19.53	21	48	69	0.623	
MT97	D11_B2P7	4.70	0.28	0.955	21.43	27	37	64	0.805	
MT98	D12_B2P7	5.29	0.79	0.947	26.51	21	50	71	0.768	
MT99	D2_B2P7	4.71	0.26	0.953	9.32	39	11	50	0.766	
MT100	D3_B2P7	3.45	0.60	0.932	12.61	35	19	54	0.732	
MT101	D4_B2P7	2.88	0.09	0.931	16.53	45	25	70	0.759	
MT102	D5_B2P7	0.89	0.03	0.331	17.40	16	97	113	0.210	
MT103	D6_B2P7	4.90	0.49	-	-	-	-	-	-	

Number	Mutant	OD	Standard deviation of the OD	r to wild type on same plate	Error [%]	Number of increased metabolites	Number of reduced metabolites	Number of varying metabolites	r to reference list	Affected enzyme (gene name)
MT104	D7_B2P7	3.52	0.07	-	-	-	-	-	-	
MT105	D8_B2P7	5.33	0.26	-	-	-	-	-	-	
MT106	D9_B2P7	6.09	0.55	0.958	21.97	20	53	73	0.773	
MT107	E1_B2P7	6.41	0.50	0.926	15.87	29	37	66	0.745	glutamate-ammonia-ligase adenyl-transferase (*glnE*)
MT108	E10_B2P7	4.47	0.50	0.916	13.82	15	43	58	0.782	
MT109	E11_B2P7	4.83	0.56	0.919	14.67	15	43	58	0.760	
MT110	E12_B2P7	5.23	1.04	0.963	27.39	23	49	72	0.775	
MT111	E2_B2P7	5.69	0.53	0.959	9.13	17	19	36	0.787	
MT112	E3_B2P7	4.47	0.33	0.947	10.36	33	14	47	0.739	
MT113	E4_B2P7	5.07	0.25	0.961	19.71	40	18	58	0.775	
MT114	E5_B2P7	6.35	0.44	0.84	18.39	36	46	82	0.646	
MT115	E6_B2P7	5.36	0.45	0.791	27.14	25	64	89	0.493	
MT116	E8_B2P7	5.43	0.48	0.882	23.53	38	47	85	0.581	
MT117	E9_B2P7	6.25	0.54	0.926	14.52	20	62	82	0.755	
MT118	F1_B2P7	6.27	0.34	0.965	18.49	23	24	47	0.764	

Number	Mutant	OD	Standard deviation of the OD	r to wild type on same plate	Error [%]	Number of increased metabolites	Number of reduced metabolites	Number of varying metabolites	r to reference list	Affected enzyme (gene name)
MT119	F10_B2P7	5.09	0.29	0.929	24.34	20	50	70	0.733	
MT120	F11_B2P7	3.19	0.11	0.88	12.29	16	56	72	0.727	
MT121	F12_B2P7	5.22	0.99	0.954	24.32	24	52	76	0.763	
MT122	F2_B2P7	5.36	0.23	0.904	7.19	30	36	66	0.743	hypothetical protein (*cg0858*)
MT123	F3_B2P7	4.77	0.53	0.948	12.59	23	17	40	0.754	
MT124	F4_B2P7	5.19	0.33	0.97	19.12	40	21	61	0.778	
MT125	F5_B2P7	2.09	0.31	0.755	22.37	34	60	94	0.629	
MT126	F6_B2P7	5.66	0.76	0.854	13.42	27	42	69	0.682	
MT127	F7_B2P7	5.19	0.05	0.832	12.79	24	41	65	0.701	
MT128	F8_B2P7	5.73	0.61	0.844	28.27	26	34	60	0.656	
MT129	F9_B2P7	5.90	0.55	0.957	21.71	20	56	76	0.743	
MT130	G1_B2P7	6.71	0.51	0.947	11.59	36	29	65	0.784	
MT131	G10_B2P7	4.95	0.86	0.945	15.94	13	45	58	0.781	
MT132	G11_B2P7	4.78	0.28	0.919	9.77	28	54	82	0.669	
MT133	G12_B2P7	1.43	0.12	0.533	30.86	20	61	81	0.374	
MT134	G2_B2P7	6.55	0.50	0.953	15.00	28	30	58	0.781	

Number	Mutant	OD	Standard deviation of the OD	r to wild type on same plate	Error [%]	Number of increased metabolites	Number of reduced metabolites	Number of varying metabolites	r to reference list	Affected enzyme (gene name)
MT135	G3_B2P7	4.69	0.42	0.957	24.15	48	15	63	0.771	
MT136	G4_B2P7	5.93	0.85	0.963	19.11	15	43	58	0.815	
MT137	G5_B2P7	6.07	0.87	0.837	24.46	35	54	89	0.635	
MT138	G6_B2P7	5.24	0.34	0.816	10.09	31	50	81	0.670	
MT139	G7_B2P7	0.91	0.08	0.31	17.41	14	98	112	0.206	
MT140	G8_B2P7	5.74	0.57	0.85	26.59	28	50	78	0.645	
MT141	G9_B2P7	6.10	0.38	0.94	15.80	24	57	81	0.734	
MT142	H1_B2P7	6.39	0.48	0.927	23.79	21	41	62	0.738	
MT143	H10_B2P7	5.67	0.27	0.955	20.43	22	57	79	0.711	
MT144	H11_B2P7	6.04	0.18	0.905	-	25	58	83	0.721	
MT145	H2_B2P7	6.56	0.94	0.948	14.43	29	29	58	0.775	
MT146	H3_B2P7	5.55	0.11	0.973	18.48	45	23	68	0.776	
MT147	H4_B2P7	6.99	1.49	0.739	28.34	16	42	58	0.579	UDP-N-acetylenolpyruvoylglucosamine reductase (*murB*)
MT148	H5_B2P7	6.06	0.07	0.887	13.64	24	45	69	0.699	

Number	Mutant	OD	Standard deviation of the OD	r to wild type on same plate	Error [%]	Number of increased metabolites	Number of reduced metabolites	Number of varying metabolites	r to reference list	Affected enzyme (gene name)
MT149	H6_B2P7	3.41	0.05	0.856	21.69	44	44	88	0.634	
MT150	H7_B2P7	5.65	0.33	0.839	12.19	35	50	85	0.647	
MT151	H8_B2P7	6.68	0.11	0.926	12.22	21	43	64	0.756	
MT152	H9_B2P7	6.46	0.67	0.953	21.21	22	30	52	0.808	
MT153	A1_B2P8	6.66	0.22	0.976	10.10	8	56	64	0.797	
MT154	A10_B2P8	4.93	1.02	0.991	10.82	13	47	60	0.817	
MT155	A11_B2P8	6.06	0.77	0.986	10.96	9	58	67	0.83	
MT156	A12_B2P8	5.56	0.09	0.982	10.10	11	54	65	0.771	
MT157	A2_B2P8	6.71	0.31	0.929	20.92	10	54	64	0.800	
MT158	A3_B2P8	0.87	0.02	0.495	44.91	7	91	98	0.517	
MT159	A4_B2P8	5.81	1.12	0.984	22.20	11	43	54	0.829	
MT160	A5_B2P8	7.34	0.14	0.99	13.80	6	64	70	0.834	
MT161	A6_B2P8	6.17	0.55	0.96	10.68	11	52	63	0.752	hypothetical protein (*cgl1708)*
MT162	A7_B2P8	6.34	0.36	0.978	13.85	9	51	60	0.783	
MT163	A8_B2P8	5.61	1.06	0.962	13.74	12	54	66	0.824	
MT164	A9_B2P8	0.74	0.12	0.411	24.65	6	93	99	0.345	

Number	Mutant	OD	Standard deviation of the OD	r to wild type on same plate	Error [%]	Number of increased metabolites	Number of reduced metabolites	Number of varying metabolites	r to reference list	Affected enzyme (gene name)
MT165	B1_B2P8	5.73	0.17	0.927	23.56	13	48	61	0.798	aminopeptidase N (*pepN, cgl2426*)
MT166	B2_B2P8	5.09	0.24	0.979	9.91	11	53	64	0.830	
MT167	B3_B2P8	4.95	0.38	0.962	10.86	10	51	61	0.834	
MT168	B4_B2P8	5.64	0.28	0.948	10.10	10	58	68	0.823	citrate-transporter/symporter (*cgl0067, citP*)
MT169	B5_B2P8	0.61	0.01	0.362	33.38	9	94	103	0.270	
MT170	B6_B2P8	5.53	0.17	0.978	14.27	14	44	58	0.839	
MT171	B7_B2P8	5.14	1.43	0.979	22.28	14	35	49	0.848	
MT172	B8_B2P8	5.76	0.48	0.984	11.61	10	50	60	0.842	
MT173	A1_B2P19	6.63	0.09	0.915	14.82	12	28	40	0.841	
MT174	A10_B2P19	7.23	0.92	0.985	22.58	10	34	44	0.741	
MT175	A11_B2P19	0.92	0.02	0.47	20.32	7	88	95	0.368	
MT176	A12_B2P19	7.55	0.63	0.975	12.01	13	41	54	0.743	
MT177	A2_B2P19	0.87	0.01	0.483	43.11	13	81	94	0.399	
MT178	A3_B2P19	7.74	0.17	0.9	34.50	11	44	55	0.821	

Number	Mutant	OD	Standard deviation of the OD	r to wild type on same plate	Error [%]	Number of increased metabolites	Number of reduced metabolites	Number of varying metabolites	r to reference list	Affected enzyme (gene name)
MT179	A4_B2P19	7.37	0.09	0.946	20.36	9	46	55	0.753	
MT180	A5_B2P19	6.93	0.88	0.944	24.47	6	28	34	0.765	
MT181	A6_B2P19	7.05	0.33	0.901	21.10	22	25	47	0.789	
MT182	A7_B2P19	7.07	0.41	0.905	18.82	25	26	51	0.808	
MT183	A8_B2P19	6.79	0.12	0.943	24.09	14	34	48	0.796	
MT184	A9_B2P19	8.10	0.65	0.974	13.91	6	30	36	0.777	
MT185	B1_B2P19	6.01	0.73	0.86	28.18	19	37	56	0.780	
MT186	B10_B2P19	6.45	0.87	0.98	11.34	14	32	46	0.820	
MT187	B11_B2P19	6.64	0.30	0.979	7.56	14	23	37	0.807	
MT188	B12_B2P19	7.55	1.08	0.98	18.51	10	31	41	0.792	
MT189	B2_B2P19	6.16	0.14	0.915	13.21	8	35	43	0.803	
MT190	B3_B2P19	5.46	0.84	0.902	19.17	28	20	48	0.854	
MT192	B5_B2P19	6.49	0.50	0.873	21.02	11	22	33	0.462	
MT193	B6_B6P19	5.91	0.70	0.859	12.35	27	37	64	0.669	
MT194	B7_B6P19	5.99	0.46	0.988	18.68	8	27	35	0.801	
MT195	B8_B2P19	6.25	0.77	0.977	18.97	8	27	35	0.719	

Number	Mutant	OD	Standard deviation of the OD	r to wild type on same plate	Error [%]	Number of increased metabolites	Number of reduced metabolites	Number of varying metabolites	r to reference list	Affected enzyme (gene name)
MT196	B9_B2P19	0.89	0.02	0.517	20.29	9	87	96	0.396	
MT197	C1_B2P19	5.94	1.65	0.929	30.79	9	23	32	0.825	
MT198	C10_B2P19	6.05	0.43	0.981	8.73	12	27	39	0.756	
MT199	C11_B2P19	6.07	0.12	0.98	11.00	16	25	41	0.753	
MT200	C12_B2P19	0.97	0.11	0.418	17.81	5	90	95	0.294	
MT201	C2_B2P19	5.72	0.06	0.928	19.75	6	26	32	0.798	
MT202	C3_B2P19	5.17	0.51	0.931	13.16	10	24	34	0.840	
MT203	C4_B2P19	6.82	0.48	0.937	13.61	2	40	42	0.836	
MT204	C5_B2P19	6.41	0.63	0.982	13.07	21	27	48	0.792	
MT205	C6_B6P19	5.67	0.30	0.98	12.60	8	34	42	0.773	
MT206	C7_B6P19	5.69	0.26	0.983	11.55	12	24	36	0.731	
MT207	C8_B2P19	6.49	0.89	0.98	15.00	19	19	38	0.801	
MT208	C9_B2P19	6.69	0.72	0.984	9.82	14	22	36	0.788	
MT209	D1_B2P19	5.82	0.52	0.929	13.04	13	18	31	0.825	
MT210	D10_B2P19	5.65	0.21	0.98	8.59	16	28	44	0.777	
MT211	D11_B2P19	5.78	0.31	0.985	7.90	14	26	40	0.779	

Number	Mutant	OD	Standard deviation of the OD	r to wild type on same plate	Error [%]	Number of increased metabolites	Number of reduced metabolites	Number of varying metabolites	r to reference list	Affected enzyme (gene name)
MT212	D12_B2P19	7.11	0.55	0.78	13.84	9	21	30	0.466	
MT213	D2_B2P19	5.04	0.60	0.918	21.29	6	29	35	0.806	
MT214	D3_B2P19	4.16	0.66	0.939	16.24	21	18	39	0.781	
MT215	D4_B2P19	6.92	1.23	0.918	13.03	2	44	46	0.768	
MT216	D5_B2P19	6.04	1.41	0.986	14.29	9	27	36	0.747	
MT217	D6_B6P19	5.23	0.28	0.98	19.02	19	24	43	0.772	
MT218	D7_B6P19	5.40	0.21	0.979	12.56	17	24	41	0.741	
MT219	D8_B2P19	6.40	0.20	0.981	17.90	15	20	35	0.746	
MT220	D9_B2P19	6.98	0.91	0.915	21.72	14	12	26	0.611	
MT221	E1_B2P19	6.41	0.81	0.952	18.31	15	17	32	0.760	
MT222	E10_B2P19	6.28	0.63	0.916	13.96	9	23	32	0.617	
MT223	E11_B2P19	6.03	0.23	0.895	18.94	23	19	42	0.611	
MT224	E12_B2P19	5.73	0.81	0.933	26.79	19	21	40	0.614	
MT225	E2_B2P19	5.09	0.39	0.9	15.14	18	32	50	0.803	
MT226	E3_B2P19	5.03	0.81	0.887	25.68	16	18	34	0.856	
MT227	E4_B2P19	6.65	1.00	0.934	20.28	11	30	41	0.834	

Number	Mutant	OD	Standard deviation of the OD	r to wild type on same plate	Error [%]	Number of increased metabolites	Number of reduced metabolites	Number of varying metabolites	r to reference list	Affected enzyme (gene name)
MT228	E5_B2P19	4.29	1.32	0.971	75.60	91	11	102	0.636	
MT229	E6_B6P19	6.17	0.44	0.985	19.27	20	30	50	0.828	
MT230	E7_B6P19	4.67	0.27	0.96	8.93	29	27	56	0.720	
MT231	E8_B2P19	0.69	0.01	0.486	27.55	7	87	94	0.382	
MT232	E9_B2P19	5.38	0.13	0.854	14.23	12	26	38	0.583	
MT233	F1_B2P19	6.73	0.39	0.972	21.89	12	20	32	0.866	
MT234	F2_B2P19	5.80	0.23	0.943	15.98	11	26	37	0.816	
MT235	F3_B2P19	6.23	0.67	0.929	16.49	10	31	41	0.827	
MT236	F4_B2P19	6.29	0.74	0.931	18.72	8	30	38	0.821	
MT237	A1_B2P21	8.17	0.48	0.943	8.97	12	22	34	0.867	
MT238	A10_B2P21	0.83	0.01	0.477	25.51	10	88	98	0.444	
MT239	A11_B2P21	0.78	0.07	0.417	35.81	12	92	104	0.415	
MT240	A12_B2P21	0.79	0.05	0.352	17.26	7	95	102	0.388	
MT241	A3_B2P21	8.00	0.06	0.833	17.36	25	37	62	0.787	
MT242	A4_B2P21	8.11	0.60	0.852	10.00	27	35	62	0.821	
MT243	A5_B2P21	7.64	0.51	0.949	27.20	29	22	51	0.847	

Number	Mutant	OD	Standard deviation of the OD	r to wild type on same plate	Error [%]	Number of increased metabolites	Number of reduced metabolites	Number of varying metabolites	r to reference list	Affected enzyme (gene name)
MT244	A6_B2P21	5.78	3.23	0.959	35.37	28	17	45	0.864	
MT245	A7_B2P21	7.47	0.12	0.982	8.70	25	14	39	0.882	
MT246	A8_B2P21	8.45	0.73	0.976	9.79	25	20	45	0.871	
MT247	A9_B2P21	7.20	0.96	0.948	17.21	11	30	41	0.765	
MT248	B1_B2P21	6.59	0.31	0.959	12.84	10	13	23	0.876	
MT249	B10_B2P21	5.87	0.10	0.983	18.71	17	26	43	0.763	
MT250	B11_B2P21	6.10	0.29	0.969	19.31	12	27	39	0.775	
MT251	B12_B2P21	6.85	0.68	0.95	12.97	16	32	48	0.753	
MT252	B2_B2P21	7.72	0.99	0.929	9.22	14	23	37	0.864	
MT253	B3_B2P21	0.77	0.01	0.465	17.00	18	94	112	0.453	
MT254	B4_B2P21	6.54	1.24	0.913	36.33	30	25	55	0.819	
MT255	B5_B2P21	7.07	0.96	0.921	20.84	19	13	32	0.930	
MT256	B6_B2P21	6.74	0.67	0.935	19.84	31	15	46	0.920	
MT257	B7_B2P21	6.39	0.12	0.912	24.32	30	15	45	0.917	
MT258	B8_B2P21	7.60	0.56	0.924	12.98	23	17	40	0.895	
MT259	B9_B2P21	6.64	0.95	0.948	19.51	7	38	45	0.764	

Number	Mutant	OD	Standard deviation of the OD	r to wild type on same plate	Error [%]	Number of increased metabolites	Number of reduced metabolites	Number of varying metabolites	r to reference list	Affected enzyme (gene name)
MT260	C1_B2P21	6.22	0.16	0.952	14.97	12	12	24	0.871	
MT261	C10_B2P21	5.55	0.15	0.919	32.22	21	32	53	0.692	
MT262	C11_B2P21	5.25	0.05	0.911	23.01	21	29	50	0.667	
MT263	C12_B2P21	6.34	0.56	0.922	14.60	16	29	45	0.736	
MT264	C2_B2P21	7.41	1.24	0.949	10.80	15	19	34	0.857	
MT265	C3_B2P21	6.05	0.43	0.929	10.41	29	7	36	0.886	
MT266	C4_B2P21	3.66	0.57	0.927	27.87	24	22	46	0.869	
MT267	C5_B2P21	1.37	0.05	0.471	18.18	35	61	96	0.430	
MT268	C6_B2P21	6.02	0.37	0.927	10.15	16	15	31	0.862	
MT269	C7_B2P21	6.14	0.16	0.935	9.99	17	20	37	0.848	
MT270	C8_B2P21	0.64	0.02	0.334	21.76	15	86	101	0.338	
MT271	C9_B2P21	6.12	1.00	0.933	12.63	14	31	45	0.741	
MT272	D10_B2P21	4.92	0.09	0.923	9.75	18	27	45	0.743	
MT273	D11_B2P21	4.98	0.16	0.945	15.39	22	23	45	0.741	
MT274	D12_B2P21	5.75	0.90	0.965	21.58	31	17	48	0.741	
MT275	D2_B2P21	5.76	-	0.571	-	30	39	69	0.628	

Number	Mutant	OD	Standard deviation of the OD	r to wild type on same plate	Error [%]	Number of increased metabolites	Number of reduced metabolites	Number of varying metabolites	r to reference list	Affected enzyme (gene name)
MT276	D4_B2P21	6.92	0.91	0.927	11.21	16	20	36	0.864	
MT277	D5_B2P21	6.07	1.16	0.832	15.50	12	21	33	0.880	
MT278	D6_B2P21	1.57	1.67	0.696	63.41	31	41	72	0.654	
MT279	D7_B2P21	5.23	0.35	0.902	13.95	19	23	42	0.811	
MT280	D8_B2P21	6.91	0.57	0.926	19.44	12	26	38	0.833	
MT281	D9_B2P21	5.54	1.12	0.918	15.94	21	29	50	0.737	
MT282	E1_B2P21	5.81	0.38	0.881	8.86	13	7	20	0.907	
MT283	E10_B2P21	4.40	0.24	0.68	11.43	18	21	39	0.831	
MT284	E11_B2P21	5.00	0.48	0.976	15.98	11	31	42	0.645	
MT285	E12_B2P21	0.63	0.01	0.459	22.05	8	96	104	0.433	
MT286	E2_B2P21	6.93	0.87	0.941	10.84	12	15	27	0.920	
MT287	E5_B2P21	6.12	0.56	0.978	7.94	18	20	38	0.759	
MT288	E6_B2P21	0.70	0.02	0.452	18.99	9	90	99	0.502	
MT289	E7_B2P21	5.53	0.48	0.985	12.49	11	34	45	0.761	
MT290	E8_B2P21	6.59	0.69	0.983	13.43	11	31	42	0.764	
MT291	E9_B2P21	5.94	0.83	0.977	10.28	17	29	46	0.646	

Number	Mutant	OD	Standard deviation of the OD	r to wild type on same plate	Error [%]	Number of increased metabolites	Number of reduced metabolites	Number of varying metabolites	r to reference list	Affected enzyme (gene name)
MT292	F1_B2P21	6.21	0.24	0.465	18.69	15	85	100	0.475	
MT293	F10_B2P21	5.30	0.34	0.985	10.80	11	29	40	0.642	
MT294	F11_B2P21	5.44	0.37	0.963	12.43	4	51	55	0.621	
MT295	F12_B2P21	5.62	0.79	0.985	15.40	14	33	47	0.627	
MT297	F3_B2P21	5.94	0.72	0.95	18.40	28	24	52	0.859	
MT298	F4_B2P21	7.37	0.63	0.992	7.25	13	21	34	0.907	
MT299	F5_B2P21	6.66	0.03	0.961	24.37	47	23	70	0.724	
MT300	F6_B2P21	2.08	-	0.612	-	11	86	97	0.572	
MT301	F7_B2P21	5.71	0.05	0.932	22.16	19	22	41	0.692	
MT302	F8_B2P21	7.22	0.57	0.983	15.94	10	30	40	0.750	
MT303	F9_B2P21	6.51	0.70	0.99	8.95	12	40	52	0.632	
MT304	G1_B2P21	6.90	0.41	0.988	9.66	20	21	41	0.890	
MT305	G10_B2P21	0.69	0.01	0.432	15.56	8	96	104	0.413	
MT306	G11_B2P21	5.59	0.16	0.99	7.97	12	33	45	0.628	
MT307	G12_B2P21	6.47	0.60	0.994	16.88	16	38	54	0.619	
MT308	G2_B2P21	7.85	0.68	0.974	7.99	14	17	31	0.908	

Number	Mutant	OD	Standard deviation of the OD	r to wild type on same plate	Error [%]	Number of increased metabolites	Number of reduced metabolites	Number of varying metabolites	r to reference list	Affected enzyme (gene name)
MT309	G3_B2P21	6.83	0.50	0.931	15.80	15	14	29	0.936	
MT310	G4_B2P21	7.37	0.26	0.985	7.32	17	39	56	0.615	
MT311	G5_B2P21	6.53	1.14	0.99	22.56	18	22	40	0.759	
MT312	G6_B2P21	6.22	0.48	0.961	16.03	16	21	37	0.727	
MT313	G7_B2P21	5.94	0.05	0.977	15.61	18	24	42	0.728	
MT314	G8_B2P21	8.61	0.61	0.987	18.89	15	47	62	0.635	
MT315	G9_B2P21	7.54	0.60	0.993	17.55	20	42	62	0.624	
MT316	H1_B2P21	7.93	0.49	0.992	11.75	3	58	61	0.901	
MT317	H10_B2P21	7.23	0.90	0.986	16.03	13	45	58	0.638	
MT318	H2_B2P21	8.34	1.17	0.989	13.51	18	17	35	0.908	
MT319	H3_B2P21	7.78	0.44	1	13.94	16	20	36	0.897	
MT320	H4_B2P21	7.95	1.81	0.984	25.74	18	42	60	0.640	
MT321	H5_B2P21	8.37	0.17	0.972	15.76	7	47	54	0.654	
MT322	H6_B2P21	8.03	0.78	0.993	16.62	22	23	45	0.747	
MT323	H7_B2P21	7.39	0.35	1	14.36	20	21	41	0.759	
MT324	H8_B2P21	7.63	0.46	0.972	17.82	20	39	59	0.642	

Number	Mutant	OD	Standard deviation of the OD	r to wild type on same plate	Error [%]	Number of increased metabolites	Number of reduced metabolites	Number of varying metabolites	r to reference list	Affected enzyme (gene name)
MT325	H9_B2P21	7.50	0.28	0.965	16.17	10	49	59	0.655	

Danksagung

Mein Dank geht an meinen Mentor Professor Dr. Dietmar Schomburg für die Bereitstellung des sehr interessanten Themas, zahlreicher Anregungen sowie der mir gegebenen Möglichkeiten, eigene Ideen zu entwickeln und viele neue Erfahrungen zu machen.

Bedanken möchte ich mich außerdem bei Professor Dr. Dieter Jahn für die Übernahme des Zweitgutachtens sowie bei Professor Dr. Petra Dersch für die Übernahme des Vorsitz der Prüfungskommission.

Besonders bedanken möchte ich mich bei Professor Dr. Franz-Josef Marner für die Beantwortung zahlreicher Fragen und vieler anregender, fachlicher Diskussionen.

Mein besonderer Dank geht an Dr. Sebastian Buchinger für die gute Einarbeitung in eine ganz neue Aufgabe sowie die stetige Motivation und die vielen produktiven Diskussionen im ersten Teil meiner Arbeit.

Bedanken möchte ich mich auch bei Manfred Kreikler von der Feinmechanikwerkstatt der Universität zu Köln für die Anfertigung vieler Sonderwünsche.

Der ganzen Arbeitsgruppe Schomburg möchte ich für die gute Zusammenarbeit und die nette Arbeitsatmosphäre danken. Besonderer Dank gilt dabei Lorenz Reimer und Timo Lühr die durch interessante Resultate im Rahmen ihrer Diplomarbeiten sehr zum Vorankommen meiner Arbeit beigetragen haben, sowie Patricia Wieloch und Kerstin Schreiber die am Quenchingprojekt mitgearbeitet haben.

Außerdem danke ich besonders Christian Jäger für die zahlreichen Diskussionen und die Kritik die nicht selten zu neuen Ansatzpunkten und Erkenntnissen führte.

Bei Sabine Thiele möchte ich mich für die Übernahme der Gerätebetreuung bedanken, wodurch ich viel Zeit und auch einige Nerven gespart habe.

Bedanken möchte ich mich auch bei Kathrin Laubert und meiner Schwägerin Astrid Spura für tolle sprachliche Korrekturvorschläge zur Verbesserung der Dissertation bzw. Publikation.

Ein großes Dankeschön geht an meine Familie für die Unterstützung seit Beginn meines Studiums. Dabei geht der größte Dank an meinen Mann René für die mir entgegengebrachte Geduld und Unterstützung sowie die vielen Motivationen aber auch die zahlreichen voranbringenden Diskussionen.